Project Number: <KLB-0401>

Design of a Biaxial Test Device for Compliant Tissue

A Major Qualifying Project Report:
Submitted to the Faculty
Of the
WORCESTER POLYTECHNIC INSTITUTE

In partial fulfillment of the requirements for the
Degree of Bachelor of Science

Submitted by:

____
Catherine Chong

____
Haydon Hung

____
Alexis Steinhart

____
Jonathan Trexler

Date: April 28, 2005

Approved:

____
Prof. Kristen L. Billiar, Advisor

Table of Contents

Authorship Page iv
Acknowledgements v
Abstract vi
Table of Figures vii
1 Introduction 1
2 Background 3
2.1 Properties of Skin 3
2.2 Why Use Biaxial Testing Device? 4
2.3 Various Biaxial Testing Systems 5
2.3.1 Two Linear Axes for Planar Specimen 6
2.3.2 Indentation / Inflation Test 12
2.4 Methods for Attaching Sample to Grips 13
2.4.1 Clamps 14
2.4.2 Sutures/Staples 16
2.4.3 Hooks 18
2.5 Test Chambers 19
2.5.1 Temperature 19
2.5.2 Saline 19
2.6 Actuators and Motors 20
2.6.1 DC motor 20
2.6.2 DC Stepper Motor 21
2.6.3 DC Servo Motor 22
2.6.4 Pneumatic/Hydraulic Motor 22
2.6.5 Linear Actuators 23
2.7 Motion Controllers 24
2.7.1 Motion Controller Board 25
2.7.2 Amplifier/Motor Drive 25
2.7.3 Feedback Device 26
2.7.4 Data Output: Proportional-Integral-Derivative (PID) 26
2.8 Mechanisms for Linear Movement 30
2.9 Force Measurement 30
2.10 Displacement Measurement 31
2.10.1 Video Display 31
2.10.2 Signal 32
2.10.3 Signal Format 32
2.11 Computer Control 33
3 Design Approach 34
3.1 Design Iteration #1 – Two Motor Design 35
3.1.1 Pros and Cons 38
3.1.2 Pass or Fail 38
3.2 Design Iteration #2 – Four Axes Design 39
3.3 Modifications to Four Axes Design 43
3.4 Design for Heated Test Chamber 44
3.4.1 Purpose and Constraints 44

3.4.2 First Design: Fish Tank Heater 44
3.4.3 Second Design: Exterior Pump 45
3.4.4 Combination of the Two Previous Designs 46
3.4.5 Third Design- Plexiglas® 47
3.4.6 Design #2 - Mylar 47
3.4.7 Final Solution 48
3.5 Sample Attachment 50
3.5.1 Using Rice Paper and Latex Samples 50
3.5.2 Graphite Markers 52
3.5.3 Applying Force onto the Latex Sample 53
4 Methodology 55
4.1 Motion 55
4.1.1 Motors 55
4.1.2 Controllers 55
4.1.3 Rails 59
4.2 Force Measurement 59
4.2.1 Force Transducer 59
4.2.2 Signal Conditioning/Filter 60
4.3 Displacement Measurement System 60
4.4 Control System Overview 61
4.5 Data Acquisition 63
5.0 Assembly of Device 65
5.1 Components 65
5.2 LabVIEW 66
5.2.1 INITIALIZE.VI 67
5.2.2 FINAL.VI 69
5.2.3 Image Acquisition (IMAQ) 70
5.2.4 Transducer Data Acquisition 71
5.2.5 Required Inputs for INITIALIZE.VI and FINAL.VI 72
6.0 Discussion 74
7.0 Recommendations 76
References 78
APPENDIX A: Standard Graphs for All Living Tissues [25] 81
APPENDIX B: The Objective Tree 83
APPENDIX C: Pair-wise Comparison Chart 84
APPENDIX D-1: National Instruments (Series Comparison) 86
APPENDIX D-2: National Instruments (Low Cost Motion Control) 87
APPENDIX D-3: Precision MicroControl Corp Motion Control 88
APPENDIX D-4: Galil Motion Control 89
APPENDIX E: Calculations Loads for Force Transducers 92
APPENDIX F-1: Plexiglas® Thermal Conduction 101
APPENDIX F-2: Mylar Thermal Conduction 103
APPENDIX G-1: Pivot Mechanism 104
APPENDIX G-2: Bearings - Vee Jewel Assembly 105
APPENDIX G-3: Dimensions of Pulley Frame 108
APPENDIX G-4: Dimensions of Pulley 109

APPENDIX G-5: Assembly of Bath Chamber 110
APPENDIX G-6: Dimensions of Chamber Base 111
APPENDIX G-7: Dimensions of Framework Pieces 112
APPENDIX G-8: CAD Drawings of Motor Mounts 114
APPENDIX G-9: Dimensions for Motor Plates 115
APPENDIX G-10: CAD Drawings of Transducer Mounts 119
APPENDIX G-11: Dimensions of Transducer Mounts 120
APPENDIX G-12: CAD Drawings for Assembly of Motors and Transducers 125
APPENDIX G-13: Dimensions of Arm 127
APPENDIX H: Excel Sheet with Part Number, Description, Company, and Price 129
APPENDIX H-1: AM Series Stepper Motors 130
APPENDIX H-2: Universal Joints 132
APPENDIX H-3: Futek Torque Transducer 133
APPENDIX H-4: Kerk Screwrail Assemblies 135
APPENDIX H-5: PID Controller 139
APPENDIX H-6: Kapton Flexible Heaters 140
APPENDIX H-7: Thermocouple Wire 141
APPENDIX H-8: Stepper and Servo Motor Drives 142
APPENDIX H-9: Motion Controller 144
APPENDIX H-10: Image Acquisition 145
APPENDIX H-11: Data Acquisition Board 146
APPENDIX H-12: Signal Conditioning Modules 152
APPENDIX I: Procedure for Running a Sample Test 155
APPENDIX J: Clinch Knot Instructions 158

Authorship Page

Introduction: AS, CC, JT

Properties of Skin: CC

Why use Biaxial Testing Device: CC

Hooks: CC, AS

Test Chamber: CC

Actuators and Motors: HH

Motion Controllers: CC

Mechanisms for Linear Movement: HH

Force Measurement: HH

Displacement Measurement: JT

Computer Control: AS, JT

Design Iteration #1: HH, JT

Design Iteration #2: HH, JT

Modification for 4 Axes Design: HH, JT

Design for Heated Test Chamber: ALL

Sample Attachment: CC, AS

Motion: CC

Force Measurement: HH

Displacement Measurement System: JT

Control System Overview: JT, AS

Data Acquisition: JT, AS

Assembly of Device: HH

Components: HH

LabVIEW: JT

Discussion: HH, JT

Recommendations: AS

Acknowledgements

We would like to thank the following individuals and groups for the contribution to this project:

- The Whitaker Foundation (RG-02-0732) for funding this project
- Steve Derosier and the work studies of the WPI Washburn Machine Shop
- National Instruments tech support for all their help with component selection and LabVIEW guidance
- Peterson Steel for donating materials (aluminum material) for the project

Abstract

The objective of this project is to design and build a computer controlled testing system for planar biaxial stretching of soft connective tissues. The planar biaxial device designed in this paper has a four-axis control system as well as four components: a temperature-controlled testing chamber, a low friction sample attachment system, a stretching/force system, and a stress/strain measurement system. The device's design is unique due to its low force capability (< 0.5N), low cost (< $15,000), and real-time computer control.

Table of Figures

Figure 1. Multi-axial Testing Device of Reihsner, Balogh, and Menzel [33] 4
Figure 2. Pulley System by Lanir and Fung [19].. 6
Figure 3. Biaxial Device by Nielsen, Hunter, and Smaill [28].. 8
Figure 4. Biaxial Device by Demer and Yin [5]... 8
Figure 5. Device by Vito [40].. 9
Figure 6. Equibiaxial Stretching by Humphrey, Vawter, and Vito [12]........................... 9
Figure 7. Billiar and Sacks System; Pulley System (left); Suture Attachments (right) [35]... 10
Figure 8. Biaxial Device of Makinde, Thibodeau, and Neale [23]................................. 11
Figure 9. Hydraulic System by Langdon et al. [16]... 12
Figure 10. Indentation Test by Lafrance et al. [15] 12
Figure 11. Inflation Test by Hsu et al. [11].. 13
Figure 12. Interchangeable Jaws on Device by Brouwer et al. [2] 14
Figure 13. Cruciate-shaped Sample by Flynn, Peura, Grigg, and Hoffman [8] 15
Figure 14. Cyrogenic Grips for Tensile Tests by Lepetit et a.l [21]............................... 16
Figure 15. Attachment of Sutures (Lanir and Fung [19]) 16
Figure 16. Results After Loading (Liu and James [22])et al.).. 17
Figure 17. Instron's Planar Biaxial Test System: Hooks and Sutures [42]..................... 18
Figure 18. Schematic of Instron's Pulley System and Sutures [42]................................ 18
Figure 19. Explanation of How DC Motor Functions [43]... 21
Figure 20. Diagram of Stepper Motor [45]... 22
Figure 21. Typical Setup for a Basic Pneumatic System [47] 23
Figure 22. Internal View of Linear Actuator [48]... 24
Figure 23. Schematic of Motion Control [48] 25
Figure 24. Ideal Position Curve [49]... 27
Figure 25. Realistic Curve 28
Figure 26. Overshooting/Undershooting Curves 28
Figure 27. Oscillation (Underdamped) Curve 28
Figure 28. Overdamped Response 29
Figure 29. Constant Oscillation Curve.. 29
Figure 30. Optimal Response from PID Control 29
Figure 31. Shape of Typical Sample... 35
Figure 32. Deformation when Edges are Fixed 36
Figure 33. Deformed Samples with Equal Loading... 36
Figure 34. Conceptual Design of a Possible Two-Motor Design 37
Figure 35. Conceptual Drawing of a Four-Motor System 39
Figure 36. Different Setup of Connecting Arm to Torque Transducer............................ 42
Figure 37. Conceptual Drawing of Final Design 43
Figure 38. Fish Tank Heater Bath Design 45
Figure 39. Exterior Pumps to Heat Bath... 46
Figure 40. Combination of Previous Two Designs... 46
Figure 41. Levels of Bath Chamber.. 49
Figure 42. Layout of Test Chamber.. 50
Figure 43. Rice Paper with Hooks 51

Figure 44. Suture Staple with Two Hooks 51
Figure 45. Latex Sample with Marking 52
Figure 46. Rice Paper with Marking 52
Figure 47. Slight Pull 53
Figure 48. Stronger Pull 53
Figure 49. Maximum Pull 54
Figure 50. Schematic of Control System 63
Figure 51. Diagram of Timed Circuits 64
Figure 52. Timed Loop with Priorities 64
Figure 53. Synchronization of Timed Loops 64
Figure 54. Displacement Measurement 67
Figure 55. Initial Image of Graphite Markers 68
Figure 56. Threshold Image of Graphite Markers 68
Figure 57. Initialize.VI 69
Figure 58. Centroids on Graphite Markers 70
Figure 59. FINAL.VI 71
Figure 60. Inputs and outputs for VI 72
Figure 61. Data in Excel Spreadsheet 73

1 Introduction

Advancements in wound healing are critical today due to various types of skin problems such as ulcers, bedsores, and skin burns. For example, approximately 700,000 patients are treated yearly for injuries ranging from minor first-degree burns to serious third degree burns [41]. Skin substitutes are essential to heal the wound properly, which are from culture tissues.

Researchers in the field of tissue engineering have produced cell-cultured tissues to further the advancements in the wound healing process. Our advisor, Professor Kristen Billiar is currently growing such cultured tissue samples in his Tissues Mechanics and Mechanobiology Lab to understand how mechanical forces alter the cellular response and to investigate the subsequent changes in the mechanics of the tissues. Generally, tissue engineered skin does not mimic the properties of native skin because it is soft, fragile, and easy to tear.

The most common way to determine the mechanical properties of the tissue samples is by the uniaxial testing method. This stretches the sample in one direction. However, it is insufficient because it does not obtain all the necessary data for a full mechanical representation of the sample.

In order to obtain a complete characterization of a planar tissue, multi-axial testing is required. This is necessary because the tissue is a three-dimensional structure and it experiences forces in multiple directions during stretching. For very soft connective tissues, it is commonly assumed incompressible through its thickness [19]. Therefore, biaxial testing is sufficient to retrieve the required data for a constitutive equation. This method stretches the sample in two directions, horizontal and vertical direction (the x and y axes, respectively).

The objective of this project is to design and build a computer controlled testing system for biaxial stretching of soft connective tissues. The device will be used to measure the mechanical material properties of the tissues while subjecting to biaxial loads. This will allow an accurate comparison between the sample and natural tissue. Through this analysis and comparison, an assessment of progress made in the field of tissue engineering can be made.

This paper includes the research obtained to provide a background for designing this device in terms of properties of skin and cultured tissues, previous systems, bath chamber, attachment methods, motion control, stretching/force system, displacement measurement, and LabVIEW. It then gives a detailed account of the design process and the reasons for the final design. Next, this paper displays the process of building the device, testing methods, and results and discussion of implications. In the final chapter of this paper is the discussion on the design and the design process with recommendations for future work.

2 Background

2.1 Properties of Skin

There is a huge demand for artificial skin and reproduction of tissue mass to serve as space fillers or replace the organs (blood vessels, skin, nerve ending, organs, etc). Currently in research is the use of polymer materials with biological surfaces to mimic the properties of natural skin/tissues. To achieve this, it is critical to understand the skin and its mechanical properties. According to Lanir and Fung. [19], "precise knowledge of the mechanical properties of the skin will be of great value to plastic surgeons in designing the size, shape and orientation of skin grafts." The process of cell culture and possibly other polymer materials is the necessary step to proceed. Subsequently, it is necessary to test the cultured material to determine the mechanical behavior. By comparing the results with the mechanical behavior of skin, it will determine whether the cultured material can withstand the native environment that natural skin is exposed to everyday. The artificial skin is highly demanded for severely burned patients, while the joints in the body are in need for soft connective tissues. To have a detailed understanding of the skin, one must look into the properties and understand the composition of it [37].

Skin plays an important role in the body because it contains, holds, and protects all the internal organs from the external environment, therefore it needs to be strong and tough. Because the skin is composed of more than one component, the skin is not homogenous throughout the body. The skin accounts for 16 percent of human adult body weight [18] and consist of mostly collagen and elastin. The collagen is responsible for the tensile strength of 1.5 to 3.5 x 10^2 MPa with the Young's modulus measuring up to 1

GPa [18]. The skin also contains elastin, which is responsible for the “reversible deformation” and can stretch more than 100 percent of its original size, and can withstand up to 20 N/m, which depends on the location of the body. Although there are still questions about the specific role of elastin [31], it is compliant and exhibits elastic behavior [32].

In order to culture tissue samples to possibly be used as skin substitutes, they must be strong and tough. Biaxial testing device is needed to test the cultured samples to study how mechanical forces affect the sample and the changes of its mechanical strength.

Appendix A shows the standard graphs for all living tissues [25].

2.2 Why Use Biaxial Testing Device?

A biaxial testing device is essential to obtaining the proper data because soft tissue is a three-dimensional structure (oriented in layers of primarily planar networks with fibers running between the layers) [18]. An ideal testing device would be an *in vivo* multi-axial testing device by Reihsner, Balogh, and Menzel [33] in Figure 1.

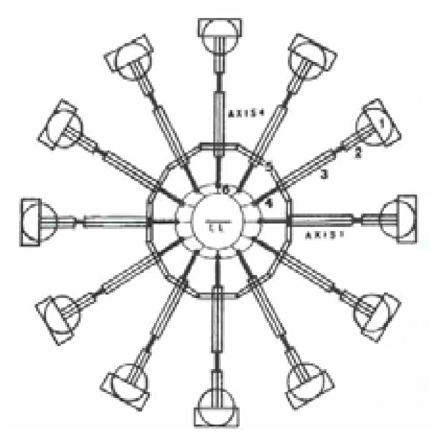

Figure 1. Multi-axial Testing Device of Reihsner, Balogh, and Menzel [33]
Determines the strain in all directions
due to anisotropic behavior of the tissue sample

The common method to test tissue samples were completed by the uniaxial devices. However, they were not sufficient to determine the mechanical properties, such as fatigue strength and tensile strength, for all directions. In one direction, the tissue may be isometric (fibers contracting but not changing in length); however, this does not apply in three-dimensional case because edges of the sample tissue are “not fixed but free to deform” [5], confirming that uniaxial tests do not provide the necessary data to derive the unique three-dimensional constitutive equations for skin [12]. Therefore, a multi-axial testing device is required to acquire all the necessary data for a stress/strain relationship [6]. (Strain is the change of length over initial length; stress is force over unit area.)

Assumed incompressibility, the data from the two-dimensional test makes it possible to achieve the full three-dimensional constitutive equation [5, 19]. Other assumptions include:

- Thickness of specimen is uniform throughout its entire length
- Loads are uniformly distributed over an area in the central region of the sample [12]
- St. Venant’s principle: The strain measurement is taken at the central region of the tissue sample because it is free from distortions [6].

2.3 Various Biaxial Testing Systems

Several research groups have and are conducting experiments with biaxial testing to test various soft biological tissue samples to derive the three- dimensional constitutive relationship. Some devices are similar, while some are completely different.

2.3.1 Two Linear Axes for Planar Specimen

This is the most common type of device used to test soft tissues under biaxial loads.

Lanir and Fung [19] were two of the earlier researchers who experimented with thin, rectangular rabbit skin samples by using this system. Figure 2 shows the device they used to acquire the force-length time relations.

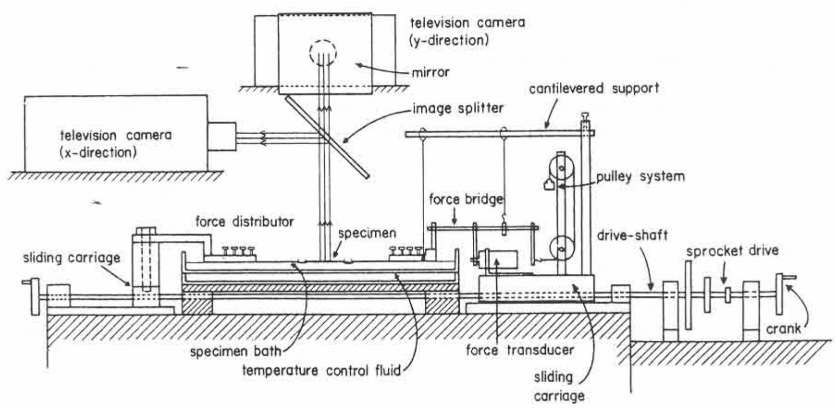

Figure 2. Pulley System by Lanir and Fung [19]
Utilizes a pulley system to allow force distributor to be pulled by a constant weight, allowing a controlled slow/rapid stretching rate

There were four major components involved in this biaxial device:

1. Environment: The specimen floats in the top half of a double compartment tray filled with physiological solution while a thermoregulation system is beneath. This is necessary to keep the sample submerged and maintained at 37 ºC.
2. Actuators/stretching mechanism: There is a hand crank to physically turn to stretch the sample, which is hooked along the edges with small staples and silk sutures.

3. Force mechanism: To measure the stress, one platform mounts on top of the sliding mechanisms while the other side attaches to a force transducer and this stretches the sample.
4. Displacement measurement: This system is a non contact displacement analyzer consists of a television camera, a video processor, and a television monitor, to measure the strain of the sample. It cannot touch the sample because it is fragile.

This system is capable of performing these experiments:

- measuring the forces in main and transverse direction vs. the extension ratio
- measuring two transverse forces and extension ratios
- quickly stretching the specimen in one direction while the other axis is kept constant
- measuring the stretched dimension as a function of time
- observing the effect of temperature on the stress-strain relationship

According to Nielsen, Hunter, and Smaill [28], the problem with Lanir's method was the time consuming preparation, the point forces needed to be separate, and the strain rates did not measure as high as physiological rates. Figure 3 shows his version of a biaxial device with a few variations to Lanir's device.

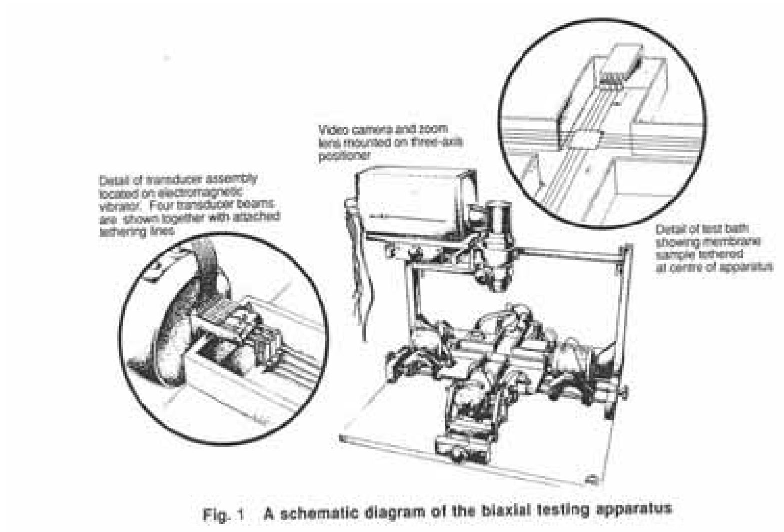

Fig. 1 A schematic diagram of the biaxial testing apparatus

Figure 3. Biaxial Device by Nielsen, Hunter, and Smaill [28]
Only used four attachments on each edge, point forces monitored individually, and loading was controlled by software system

The figure below is a device by Demer and Yin [5], using an isolated canine myocardium

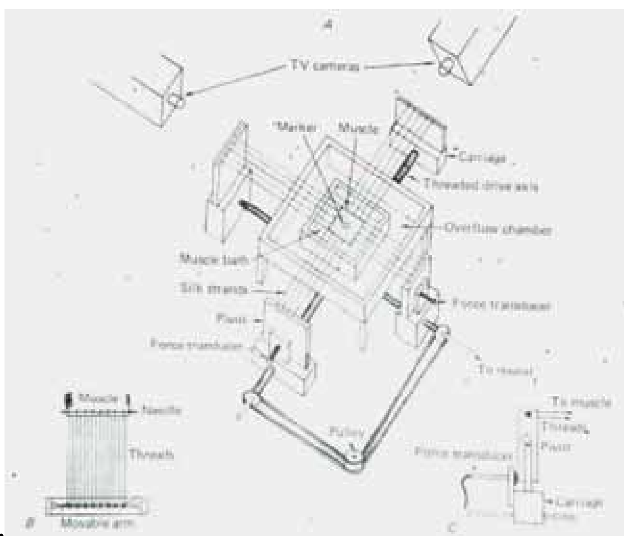

.

Figure 4. Biaxial Device by Demer and Yin [5]
Sample located at center of bath with four attachments on each edge, utilizes the pulley and chain system, two video cameras used to monitor the targeted area

w, Yin, and Zeger [3] used canine pericardium to find the pseudo strain-energy function by characterizing its property. May-Newman and Yin [26] and Chew, Yin, and Zeger used the same device as before except there was no pulley system attached to the motors.

Vito [40] used aorta samples from dogs to find the continuous axial loading and unloading, while maintaining the diameter.

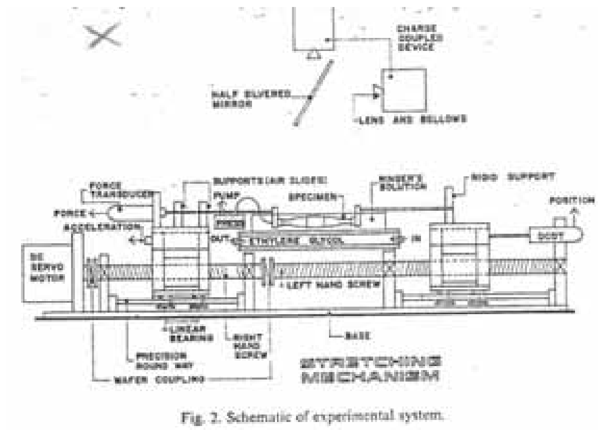

Figure 5. Device by Vito [40]
Used servomotors to drive each axis, needs to improve on processing speed and ease of software development, rate of loading was 0.025 cm/s producing a length 0.5-1.0 cm

Humphrey, Vawter, and Vito [12] worked on a technique to get an accurate tracking of the markers on the surface of the tissue sample.

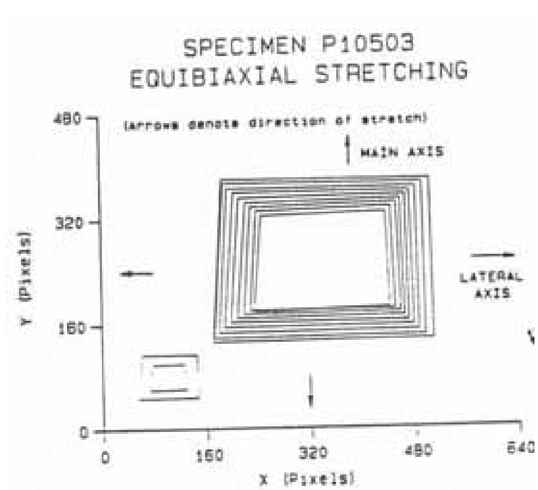

Figure 6. Equibiaxial Stretching by Humphrey, Vawter, and Vito [12]
Observation when tracking deformation of sample during equibiaxial stretching

Sacks and Chuong [36] has done related testing with similar devices, a pulley system is involved to insure there were equal tension for each pair of the suture lines

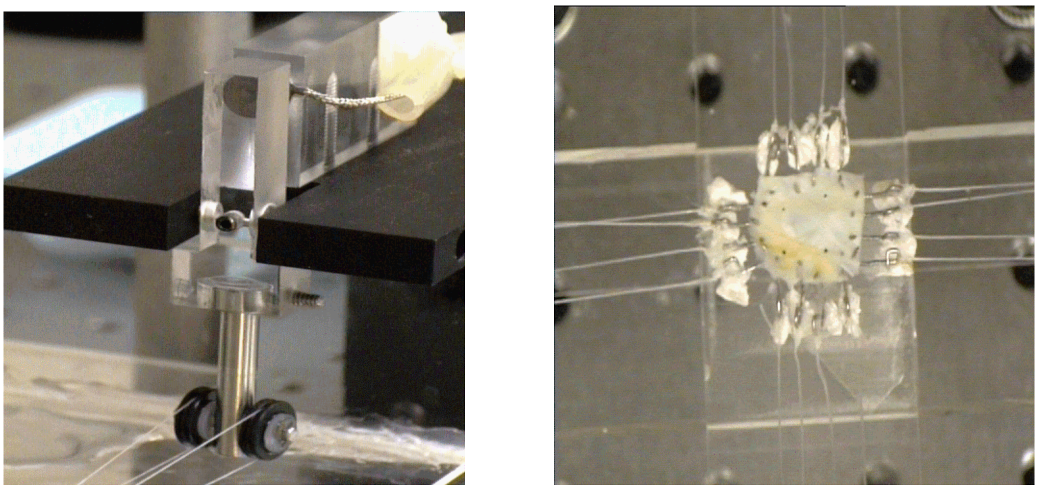

Figure 7. Billiar and Sacks System; Pulley System (left); Suture Attachments (right) [35]
Pulleys distribute forces equally onto the sample, sutures
are used for the specimen to shear freely

Mankinde, Thibodeau, and Neale [23] concentrated on developing a biaxial testing device for a cruciform shaped specimen.

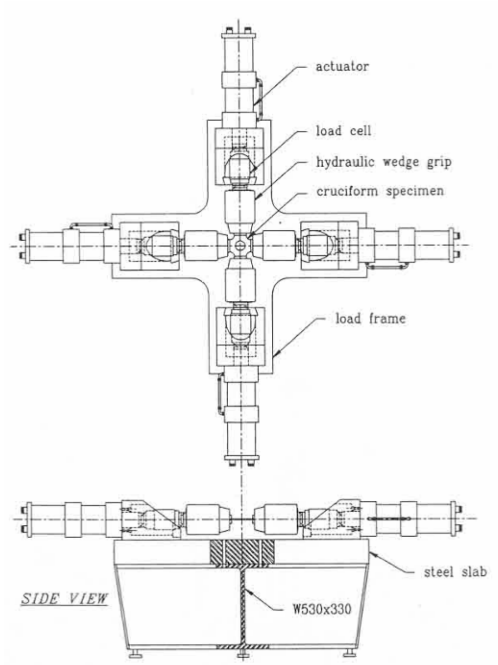

Figure 8. Biaxial Device of Makinde, Thibodeau, and Neale [23]
Loading system involves load reaction frame and load train, out-of-plane design was ideal because of low cost, ease of manufacturing, and assembly

Langdon, Chernecky, Pereira, Abdulla, and Lee [16] used a custom-built hydraulic testing system, using four independent servo-hydraulic actuators. This system used very up-to-date technology, and was far more scientific and technical than the previous designs. Figure 9 shows all the involved components and how they connect to each other to get the results.

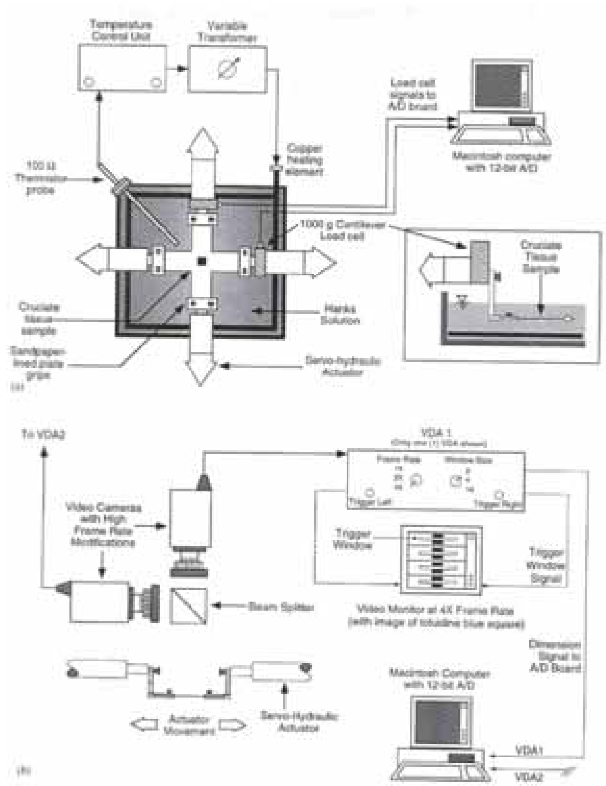

Figure 9. Hydraulic System by Langdon et al. [16]
Cantiliver grips are lined with sandpaper to hold samples,
uses dichroic beam spliter and two high frame-rate cameras
to view the central region

2.3.2 Indentation / Inflation Test

Lafrance, Yahia, Germain, Guillot, and Auger [15] used an indentation test for biaxial testing on living skin equivalents (SE) and dermal equivalent (DE).

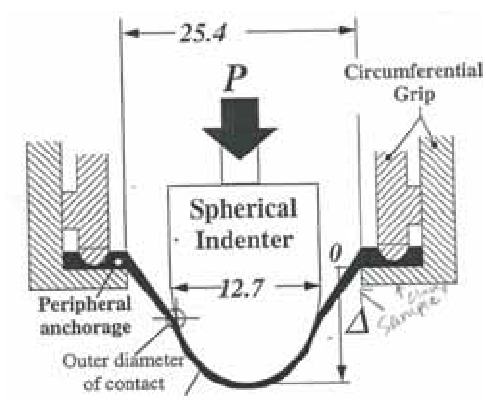

Figure 10. Indentation Test by Lafrance et al. [15]
A circumferential grip clamps and centers the samples
with the load axis of the spherical indenter

Van Noort, Black, Greaney, and Irvin [38] used an inflation device to measure the stress/strain relationship. Perspex rings hold the tissue while the pressurized water fills the test chamber, causing the tissue to inflate until the point it bursts. This method provides realistic measurements to help research in wound healing. Hsu, Lui, Downs, Rigamonti, and Humphrey [11] also proceeded with a similar type of device.

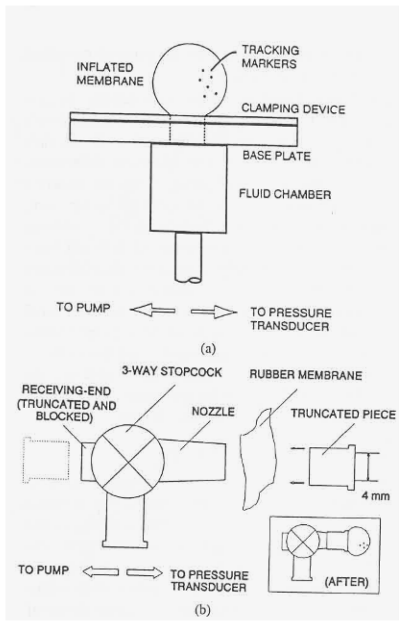

Figure 11. Inflation Test by Hsu et al. [11]
Fluid chamber maintains the pressure from the transducer and the pump,
3-way stopcock controls the inflated membrane

The inflation devices are excellent devices to obtain mechanical properties of the skin in all directions, however, it lacks the versatility of a planar test and the sample's size and range are dependent on the size of the nozzle and pressure

2.4 *Methods for Attaching Sample to Grips*

There has always been a problem with the method of attaching the sample to the grips (such as clamps, sutures with hooks, etc.). The reason for the concern is that the attachments introduce local stress concentration at certain points and may cause the strain field to be non-uniform. It can alter the geometry and cause uneven loads at the attachment sites. It is necessary to keep the original orientation, fiber lengths, and boundary loadings preserved when mounting the sample because without maintenance, the data is not valid for an *in situ* testing [10].

There are different methods of attachment, which include gluing the sample to the grips, but only for very thin samples. For thicker samples, gluing could cause shear stress/strain [21]. The solution to this problem is to take direct measurements of the tissue strain near the center of the sample because it will be adequately remote from the grips.

2.4.1 Clamps

Brouwer *et al.* [2] designed a device to have interchangeable jaws. The jaw opens and closes at a constant, precise velocity until it reaches a set position and force.

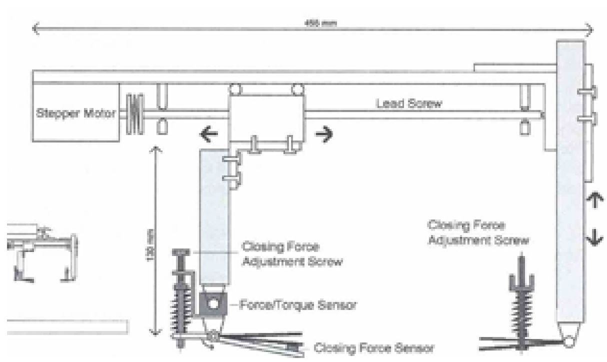

Figure 12. Interchangeable Jaws on Device by Brouwer et al. [2]
Button force sensor receives the required force
and stops the jaw from operating

Reihsner, Balogh, and Menzel [33] used actual clamps with 400 grid abrasive paper, which was glued to the inside surface of the clamp. This allowed for "optimal compression of the specimen between the clamps can be found empirically as 'mid position' between slipping and jaw break".

Langdon *et al.* [16] used a cruciate shape for the samples (3 cm with the central region of 2 cm) because it retains continuous fiber geometry of the tissue. Figure 13 shows an example of a cruciate shaped sample by Flynn, Peura, Grigg, and Hoffman [8].

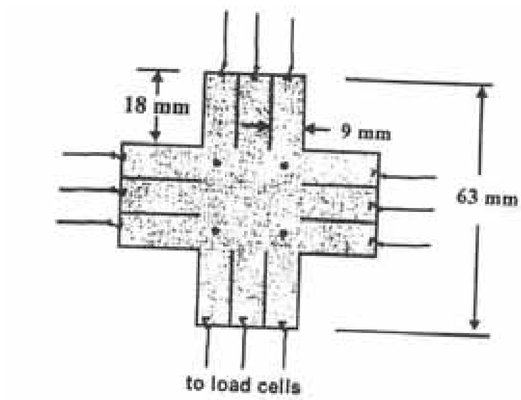

Figure 13. Cruciate-shaped Sample by Flynn, Peura, Grigg, and Hoffman [8]
Clarifies the idea of what a cruiciate form looks like

The sample was mounted onto four plates, surfaced with #180 grit waterproof sandpaper, and the plates tightened with screws. An alignment jig was necessary to align the grips and arms properly.

Lepetit, Favier, Grajales, and Skjervold [21] developed cryogenic grips for tensile tests (mostly used for ligaments and tendons), which were done in two ways (Figure 14). The first method uses cryoclamps, which the ends of the sample are frozen and mechanically clamped. This leads to damages or breaking the frozen area. The second was cryofixation, in which molds the tissues into ice blocks, but thawing the samples is necessary.

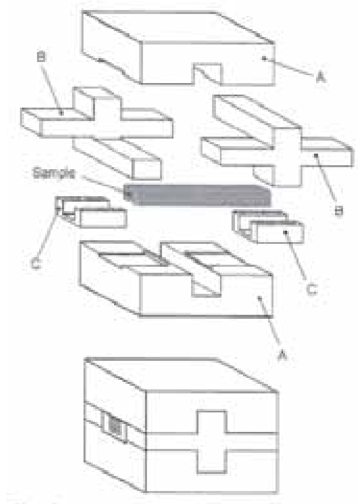

Figure 14. Cyrogenic Grips for Tensile Tests by Lepetit et a.l [21]
This is a 3-minute process and allows for low resistance properties.

One concern for using clamps is slippage, which occurs when the clamp is not tight enough. This causes the grip's displacement to be inaccurate and making the data invalid. If the clamp is too tight, this could lead to damage of the sample on the edges.

2.4.2 Sutures/Staples

Figures below show how the square/rectangular samples are attached to the device using sutures/staples.

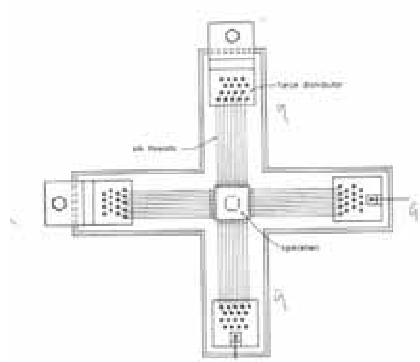

Figure 15. Attachment of Sutures (Lanir and Fung [19])
Each side attached to motor carriage
with surgical staples

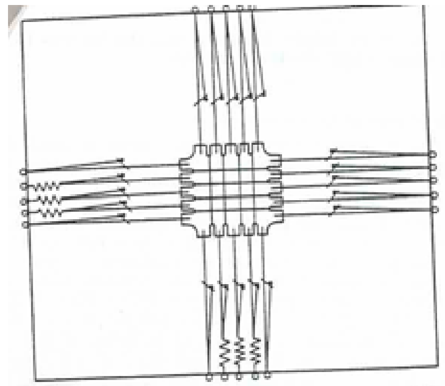

Figure 16. Results After Loading (Liu and James [22])et al.)
Edges of the sample deforms due to
the applied load

Gloeckner, Sacks, Billiar, and Bachrach. [9] used two loops of suture around each of the two small pulleys. The horizontal common axle connects to a vertical pivoting rod (to allow frictionless rotation). Sacks [36] also used 000 silk sutures, but they were looped 5 times around each side. The samples were in their dehydrated state with the water bath empty when mounted to the controlled sample onto the device. Once mounted, saline filled the bath at room temperature, which left the sample to re-hydrate for an hour. For his next paper [35], there were only two loops of suture for each side (mounted on a pulley)and held by four stainless steel staples.

The 25 mm x 25 mm sample used a 5-0 suture with five continuous loops per edge (1 loop/5 mm). Within the sample size, the clamping does not affect the 15 mm x 15 mm region at the center [14]. May-Newman and Yin [26] also did a similar setup.

Lanir and Fung [19] used a rectangular shaped sample and had the specimen float in physiological solution. They used 68 small staples; each connected by a silk thread that screw onto the force-distributing platform. This allowed independent adjustment of each thread. Because of the staples and hooks, there exists a stress at the edges (1/20 normal stress); however, the central region (benchmark) was not be affected. In the case of the sutures, the higher the stress, the more rigid the sutures will have to be.

2.4.3 Hooks

Currently, many material testing machines, such as the one developed by Instron [42] (Figure 17 and 18), utilize hooks to attach the sample to the testing device.

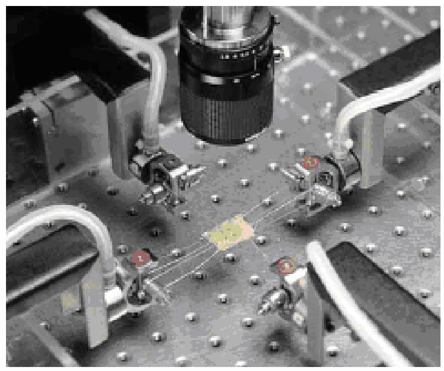

Figure 17. Instron's Planar Biaxial Test System: Hooks and Sutures [42]
Samples placed in and removed from the device quickly and easily

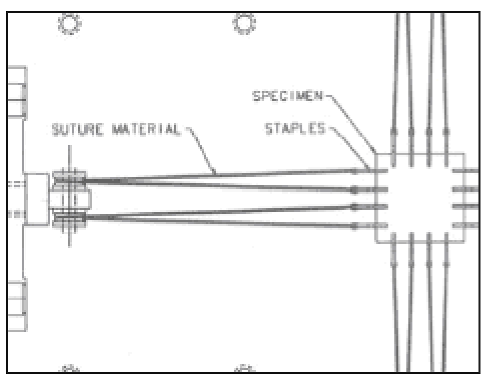

Figure 18. Schematic of Instron's Pulley System and Sutures [42]
Hooks with sutures provide efficient mounting system

Using hooks are ideal for most devices because there is less damage when attaching the sample to the device. The deformation will only occur at the point of the attachments.

2.5 *Test Chambers*

Many samples go through mechanical tests without requiring special considerations. However, because it is necessary to have a "natural" environment for the samples, there are two main factors to keep in mind when handling the samples: temperature and saline solution.

2.5.1 Temperature

The temperature has an effect on the mechanical properties of the sample [19]. Heat can change the composition of the sample by causing it to increase in stiffness or become more flexible. For example, drastic chemical changes can occur when the temperature is elevated for a collagen, which alters the physical properties [14]. This solution may achieve different desired temperatures by using foil heaters or a thermocouple to maintain the temperature.

2.5.2 Saline

For the many connective tissues, it is necessary to submerged them in saline solution throughout the experiment (before putting it on the machine until after the testing is completed). However, the solution may cause the tissue sample to swell. For example, Lanir and Fung [19] observed swelling in his samples within 3-4 hours of being in the saline.

In the past methods:

- the sample was immersed 10-15 mm below the saline surface [14]

- DMEM solution has been used with HEPES to have the pH value of 7.2 (which is near human pH value) [15]
- Lanir and Fung [19] kept the solution at pH 7.4. The test chamber is unique.
- Nielsen, Hunter, and Smaill. [28] used a roller pump to circulate the saline solution throughout the experiment. The temperature ranged from 4 degrees to 40 degrees C.

These examples show that it is a crucial aspect to keep the samples near its native state (pH value of 7.4, human body temperature) and also to use the proper physiological solution.

2.6 *Actuators and Motors*

An objective stated for this project was to enable the device to stretch the samples automatically. In order to achieve this, there needs to be a component that will drive the device.

2.6.1 DC motor

This is one of the most primitive methods of converting electrical energy into rotational mechanical energy. The armature of the motor rotates when a current input signals the motor. These motors are relatively cheap, and very simple to operate.

With this simple mechanism, controls are limited to on, off, and variable velocity. Removal of the current input is necessary to stop the motor. Even though the power source may be off, current does not have the ability to stop instantly, which causes the armature to slow down before stopping. Even if the time is very short, a small moving current may move the armature a few degrees. The reasons described above show that a DC motor is not a good positioning device.

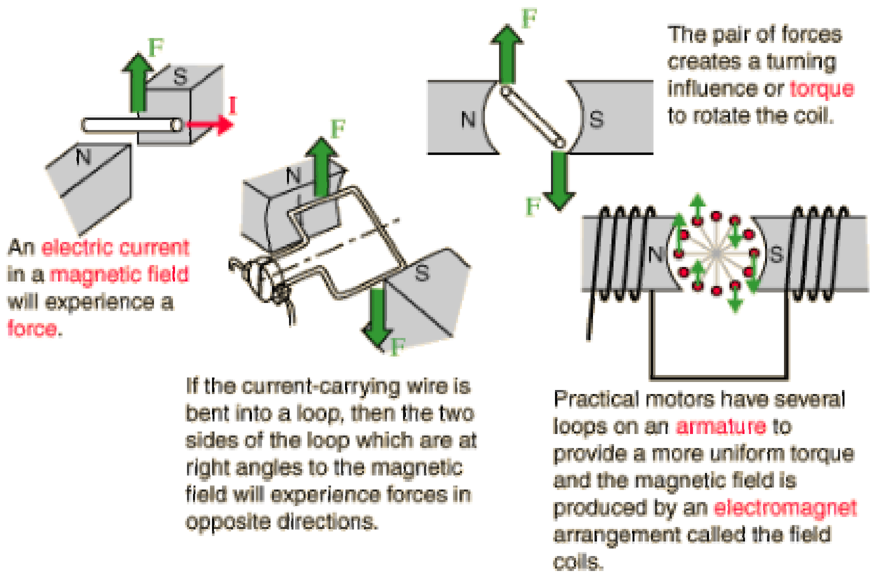

Figure 19. Explanation of How DC Motor Functions [43]
Constant current input makes the motor produce a constant rotational output, a changing current input changes the rotational velocity

2.6.2 DC Stepper Motor

This is a DC motor with more than one electromagnetic pole but has a rotating arm of a stepper motor with a constant north or south pole. The outer poles charge from on and off. Stepper motors are simple rugged devices that are low in cost, high in reliability, and easy to operate. They have high torque at low speeds, however, the torque decreases at higher speeds [44]. Stepper motors are able to rotate continuously, however it rotates in steps. It must briefly stop at each step before moving onto the next step. It does not have the smooth velocity a regular DC motor would have.

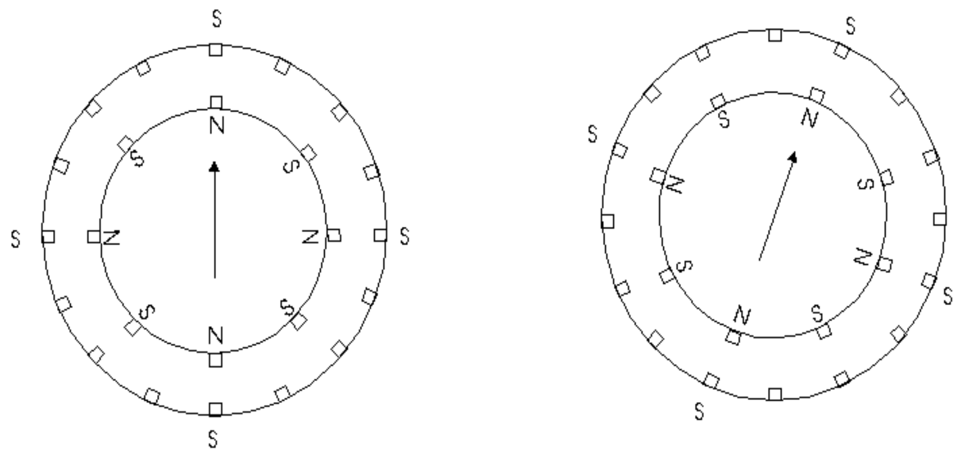

Figure 20. Diagram of Stepper Motor [45]
Left: a stepper motor held at an initial rotation Charged poles at the top, bottom, left, and right are south poles.
Right: the poles in the outer ring does not charged anymore while the new poles (in counter clockwise to the previous poles) are charged.
To rotate the arm, charge the poles to one pole clockwise or counter clockwise to the previous pole. The more divisions and number of poles there are, the more steps the motor is able to have, which makes it possible to have micro stepping.

2.6.3 DC Servo Motor

Servo motors are DC motors (with high torque) while being able to position accurately. This is possibly because servo motors are closed-loop systems while stepper motors are open-looped systems. When the controller gives a signal to the stepper motor, it assumes that the motor has moved a certain distance. On the other hand, servo motor need to know that it has moved that distance. There are encoders built in the back of servo motors, which tell the controller the exact number of revolutions and position of the rotating arm. Because of this feature, servo motors are extremely costly. One could place an encoder feedback at the end of a stepper motor, but it does not have high torque as the servos do [46].

2.6.4 Pneumatic/Hydraulic Motor

Compressed air or fluid drives the pneumatic/hydraulic motors to run instead of a current input. A piston chamber resides within the motor, where there are two pathways for fluid to enter. Since the armature of this motor moves in a linear manner, conversion from a circular output to a linear output is not needed. However, the armature needs some sort of fluidic input, usually compressed gas, to power the movement. .

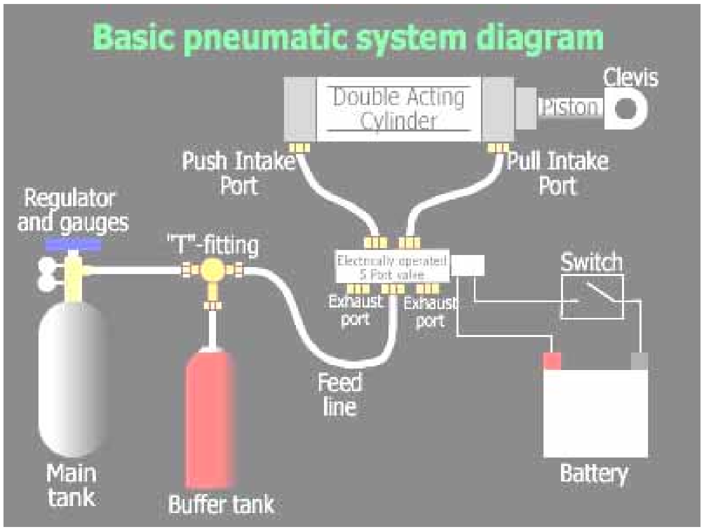

Figure 21. Typical Setup for a Basic Pneumatic System [47]
An installation of a network of tubing and controller for airflow is necessary, one pathway pushes the piston out while bringing the other piston in

2.6.5 Linear Actuators

Linear actuators are basically stepper motors attached to a threaded slider mechanism. A belt or gear (depending if a higher velocity or torque is required) connects the stepper motor and threaded slider. The cost of this system may be more expensive than by purchasing the two components individually. Versatility of a package system may also be lower than a custom system.

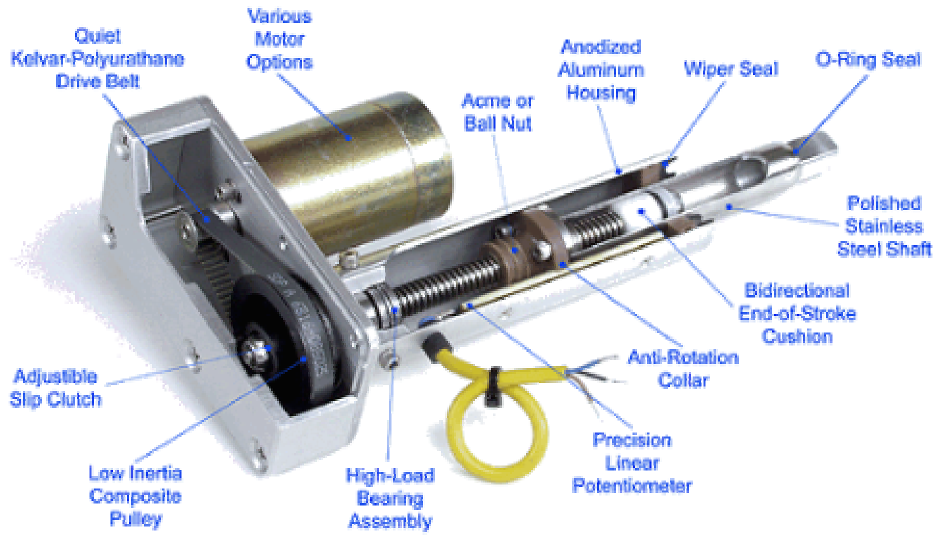

Figure 22. Internal View of Linear Actuator [48]
Linear actuators are prepackaged component (has motor and slider mechanism) guaranteeing to be compatible with one another

2.7 Motion Controllers

Once selecting the motors, then it is easy to decide on a motion control system. This closed-loop motion control system involves the motion controller board and the amplifier/motor drive along with feedback devices, the motor drive and amplifier is the same item.) As there are movements, there are feedback devices like position sensors. The sensors provide information back to the controller, where the controller can tell what position and velocity the motor is operating. Figure 23 explains the flow of motion control.

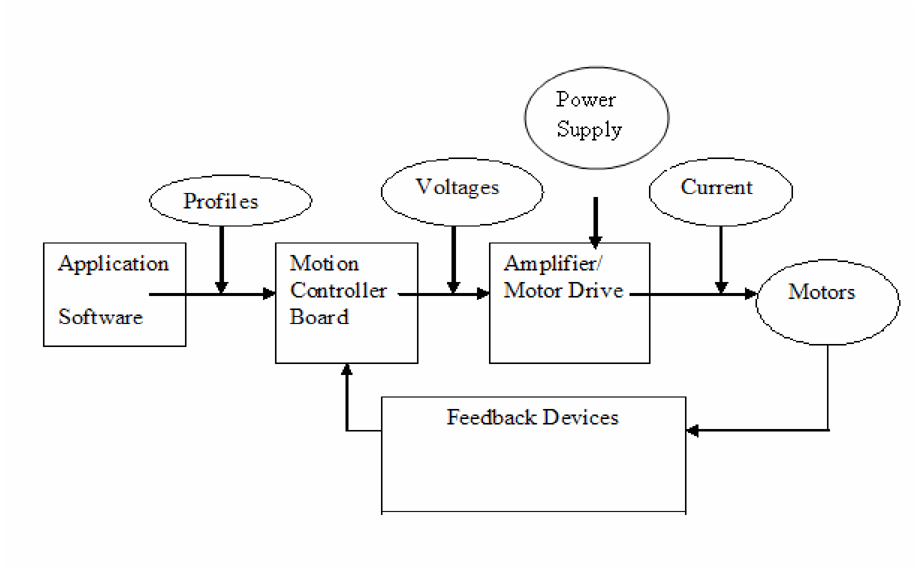

Figure 23. Schematic of Motion Control [48]
User can control various motion commands for motors to perform,
motion controller sends the commands to motor drives as (+/-) 10 voltage step signals,
signal converts to current, which the motors can read
motor converts current to torque and produces motion,
feedback devices provide information back to controller

2.7.1 Motion Controller Board

The motion controller board takes the motion profiles and calculates the trajectories (by using target position, velocity, and acceleration) so the motor will have the right amount of torque needed to cause motion. Having this controller board will prevent other interference (as if loading up another program will not delay or stop the motors from working). The controllers also get feedback from position sensors, which ensure reliability, determinism, and stability of the system.

2.7.2 Amplifier/Motor Drive

e all the signals are converted, then flows to the amplifier/motor drive as voltages. The type of motor drive must match the motor type (i.e. if stepper motors are used, then a stepper motor drive is necessary). Another important factor to look into is the current supply. If the current is too much for the motors to handle, then it will most likely damage the motors. If the current is too little, then the motors will not run and work at the speed it is capable of because it will not have the full amount of torque.

2.7.3 Feedback Device

Various types of devices to stop the motor from continuing the motion:

1. **Limit Switch:** The purpose of this device is to signal the end of travel or to prevent the motor from exceeding the necessary distance. Without a limit switch, the motor will reach the farthest position and the motor will continue to run, damaging it. With the limit switch, the motor would reach the limit switch, signaling the controller to stop running the motor and bring it to a complete halt. Disabling the limit switch will allow the motors to run.
2. **Home Switch:** This allows the user to set the limit for the positioning of the motor after reaching this point. The user can set the encoders to the value of zero or to any arbitrary number. If the motor hits the limit switch before the motor switch, the motor will reverse its direction until it reaches a home switch or another limit switch.
3. **Index:** This component produces a signal for every revolution that motor makes.

2.7.4 Data Output: Proportional-Integral-Derivative (PID)

It is significant for our system to have a continuous flow of data output because it is necessary to see the continuous movement of the soft tissue sample at a constant rate. The proportional-integral-derivative (PID) controls the output at a set level (determined by the user) even when the continuous parameters are wavering over/below the set level.

The PID also changes the process level from one point to another, instantly and accurately. There are three components for the PID control.

1. **Proportional Control**: (Ratio Control) Adjusts the difference between the set level and the current level, therefore the correction is in proportion with the measure of error.
2. **Integral Control:** (Reset Control) Returns the process back to the original set point by detecting the difference between the error and the set level and the amount of time the error continued.
3. **Derivative Control:** (Rate Control) The corrective signal to fix the current point to the set point is dependent on the rate of change of the signal.

For a closed-feedback loop, this is a typical PID function.

An example of a basic control theory (Figure 24 – Figure 30 taken from National Instruments [49]), the controller is a dial, which is set for the position point (in degrees).

If the dial were set from 0 ° to 108° in 3 seconds, then ideally, the user would like an instantaneous response to the controller like in Figure 24.

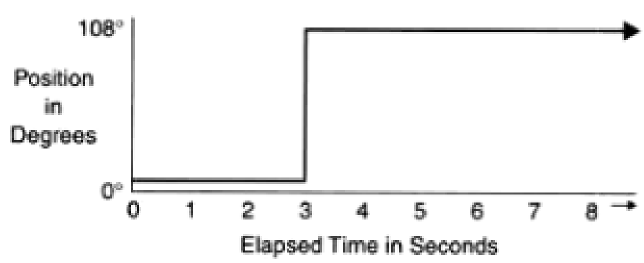

Figure 24. Ideal Position Curve [49]

However, this will not happen. More realistically, there would be a linear increase up to 108 °, which is seen in Figure 25.

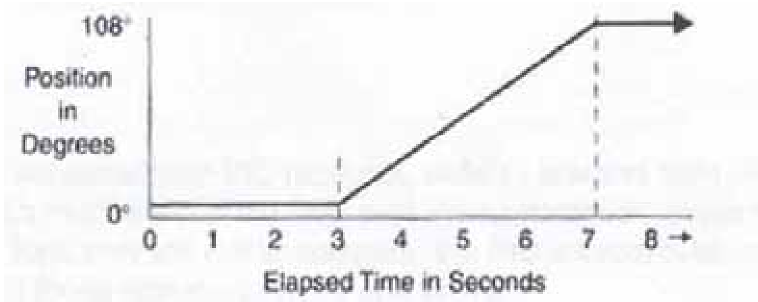

Figure 25. Realistic Curve
Takes longer to reach desired position

Figure 26 shows the curves undershooting or overshooting the desired mark.

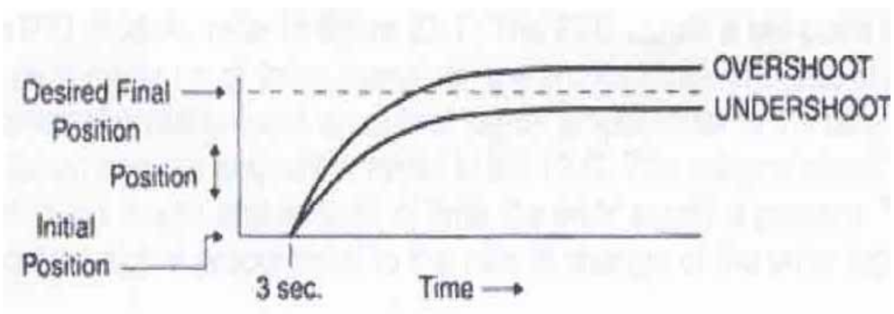

Figure 26. Overshooting/Undershooting Curves
Overshooting: the amount of signal exceeds the set level when shifting from one voltage to another
Undershooting: ratio of signal that fluctuates between two set levels (amplitude usually lies below the desired position)

The next figure shows an oscillation waveform (underdamped)

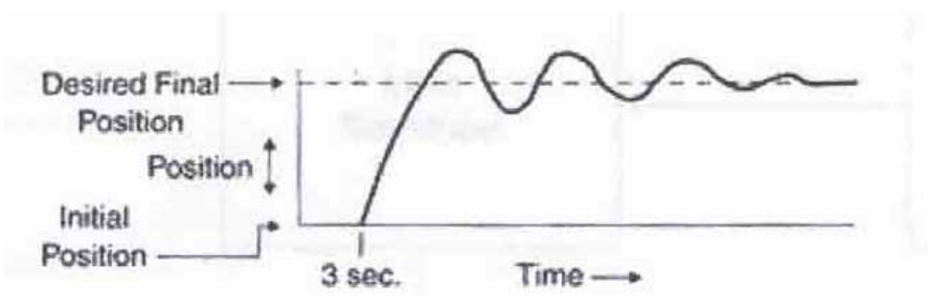

Figure 27. Oscillation (Underdamped) Curve
Takes a few seconds before it stabilizes in its proper position.

Another type of curve is a damped response.

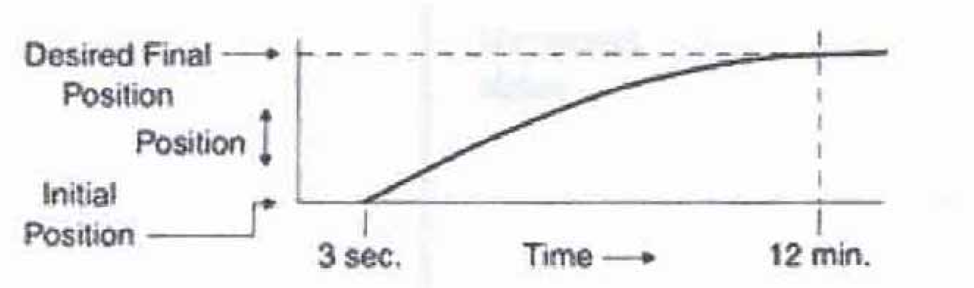

Figure 28. Overdamped Response
Curve is an exponential curve but takes
longer amount of time to reach the final position

The last type of curve is a constant oscillation curve at the desired position.

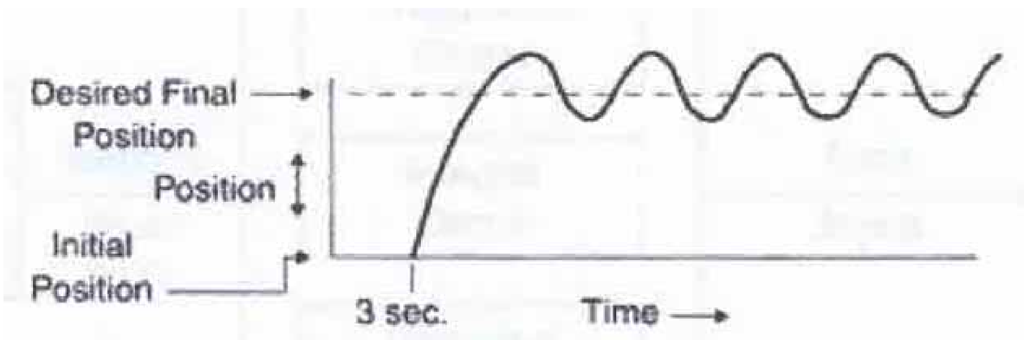

Figure 29. Constant Oscillation Curve

These five curves are not ideal, especially if accuracy and swiftness are necessary.

The most realistic response to get from a PID control is the figure below.

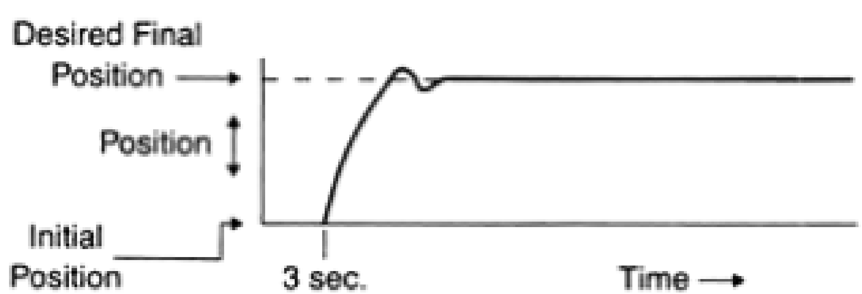

Figure 30. Optimal Response from PID Control

2.8 *Mechanisms for Linear Movement*

Not all of the motors listed previously provide linear movement. Certain DC motors do come in a linear form; however, their strokes are limited by the size of the motor. The most common method of transforming rotational force from a motor to a linear force is to put it through a mechanical slider. These slider mechanisms typically allow the movement in one axis while keeping the other two axes and rotation still. Low friction types have bearings within the slide. Unlike actuators, which extend out from their resting position, slide rails supports on either left or right side, and a platform is what moves along the axis. Because of this, rails are capable of handling a much higher perpendicular torque than linear actuators.

Some common types include screw drive, ball screw drive, belt drive, and chain drive. Belt and chain driven drives are simple mechanical devices where the belt/chain attaches directly to the motor shaft and the slide block. The motor shaft is perpendicular to the motion of the slide block. On a ball screw drive, the motor shaft is parallel to the motion of the rail block, which attaches to a threaded rail. This will rotate when the motor rotates. Depending on the pitch, one revolution of the motor may be one sixteenth of an inch to one-quarter inch. Screw rails are capable of moving at much smaller intervals, however do not have as high of a velocity and acceleration as belt or chain drives. Left and right hand threads are available along with different pitch angles.

2.9 Force Measurement

Since stress is the measure of force over area, there needs to be a device to measure the force produced by the actuating mechanism. Knowing that we must ultimately achieve linear motion and that many motors produce a rotational force, linear force transducers and torque transducers are ideal. Such transducers are available in a variety of different sizes and ranges. Some work in tension, others work in compression, and some work in both tension and compression. The most common connection these transducers have is threaded males inputs. The output is usually a signal output, which connects to an electronic device.

There are two features to consider for the transducers. It is possible to place an overload stop in the transducer, allowing the transducer to work in a certain range. Once the load has peaked, a mechanical stop in the transducer prevents it from taking any more loads. It is an option designed to prevent excess load from breaking the transducer. The design of the apparatus determines the placement of the transducer. There are submergible load cells that have the capability to function when submerged in solution.

2.10 *Displacement Measurement*

In order to measure the displacement of the tissue samples during loading, video cameras are necessary to perform non-contact image analysis. Out on the market, there are many different types with a variety use of applications. The four major distinctions between cameras are color, signal, signal format, and cost. There are advantages and disadvantages for each of the options within these classes.

2.10.1 Video Display

Video cameras come in two types of display: color and monochrome. Color cameras provide greater versatility in image display. Depending on the application, color detail may be necessary. Monochrome is a black and white display of the image captured. Although color detail is absent, for applications which do not require color, monochrome is usually the preferred option. The advantages of monochrome over color include approximately 10% higher resolution than single-chip color cameras. In addition, monochrome cameras have a better signal-to-noise ratio, increased light sensitivity, and greater contrast. Monochrome cameras are also typically cheaper than equivalent color cameras.

2.10.2 Signal

Color and monochrome video cameras both are available in analog and digital signal outputs. The main advantage to an analog signal is that it is usually lower in cost than a digital signal camera. However, if high performance is more important than cost, a digital signal is usually the best option. Digital signal cameras typically have higher resolutions, higher frame rates, less noise, and more features. A disadvantage to digital cameras is they are very costly.

2.10.3 Signal Format

Analog and digital signals are available in a variety of signal formats. The most common analog signal formats are NTSC (color signals) and EIA (monochrome signals) composite formats. Other formats include Y-C s-video, and RGB (red-green-blue) formats. Both Y-C and RGB split color information into separate channels, which results in superior image quality. Types of digital signals include Cameralink, IEEE-1394 firewire, RS-422, and RS-644. Cameralink and IEEE-1394 are the most common formats. Digital signals require a computer interface to display the images on a monitor. An advantage to IEEE-1394 cameras is that it is possible to connect the cameras directly to the computer with a firewire interface using a single cable. Cameralink cameras require a separate acquisition card for connection to a computer interface [30].

2.11 *Computer Control*

In order for the device to run, as well as manipulate the forces and linear motion, a computer control system is essential. This system will not only control the device during the stretching of the tissue samples but it will also calculate the stress and strain of the samples. The computer control system will need to graph all of the acquired data as well as display the images taken by the camera.

LabVIEW is a general visual language, which is made up of two main components. The first is the front panel, which is the user interface. This display consists of various inputs controlled by the user and outputs that display data. The second is the block diagram, which contains the written code. This displays various component icons through which data flow is wired. The front panel and the block diagram are interconnected and relay information between each other. Together the two components form an easy to use control program.

3 Design Approach

There are two common types of biaxial testing performed on elastic type materials: the linear stretch test and the inflation test. Since the inflation test displaces samples in the z direction, a camera needs to be parallel to the x-y plane. A second camera (placed either perpendicular to the sample or at some offset angle) is required to record the sample's initial properties.

The linear stretch test stretches the sample along the x-y plane. The sample, in theory, remains on the two-dimensional plane; therefore, a second camera is not needed. Both types of biaxial testing involve very different approaches and requirements, and based on the allotted resources, it would have been unreasonable to pursue both. Inflation testing lacks the versatility of a planar test and the sample's size and range are dependent on the size of the nozzle and pressure. In addition, the client has an inflation device; therefore, the team focused on designing a planar biaxial testing device.

When designing this device, we needed to keep in mind the client's needs and the physical constraints to building this device.

- Client's Need
    - Low cost - budget of $10,000
    - Small and compact- to fit on a laboratory bench
    - Able to read low forces- samples are compliant and fragile, so it can only withstand small loads before it reaches its fatigue strength and begins to tear
    - Real-time data output

- Physical Constraints
    - Biocompatibility- device must not react with the biological tissue samples and the physiological solution
    - Non-contact displacement analyzer- needed to take the measurements without touching the sample

These constraints were determined by using the objective tree (Appendix B) and the pairwise comparison chart (Appendix C).

3.1 Design Iteration #1 – Two Motor Design

The basis of this design was to reduce the number of components and controls needed to operate the device. Before any cost analysis began, designs were based upon user friendliness and low cost. There were three major areas to look at: movement, force feedback, and displacement feedback.

In a uniaxial test, one end of the sample is stationary while the other end moves. A biaxial setup puts two of these together, which links both axes to one driving source. However, this did not fit within the specifications of versatility because each axis would loose the ability to have independent driving forces. A simple solution to this problem was to use two driving mechanisms. Figure 31 shows a typical sample shape.

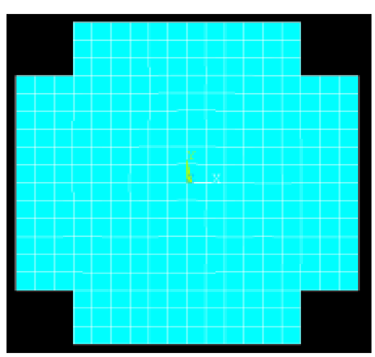

Figure 31. Shape of Typical Sample

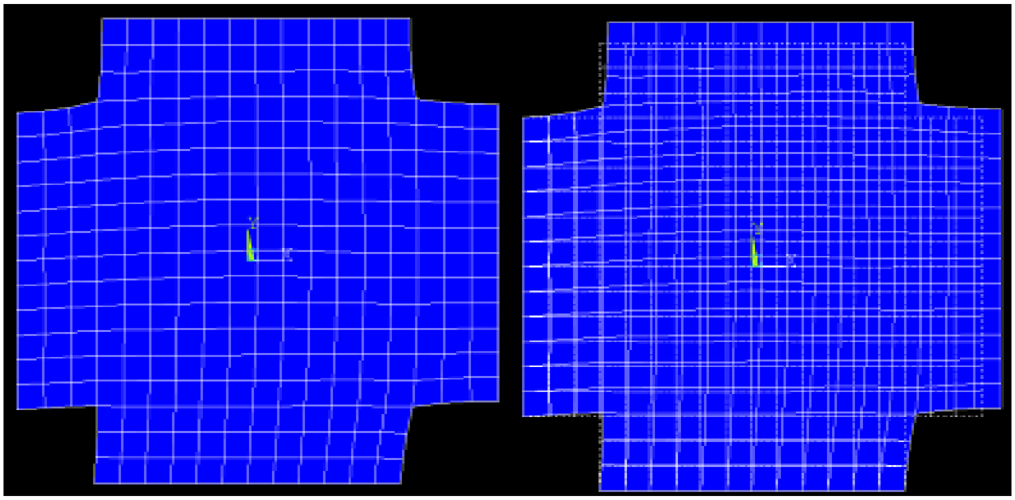

Figure 32. Deformation when Edges are Fixed
Left: Shows the deformation when the – x and –y sides are fixed, while the load is applied to the other two sides.
Right: Undeformed shape superimposed on the deformed shape.

The center of the sample changes between the start of a test to the end. It would be more advantageous to keep the center of the sample at one location like in Figure 33.

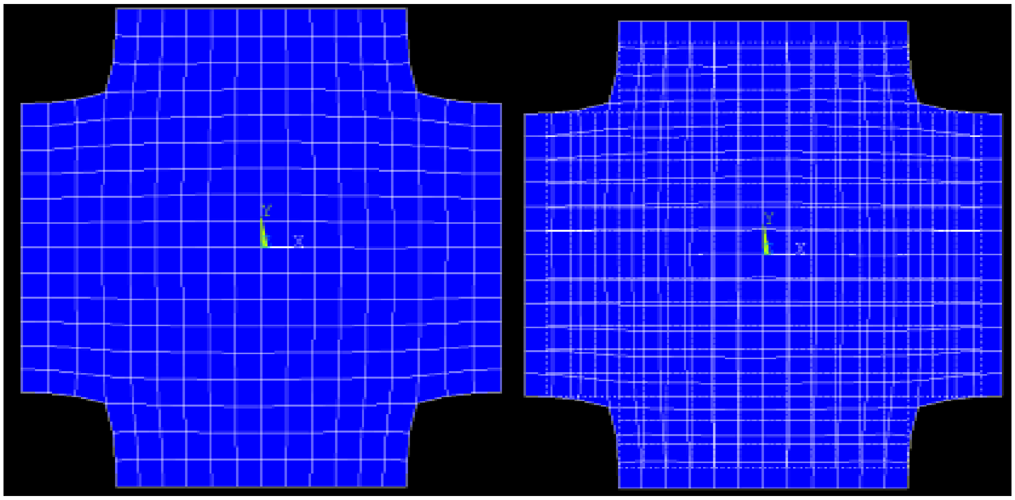

Figure 33. Deformed Samples with Equal Loading
Left: Example of a deformed sample with equal loads applies in all four directions. (Note the center of the sample is stationary)
Right: Undeformed shape superimposed on the deformed shape.

Rather than directly connecting the driving mechanism to one direction, the mechanism connects to both the positive and negative directions. Because there is no need to pull one axis unevenly in each direction, one mechanism can pull a certain amount in the +/- x direction and the +/- y direction with the same amount of force. There are manual adjustments on the device to enable proper tension and centering of the sample.

One way to achieve synchronous movement in two directions is with a threaded guide rail attached to a rotational motor or duel rod linear actuators (Figure 34). These blocks attach to the arms that extend over the bath and into the solution where sutures and hooks grip the sample. The arms from each rail would never collide with one another. There is plenty of room for a mounting system for the camera; however, the arms coming off the rails are extremely intricate.

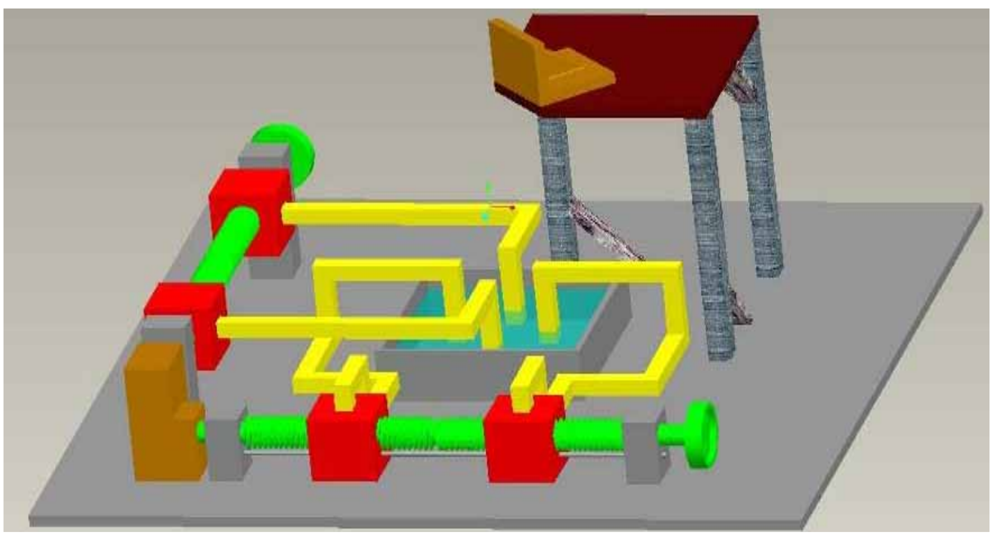

Figure 34. Conceptual Design of a Possible Two-Motor Design
Motor spins in one direction: guide rail blocks move apart.
Vice versa if the motor spins in opposite direction.

There were only two types of transducers suitable for this design: linear force transducers and torque transducers. It was possible to place linear force transducers in the saline solution between the sutures and the arm connecting to the rail. A torque transducer would need to hang over the saline bath, supported by the rail block with a lever arm that dips into the solution.

Finally, any non-contact displacement sensor would also work. A camera, for example, mounted over the sample could work, provided there is enough lighting. There was room between each drive mechanism on the base plate because we planned for supports to be built for the overhead camera table. The overhead table would hold the camera, which would reside directly over the sample.

3.1.1 Pros and Cons

This design was appealing because of the fact that there were fewer parts than other systems. Rather than having four control variables, there are only two: one for each axis. This resulted in having a compact design, which met the client's need. However, the hand cranked centering device was not as accurate as a computer-controlled jogging system. It was also difficult to reach into the device to adjust the sample's centroid location with components in the way. The cost of machining special arms that would properly fit would most likely outweigh the advantage of fewer necessary movement mechanisms.

3.1.2 Pass or Fail

Due to the complexity of the parts, this design failed to meet our needs and our client's. Parts may overlap one another or become in the way of the camera. As simple as the theory may sound, it would most likely be more difficult for the team as well as the client to use the device.

3.2 Design Iteration #2 – Four Axes Design

Our next design involved four axes of motion instead of two. Each axis contained one motor, one linear actuator, one transducer, and one machined metal arm, which connected to the specimen (Figure 35).

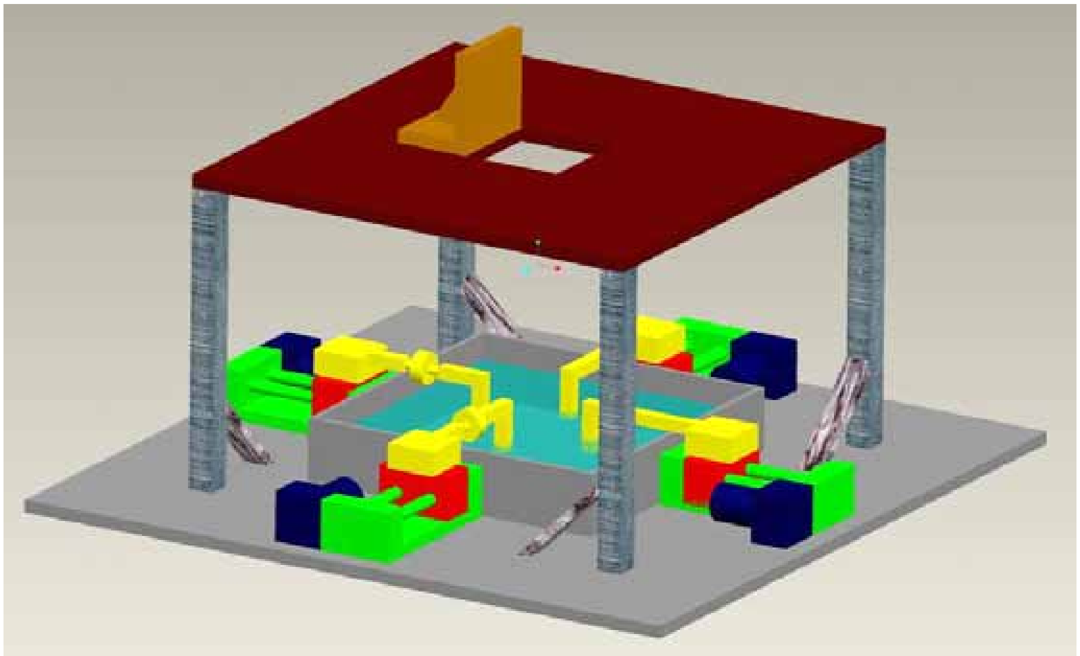

Figure 35. Conceptual Drawing of a Four-Motor System
One motor on each side of sample for more control
on each axis and can have versatility

Each actuator has an extension arm that protrudes and contracts along its axis. Then each actuator arm is attached to a machined connecting arm, which extends over the outer wall of the bath and downward into the bath. A wire and hook system will then connect from the end of the connecting arm to the specimen through a suture. As the motor drives the actuator to contract its arm, the connecting arm and hooks will stretch the specimen.

The square-shaped bath (2.5 cm x 2.5 cm) contains a saline solution, which the specimen floats in. The bath is removable and most likely will be made of hard plastic to avoid corrosion. Outside each of the four corners of the bath is a metal cylinder. On top of the metal rods is a metal tabletop. This table holds the camera directly above the specimen.

Advantage to the four axes design:

- More control of each individual axis
- Easier to center the specimen before testing- actuators adjust to center the sample for the camera
- Versatility- certain actuators can be stationary while an individual axis stretched the specimen
- Stationary overhead camera-
    - In the two axes design, centering the sample is not possible because the two opposite arms can only move outward or inward together. Therefore, to trace the markings, the overhead camera would need to move in the horizontal plane, in addition to the z-axis. This is not necessary for the four axes design.
- Less complicated design and less machining required – only requires four identical, short arms.

Disadvantages of four axes design:

- Individual control of each axis- requires separate motor, actuator, and transducer.
    - Results in high costs

- Larger in total size- having four motors, actuators, transducers, and machined arms makes the design larger. This does not meet our advisor's constraint for small space.

After looking into the initial four axes design, some problems were realized which needed to be changed. The first mistake that we found was in the maximum distance that each arm would have to stretch. Initially, we assumed that it would have to travel approximately 3 inches to stretch the tissue samples sufficiently. By taking the minimum size sample of 10 mm, and the maximum size sample of 30 mm, we can determine the correct distance of motion needed. Assuming a maximum stretching of 200%, we obtain a total distance of 80 mm of stretching by the sample and 40 mm of displacement by each arm. Results can be shown in the below equation.

MathCAD equation:
KNOWN VALUES:
Maximum initial specimen length ($L_{i(max)}$): 30 mm
Mininum initial specimen length ($L_{i(min)}$): 10 mm
Maximum strain (ε_{max}): 200%
Number or arms per axis (APA): 2

UNKNOWN VALUES:
Maximum distance of stretch (D_{max}) = ?
Maximum distance of movement (S_{max}) = ?
Distance of movement for each arm (D_{arm}) = ?

$(L_{i(max)} + (L_{i(max)} * \varepsilon_{max})) = 90$ mm $\rightarrow$ maximum distance of stretch (D_{max})
$D_{max} - L_{i(min)} = 80$ mm $\rightarrow$ maximum distance of movement (S_{max})
$S_{max}/APA = 40$ mm/arm (~1.6 inches) $\rightarrow$ distance of movement for each arm (D_{arm})

Therefore, the distance of movement for each arm became 2.5 inches each to be safe.

We also realized that the size of our bath was not large enough. When the actuators fully contract, the machined arm will collide into the inner wall of the bath. Therefore, the dimension of the bath increased to avoid this problem. Another length problem was that we had estimated the motor length incorrectly. The initial length of 2 inches was incorrect and so the new length is approximately 3 inches.

A major change in the four axes design came when we chose different linear actuators and rotational torque transducers. Instead of a linear actuator with an extending arm, we chose a rail system actuator for this design. Due to the rail system, machining is necessary for the connecting arm to extend up and over the actuator end and outward over the bath wall.

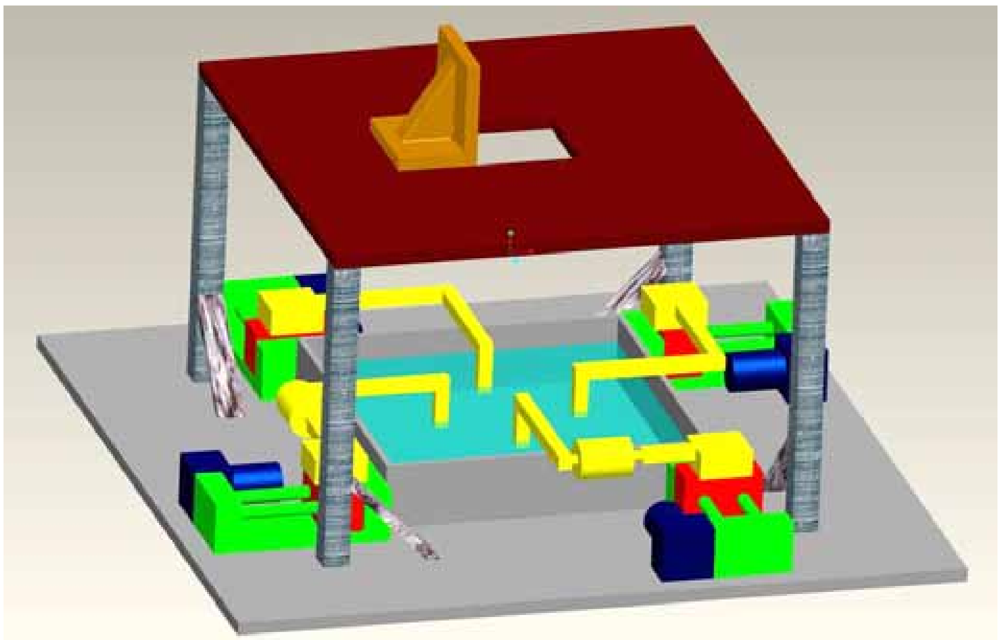

Figure 36. Different Setup of Connecting Arm to Torque Transducer
Connect each transducer to vertical stainless steel rod that extends downward into bath, then attaches to sample through a suture and hook system, rail and motors are offset to side to make room for torque tranducers

After listing both the advantages and disadvantages of the design, we chose iteration number two because the advantages outweighed the disadvantages when compared to our other iterations. Even though the four axes design was more expensive than the two axes design, the difference in total cost was tolerable. This was because we could build the four axes design while staying within our budget and provided much greater experimental versatility and control. The four axes design also provided a less complex design and required less machining. These factors all contributed in the design selection process, and choosing iteration #2 as the design.

3.3 Modifications to Four Axes Design

During the fabrication and assembly process, various components were changed. The basic concept of the device was not changed: it is still a planar biaxial device with four independent motion controls, two torque transducers and a camera. The reasons for component changes were that certain materials were easily accessible to us, and that time and cost considerations changed what we were able to use. Below is a CAD drawing of the modified design.

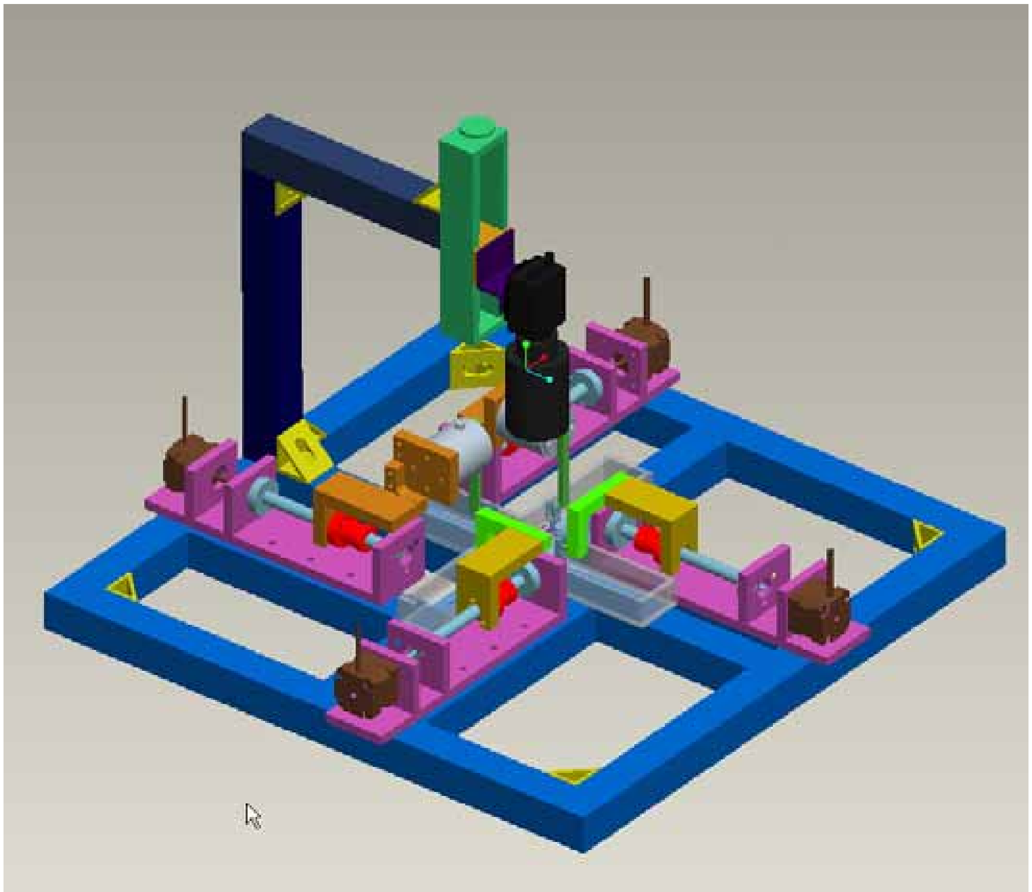

Figure 37. Conceptual Drawing of Final Design

The final layout is smaller than design #2. The most notable change is the use of extrusions over plating. They are lighter and require less fabrication time. This design was also created with draws for all components so that they may be machined properly.

3.4 Design for Heated Test Chamber

3.4.1 Purpose and Constraints

The test chamber is a critical component in the biaxial device. In this bath will be a tissue sample submerged in physiological solution, while a heating system maintains the temperature testing area at 37 ºC.

The problems presented in designing the test chamber were:

- It must be biocompatible, so whatever material we use cannot react negatively with the solution/tissue sample
- Maintaining constant human body temperature (the solution)
- Easy to clean and prepare for the experiments
- Design constraints for the test chamber (must be transparent to observe the tissue sample and must not reflect because of the camera).

A variety of design iterations were developed for the heated test chamber. The following three designs include a two chamber, inner and outer, bath. The two-chamber system would provide an encompassing heated solution around the inner bath. These methods were was not chosen for the final design for various reasons.

3.4.2 First Design: Fish Tank Heater

The first design involved a small separate 5-gallon tank, which would sit along side the device. A simple fish tank heater would be used to heat the water in the tank.

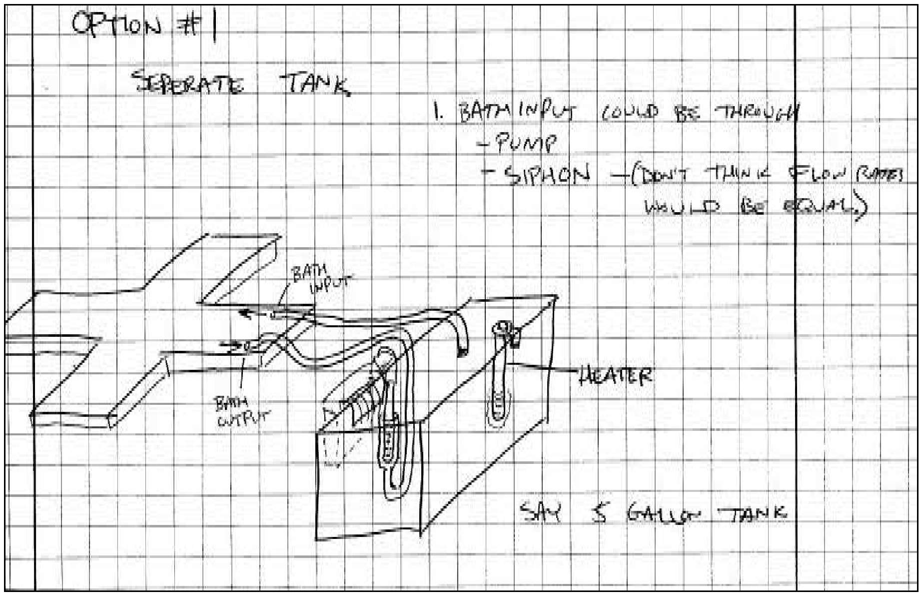

Figure 38. Fish Tank Heater Bath Design
Fish tank filter would suck water from bath through tube into tank, then siphon would displace the water through the tube back into bath

Advantages for this design include being low cost and easy to build. However, we did not select this design because of its various disadvantages. The filter and siphon system would provide flow rate discrepancies, which would produce circulation problems. Also, the fish tank-heater range was too low and would not heat the water up high enough to maintain body temperature of the saline solution.

3.4.3 Second Design: Exterior Pump

The second design did not utilize a separate tank, but instead used only an exterior pump. This small pump would be situated next to the device and connected to tubes running into the bath. Advantages included its good circulation and even flow rates. We also did not choose this design because a suitable heating system could not be found. Without the separate tank, there was no location for a heater to heat the water between the two chambers.

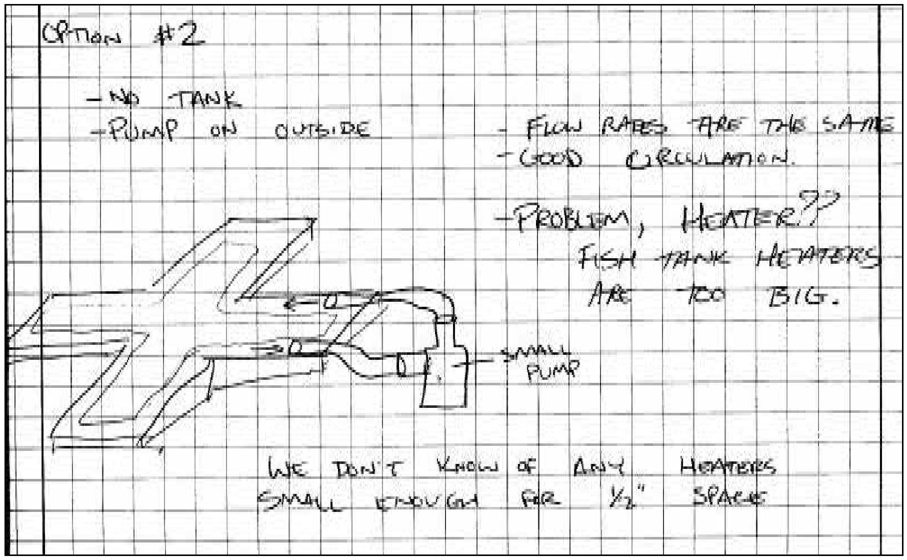

Figure 39. Exterior Pumps to Heat Bath
Uses a small pump to flow water through bath and provides good circulation,
flow rates are the same since there is no tank and the pump is on the outside.

3.4.4 Combination of the Two Previous Designs

The last two-chamber design was a combination of the first two designs. This included a separate 5-gallon tank situated next to the device.

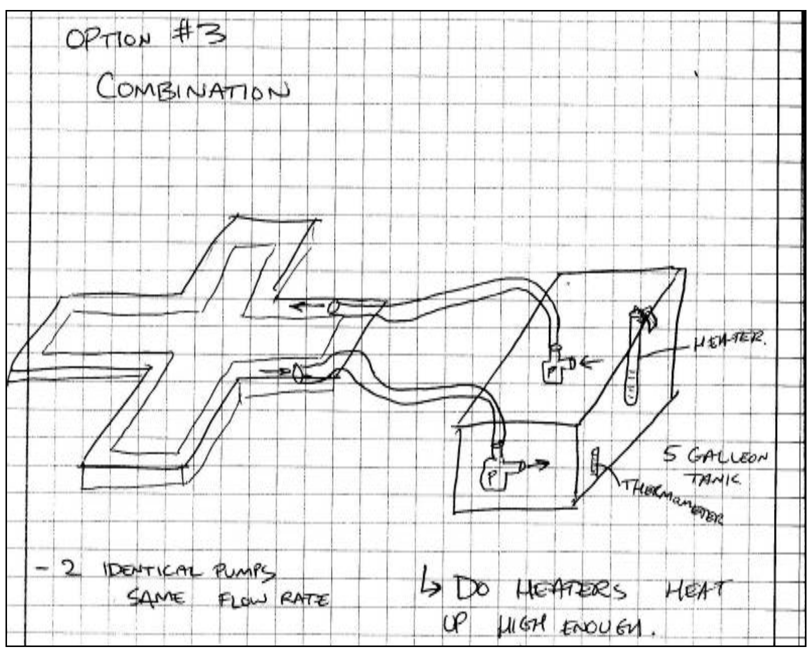

Figure 40. Combination of Previous Two Designs
One pump sucks water from bath into tank and the other pump would put
water back into bath, with identical flow rates,
small fish tank heater placed in tank to heat water

Advantages for this method include an even flow rate, good temperature control and low cost. Initially this design seemed promising, however the limited range of the fish tank heater proved detrimental. We did not choose this design because the circulating water would not be able to be heated high enough to maintain body temperature in the inner solution.

3.4.5 Third Design- Plexiglas®

Plexiglas® is an acrylic sheet that is transparent like glass, but stronger. This type of plastic is an ideal material because it is transparent, lightweight, non-reflective, rigid, biocompatible, and easy to acquire. However, it has a low thermal conductivity (0.18 W/mK). We began by creating a chamber with ¼ inch thick clear acrylic plastic. This however, created a problem with heat transfer, for it did not conduct heat very well. To solve this problem we looked at two possible solutions: either use a much thinner piece of acrylic, or find something with a higher thermal conductivity that will not react with the solution.

Going to the local plastic distributor, we were able to acquire a thin sheet of acrylic (about 0.0625 inch thick). With this acrylic sheet, the temperature we would need to set the heaters at will be 77 ºC.

*Please look at Appendix F-1 for the calculations for heat transfer.

3.4.6 Design #2 - Mylar

Because the temperature of the heaters needed to be 77 ºC, we decided to find another material that would require less amount of heat to get the physiological solution to 37 ºC. The one possible material is thermoplastic film called Mylar, which is made from ethylene glycol and dimenthyl terephthalate. The material properties of Mylar makes it an ideal product for the project because it is strong, clear, has high mechanical properties, can withstand the range of temperature we need, and is can be extremely thin (paper thickness) [52]. Even though the thermal conductivity is lower than the acrylic sheet, (0.155 W/mK), the thinness of the sheet (about 1mm) provides better heat conduction. However, it was hard to acquire a non-reflective Mylar because the company only sells it at bulk, raw form and would not provide a sample.

*Please look at Appendix F-2 for the calculations for heat transfer.

3.4.7 Final Solution

The acrylic bath was chosen because it was easily accessible, unlike the Mylar. Even though the temperature was higher than we would like, it will work well with the project.

The final design constituted of only one bath. The bottom most layer of the bath was a ¼ inch thick aluminum plate. Flexible Kaplon heating pads are attached to the bottom of the aluminum plate. The high conductivity of the aluminum distributes heat throughout the plate, which achieves even heating. On top of the aluminum plate, a thin sheet of acrylic was attached using a conductive resin. The sheet of acrylic was 1/16 of an inch thick, and was needed to maintain the biocompatibility of the bath. Acrylic with a thickness of ¼ inch was also used for the walls of the bath (Figure 41).

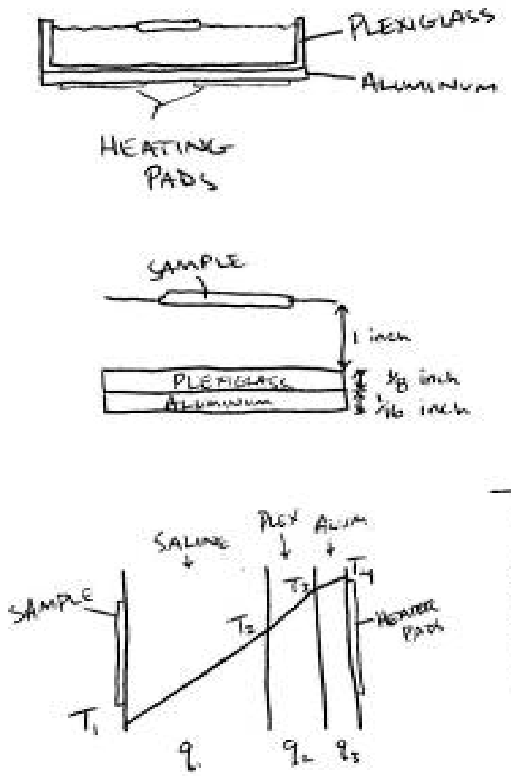

Figure 41. Levels of Bath Chamber
Heating pads below the aluminum heat the saline within the acrylic chamber to maintain a constant heat on the sample.

The increased thickness of the acrylic walls increased the insulation and reduced undesired heat loss. The heating pads are connected to an Omega temperature controller. A thermal couple is situated into the center of the saline solution and indicates the solution temperature to the controller. This controller can be set at any desired temperature and maintained at a constant level. The advantages of this design include its simplicity, absence of circulation or pumping, even heating, and superior temperature control. Figure 42 is a schematic of the final design chosen for the heated testing chamber.

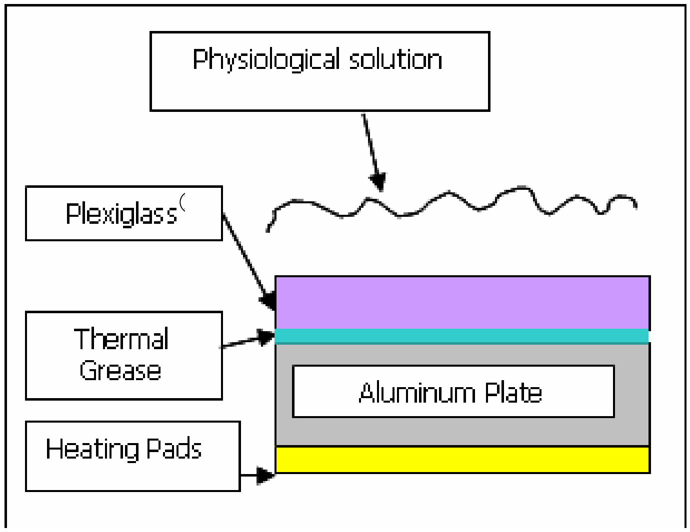

Figure 42. Layout of Test Chamber
The aluminum plate conducts the heat from the heating pads to the acrylic sheet. The thermal grease provides an interface with the bath so there are no air-pockets and with the aluminum plate the heat is distributed evenly to the entire bath.

3.5 Sample Attachment

Once the bath had been designed, a mechanism for attaching the sample to the device was needed. This section identifies the main components of sample attachment and various design iterations for attachment.

3.5.1 Using Rice Paper and Latex Samples

We decided on fishhooks and suture lines to hold the sample for our device. The fishhooks are small (#28) and the sutures are 5.0 silk or nylon material. The sutures were tied to the fishhooks by using a Clinch Knot (Appendix J).

Vietnamese spring roll rice paper was chosen to test on because of its low strength which is similar to cultured tissue. The rice paper was cut in 1" x 1" size and submerged in lukewarm tap water for thirty minutes. Then it was taken out and by using needle nose pliers, we were able to hook through the rice paper without causing deformation to the edges. Just for experimentation, only two hooks were applied in a uniaxial direction.

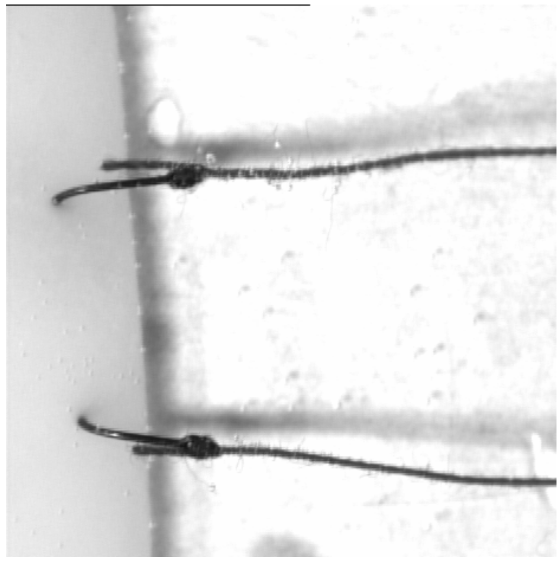

Figure 43. Rice Paper with Hooks
With a light background, this is the sample before any forces were applied.

However, the test failed because the hooks sliced right through the edges. Therefore, another way of hooking onto the sample was using a suture staple.

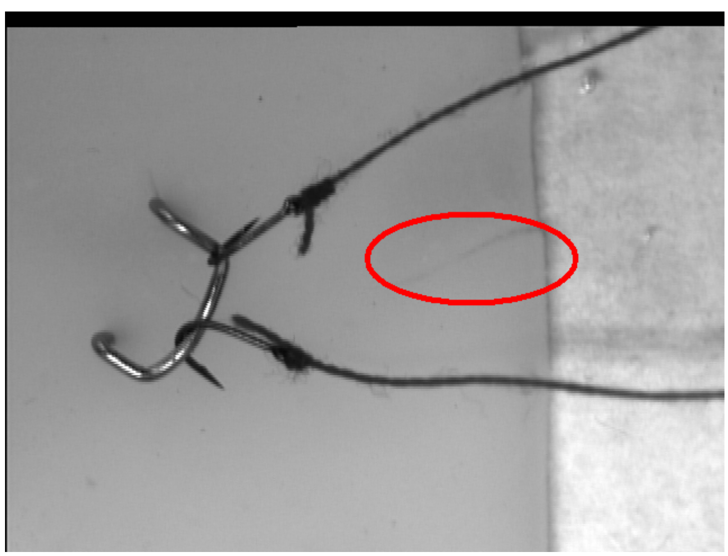

Figure 44. Suture Staple with Two Hooks
The circled area highlights where the hooks tore through
from the previous experiment.

So then, after having a hard time with the rice paper, we decided to use Latex. Latex is stronger than the rice paper; therefore, the hooks will not tear through the edges.

3.5.2 Graphite Markers

We acquired a graphite pencil from the local arts/craft store to mark on the rice paper and Latex samples.

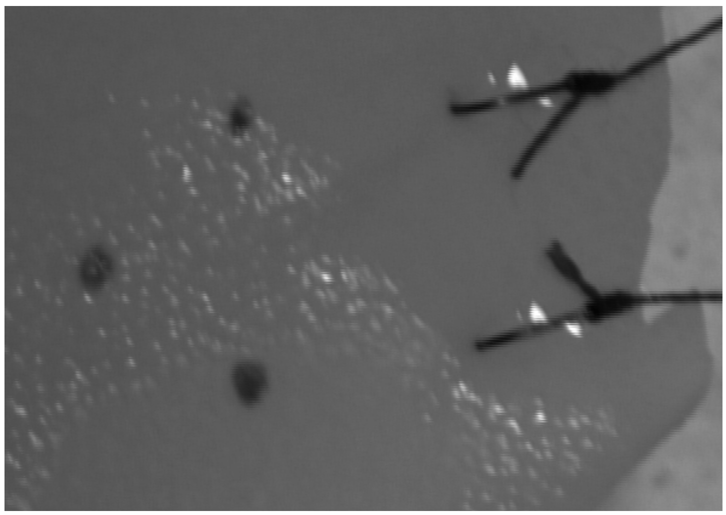

Figure 45. Latex Sample with Marking
The graphite marker marks very well on the Latex sample.

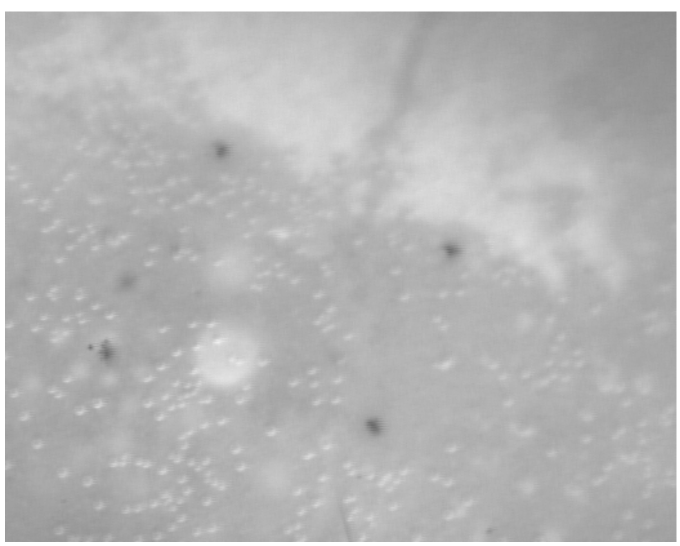

Figure 46. Rice Paper with Marking

The marking does not show up as well on the rice paper.

The solution to this problem is to use an actual graphite piece and gluing it onto the sample piece by using Krazy glue.

3.5.3 Applying Force onto the Latex Sample

Feeling confident about the strength of the Latex sample, we decided to pull the hooks and see how far it can stretch before deformation occurs at the edges.

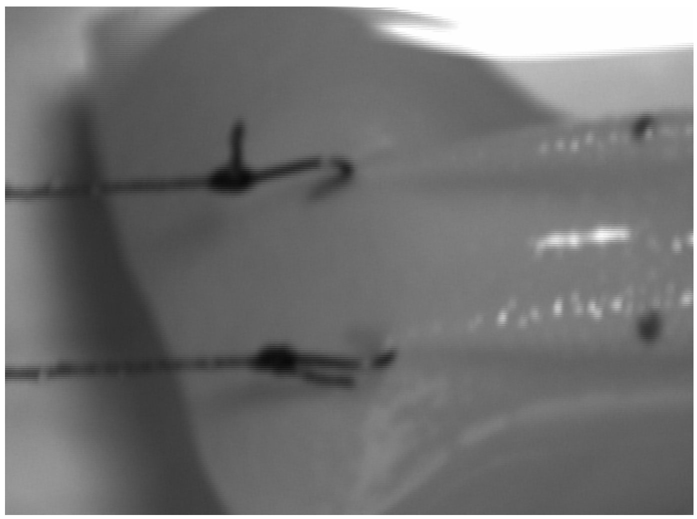

Figure 47. Slight Pull
This is a slight pull on the Latex sample.

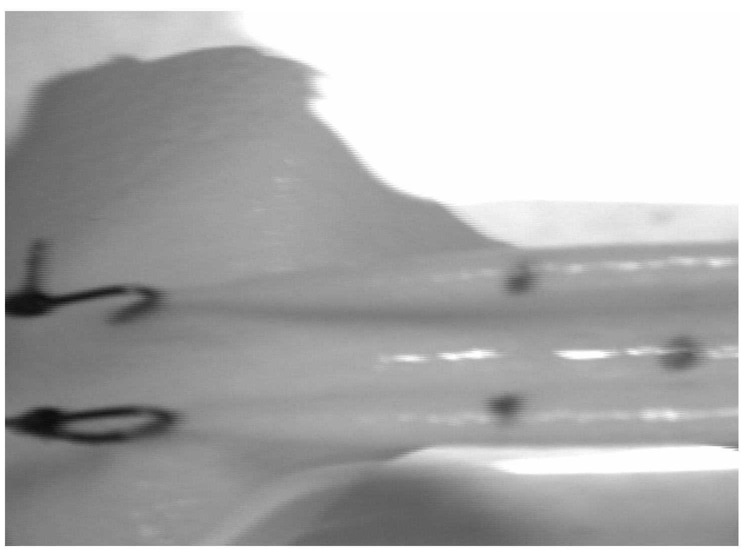

Figure 48. Stronger Pull

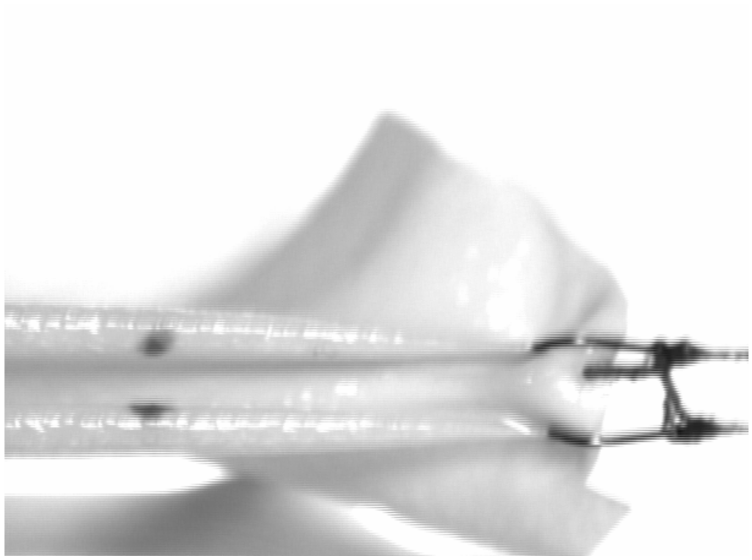

Figure 49. Maximum Pull

4 Methodology

4.1 Motion

4.1.1 Motors

Based on our design, the cheapest piece of equipment, which is adequate for the task, is a stepper motor   Stepper motors provide the proper controlled movements at the proper velocities. There is no need for an encoder feedback like one would find on a servo, because a camera takes care of that. DC motors are simple on/off motors, most widely used for constant velocity. Once the power is off, the armature still continues, which would not work for this application. Pneumatics and hydraulics were also ruled out because not only would there be a need for a fluidic supply, there needs to be a power supply, which controls the fluids going into the pistons.

The size of stepper motor needed for this device was size 17" or 23" stepper motors. US Digital Corporation sold size 23" stepper motors for $59, and Advanced Micro Systems size 17" stepper motor. Intelligent Motion Systems created their own line of stepper motors called MDrive. These stepper motors have encoders connected to the end of the motor, which provides a closed loop feedback. The video system captures the position feedback for this system, thus, those encoders are not required.

4.1.2 Controllers

After deciding to use stepper motors, our controller board must be compatible with these motors. Three different companies were concentrated on for our motion control system. Three important criteria we kept in mind when finding the right type of motion control for our system: 1. must be compatible with LabVIEW 2. compatible with stepper motors 3. Low-cost (under a $10,000 budget)

1. *National Instruments*:

This Texas based company was the first choice for motion controllers because it uses LabVIEW so there are no concerns whether or not our controller board would be compatible with the computer software. There were different categories for controllers:

a. *NI 7330 series (Low cost component)*: These devices are used for simple point-to-point applications and come in 2 or 4-axis stepper motor control board. They have Real-Time System Integration (RTSI), which allows smooth communication with the data acquisition board. The price ranges from $745 to $1045.

a. *NI 7340 Series (Mid Range Stepper/Servo Control)*: This device applies to control stepper and servomotors. It meets the high performance needs by the users, like contouring and electronic gearing. Since it involves more power, a third party motor drive is necessary. The price ranges from $895 to $2195.

b. *NI 7350 Series (High Performance Stepper/Servo Motion Control)*: This device can go up to eight axes and can configure to a stepper or servo control. It has all the added features like blended motion trajectory, hydraulic control, and 64 lines of digital I/O. These features however are more then we need. The price ranges from $1695 to $2595.

*Please look at Appendix D-1 for the features of each series

After comparing the features, we narrowed it down to the NI 7330 series because the other two series provided features that were not necessary for our system. Within the NI 7330 series, there were three different controller boards:

a. NI PCI-7332: This controller is for a two axes stepper controller, which we could not use because we needed a four axes controller.

b. NI PXI-7334: This is a four axes stepper controller; however, there is a trigger bus component in the computer, which is more than we needed. We needed the PCI card for our system.

c. NI PCI-7334: This was our choice for the motion controller because it is a four axes stepper controller and contains a PCI card. In addition, the price was reasonable ($945).

*Please see Appendix D-2 for detailed features of each controller.

Along with the controller board, we also needed a motor drive. The only motor drive that was compatible with the PCI 7334 was the MID-7604, 4 axis Integrated Stepper Driver Power Unit with the power of 115 V, which converts to 2 amps. The price for this motor drive was $1,975.50. Along with the cable needed to connect the components, the total price from National Instruments was $2,961.00. (This includes the educational discounts.)

2. *Precision MicroControl Corp*: Comparing the controllers to the NI PCI 7334 controller, the MFX PCI 1040 is very similar for features. It is compatible with LabVIEW; however, the price is too high. It cost $1,395.00 for the controller and there would need to be additional cable/wiring. In addition, this company did not provide motor drives, meaning we would have to search for other companies to provide the power. Therefore, we decided not to order the controllers from this company.

*Please see Appendix D-3 for features

3. *Galil Motion Control*: The DMC -1842 PCI bus was a similar controller to the NI PCI 7334. It uses a four axes system, which can have a combination of stepper/servo motors. Multitasking is possible with the maximum of eight programs at the same

time. There were also various modes of motion like point-to-point positioning, contouring, linear and circular interpolation, and electronic gearing. However, the additional features on the controllers are not necessary for our system and the price was a bit too high for our needs ($1,195.00). The motor drive needed for this controller was the AMP-19540 and cost about $795.00. The great thing about the Galil Motion Control system was there was no extra cabling needed, unlike the National Instruments.

Another type of controller from Galil that we researched was the DMC-2143, which connected to the computer by Ethernet; therefore, an IP address was necessary. Again, no extra cabling was required to connect the controller to the motor drive. If we had purchased the motion control system from Galil, we would have saved approximately $1,000.00. However, after talking to the application engineer from Galil, there were still some uncertainties about the products. He also mentioned that we would have had to provide our own power supply for the motor drive, and we would have had to build some kind of fixture with a DIN rail mount to secure it well or else it would stand-alone. This meant that more money was required to run this system. In comparison with the National Instrument system, it was not as advantageous as we initially thought.

*Please see Appendix D-4 for specs.

We chose to use the National Instruments' motion control system.

4.1.3 Rails

A screw-driven slide connects to the end of the motor to translate the rotational motion of the motor to linear motion. We chose a Kerk SRZ4005Tx6" rail because of its low cost and its customizing ability. Looking at the design and examples of working devices, a stroke size was calculated. Although the targeted samples may not require the full range of the rails, there may often be error, or other samples placed in the device. These rails are relatively cheap, and they work. Companies such as Thomson Industry produces linear rails, however they are plain slides without a method to drive them.

4.2 Force Measurement

4.2.1 Force Transducer

The first idea used was to make a linear force transducer compatible with the system, as it was the easiest to work with. Even after searching everywhere, we could not find a linear transducer that was less than 50 grams, nor one that was submergible. Transducers specialized for biomedical applications were hard to work with, as we designed each part for a specific task.

Rotational transducers however do have a low enough range and adjustable lever arm lengths. We selected a Futek TFF-400 20 oz-in. rotational transducer with overload protection. Calculations in Appendix E demonstrate how we chose the range of the transducer.

4.2.2 Signal Conditioning/Filter

During the search for a controller board and a filtering system, the most important specification needed, besides being compatible with force transducers, was the need to connect to LabVIEW. The proper filter and circuit board we selected based on the force transducer. The filter part chose was a SCC SG24 2 channel full bridge filter, which fits into a power bus (SC-2345. A noise rejecting cable connects this to the NIPCI – 6221 M Series DAQ board. We purchased all of these components from National Instruments. There was also software available for interpreting the data. It was because that all these components would work together with the software, and the price was reasonable National Instrument parts we selected.

4.3 Displacement Measurement System

We did extensive research on displacement measurement systems to fully understand the many components of such a system. There are many options to choose from when selecting a measurement system. Display, signal, signal format, cost, lens, and frame grabber board considerations are necessary.

The camera and vision system chosen for our final design was a Sony XC-ST50 CCD Camera. The camera is monochrome and has an analog signal. We chose a monochrome camera instead of color because monochrome has a greater quality of resolution. The advantage of color would be in its visual versatility. However, for this application, we did not need color since the measurement system would just have to differentiate between the light specimen and the dark carbon markers. Monochrome cameras were also slightly less expensive than their color equivalents. The selection of an analog camera over a digital camera we made was primarily on cost. Digital camera packages, which included an additional digital driver, were approximately twice the cost of analog camera packages. It was determined that the finances were not available to spend in excess of two thousand dollars for a digital camera system. This decision was acceptable because an analog camera would sufficiently perform the tasks needed for this application. The signal format decides whether the signal is digital or analog. Because of this, our selection for signal format was EIA (Electronic Industries Association).

These factors determined the type of camera system, which we purchased. We discussed other factors were with a professional from Edmunds Industrial Optics Inc. including lens size and focal range. We also chose a maximum viewing area of 90 mm^2 for our application. The lens (Edmund's Y54-363 10x CCD C-Mount Lens) we chose, based on the recommendation from an Edmunds professional, contains a ½" CCD format. This CCD format is the field of view that the lens is able to focus on. To reduce total project costs, we did not purchase this lens. We then acquired a lens currently from Professor Billiar's lab. If this lens does not achieve the desired performance, we will purchase the initial lens selected. We selected a frame grabber board PCI 1405 single channel color/monochrome based on the Edmunds professional advice. This board will adequately convert the frame-by-frame signal into a format compatible with LabVIEW software.

4.4 Control System Overview

A control system has the primary function of collecting and analyzing feedback from a given set of functions in order to control these functions. Monitoring or systematically modifying parameters can implement this control. In this case, the control system chosen is a computer system with LabVIEW software.

The team chose LabVIEW because of its multipurpose system, which can do everything from controlling the input of data, to acquiring the results, as well as analyzing and graphing those results. Since LabVIEW already exists on the WPI campus, it was cost-effective as well as time conscious. Instead of spending time designing and implementing an entire control system, we only had to build our program within LabVIEW.

This control system controls the rate at which the motors run the movement of the actuators, the temperature of the saline bath, and the camera. Each of these elements has their own circuit in LabVIEW and a simple key on the front panel controls the element. The controller boards help to connect the components such as the motors, the actuators, the camera and the bath heater to LabVIEW through the input/output connections.

In the schematic below, the elements of this device, which are controlled by LabVIEW, are shown as well as how they connect from one to another. Also seen in this diagram are the controller boards and their connection to LabVIEW. Overall, this system was the most effective way of controlling our device and has the ability to collect data.

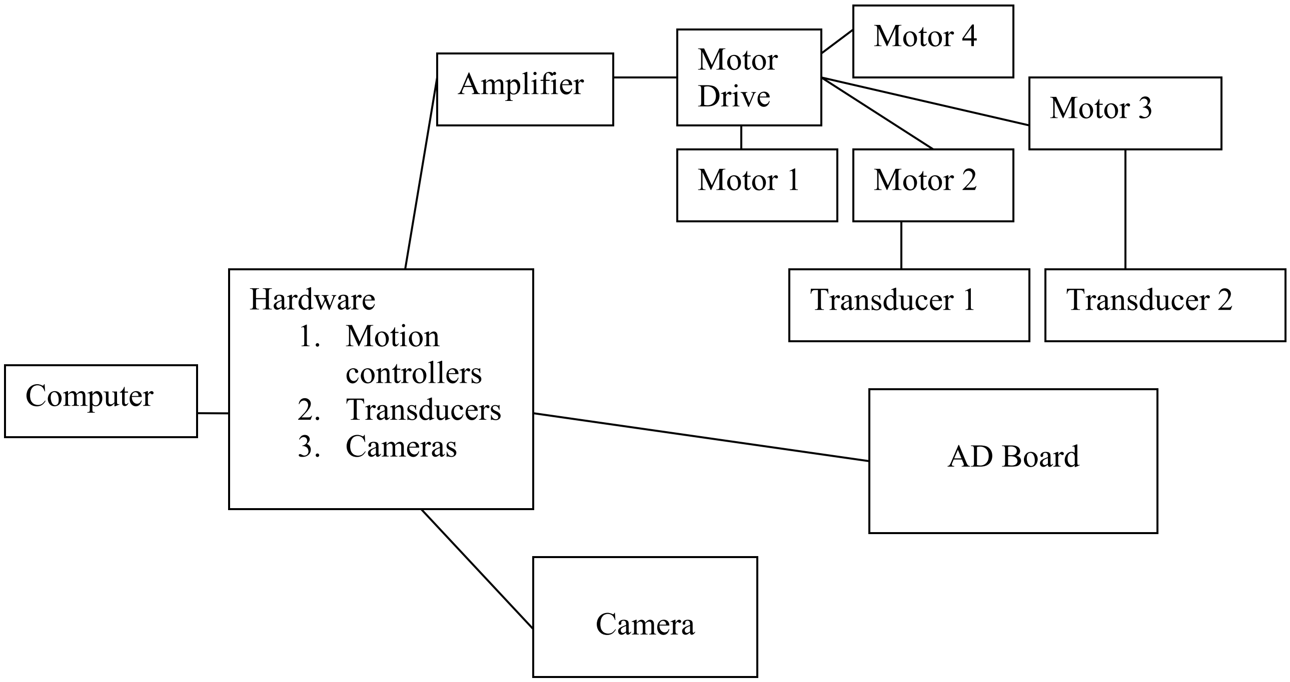

Figure 50. Schematic of Control System

4.5 Data Acquisition

Once the user can control the system, next comes the acquiring of the data that the system produces. Data acquisition is the process of receiving data from both internal and external sources. It uses a combination hardware and software to measure the data quantitatively.

The choice for this project was, again, LabVIEW since it has a data acquisition system already built in. The LabVIEW also has machine vision software (which takes output from the camera in real time) and has a timed loop, which allows the user to develop multi-rate real time applications using a high-level program interface. In this application, each loop is assigned a unique priority, with a maximum of 128 real time tasks. In this project, tasks were assigned individual loops and place on timers as seen in the figures below. The bottom figure synchronized multiple loops to start and stop together which was instrumental in controlling the many components of the device including the motors and the actuators. This was important since it could stop the whole system at the same time so as not to destroy the sample.

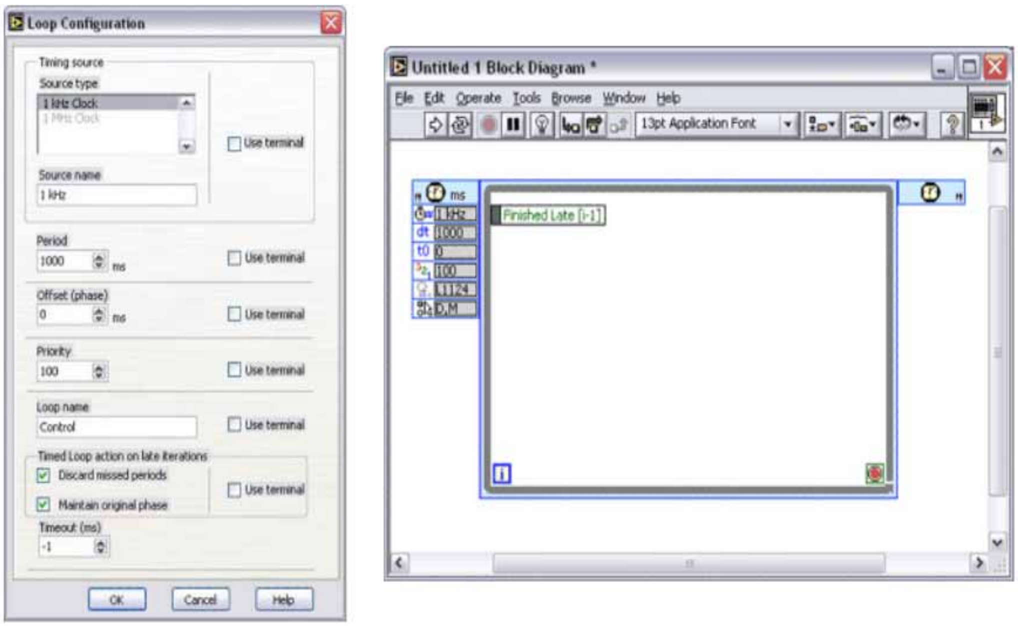

Figure 51. Diagram of Timed Circuits

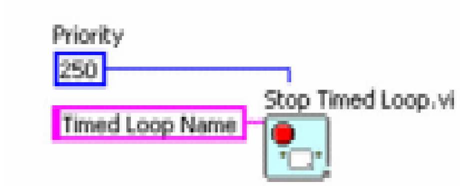

Figure 52. Timed Loop with Priorities

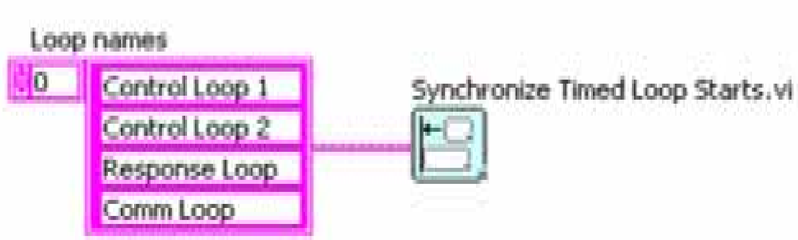

Figure 53. Synchronization of Timed Loops

LabVIEW not only acquires the data but also displays it on the front panel of the VI. This allows for graphing of the data and provides ease in the analysis of the data.

5.0 Assembly of Device

5.1 Components

The assembly of all components for the device can be found in APPENDIX G. The Schematic section includes CAD drawings of fabricated components. Specification information can be found in APPENDIX H, which also includes the company where the components were purchased. Along with APPENDIX H, there is an excel sheet with price and what company we ordered from. The components are listed based on section in the following order:

- Sample Attachment
- Bath Chamber
- Framework
- Stretching
- Force Measurement
- Displacement Measurement

Now we will discuss basic construction information:

- 6061 Aluminum was used as much as possible. It is inexpensive and easy to machine.
- Bolts and screws were used rather than welds to attach components. Screw sizes were chose based on the spec of the components. Custom parts all used #8-32 screws.
- Most of the plastic used was Acrylic (Plexiglas®). However, Lexan is a much better material to use because it does not chip as much during machining, and so it was used for the pulley frame.

- Plextic® was used to attach plastic to each other (used on the frame and arm). This substance melts the two plastics together and holds the two in place.
- An aluminum plate of the same dimension (except ¼" thick) of the chamber base was fabricated.
- Thermo grease was used to eliminate the air between the heating pads and aluminum plate, as well as the plate to the plastic.
- Stock metals were purchased from Peterson Steel and plastic stock from Plastics Unlimited.
- Electronic components were purchased from radio shack or the ECE dept. stock room. Many cables, including the stepper motors, heating pads and PID controller unit were extended. Match cable sizes up, solder and wrap with heat shrink.

The shafts on the motor (metric) and rail (English) were mismatched. The bore on the flexible couple on the motor end was drilled out to the correct size. The couple will only fit on one way.

5.2 LabVIEW

In order for the biax device to work properly, the entire system needs to be networked together. Using the software program LabVIEW, the system can be easily controlled and monitored by the user. LabVIEW is a graphical, data flow programming software which enables signal acquisition, measurement analysis, and data presentation. The end program provides the user with an easy user interface and process control. Two programs were written to integrate and control the motors, image acquisition (IMAQ), and the force acquisition. The following section explains the performance of the Labview programs and its control and display.

5.2.1 INITIALIZE.VI

The first program is called INITIALIZE.vi and is used for preparing the sample for an experiment. This program is used for attaching, tightening, and centering the sample, as well as for adjusting the threshold range. IMAQ is needed to monitor the sample's movement during preparation and stretching.

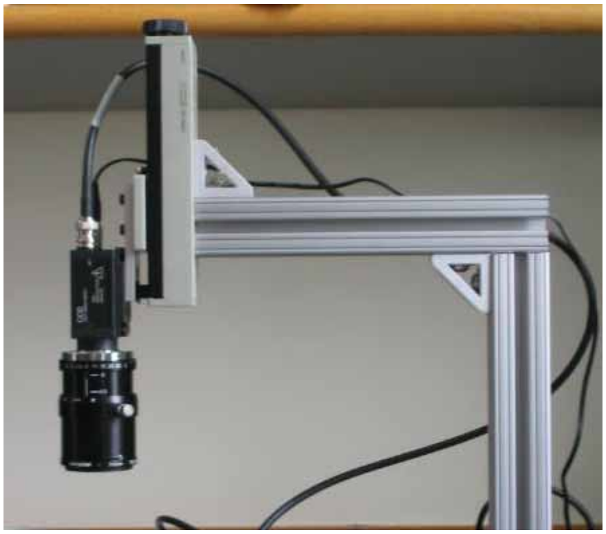

Figure 54. Displacement Measurement
Camera model Sony XC-ST50 used to measure the displacement of graphite markers on sample

The LabVIEW program obtains an image signal from the camera through a NI PCI-1405 image acquisition board.

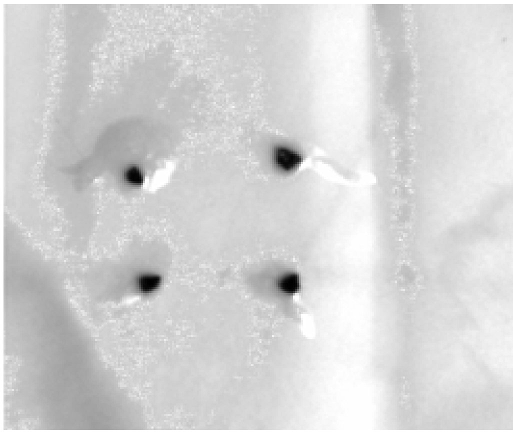

Figure 55. Initial Image of Graphite Markers
Sample with four graphite markers, after centering the sample.

This image is then threshold to locate the four graphite markers through contrast recognition.

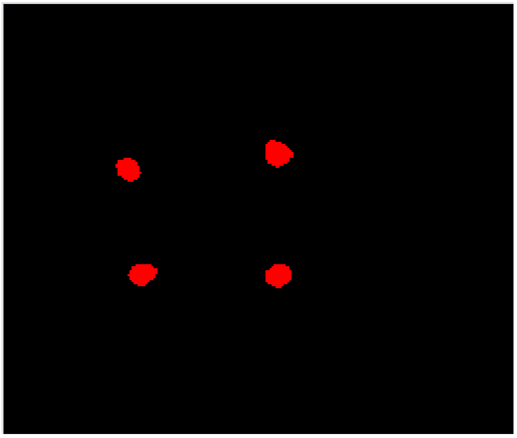

Figure 56. Threshold Image of Graphite Markers
Displays the graphite markers on the interface in real-time and shows the user the locations of markers.

Each pixel is displayed in either black or red, depending on whether the contrast is dark or light. There is a threshold range control on the interface to allow the user to adjust the range depending on the lighting environment. The user is also provided with buttons for easy motor control.

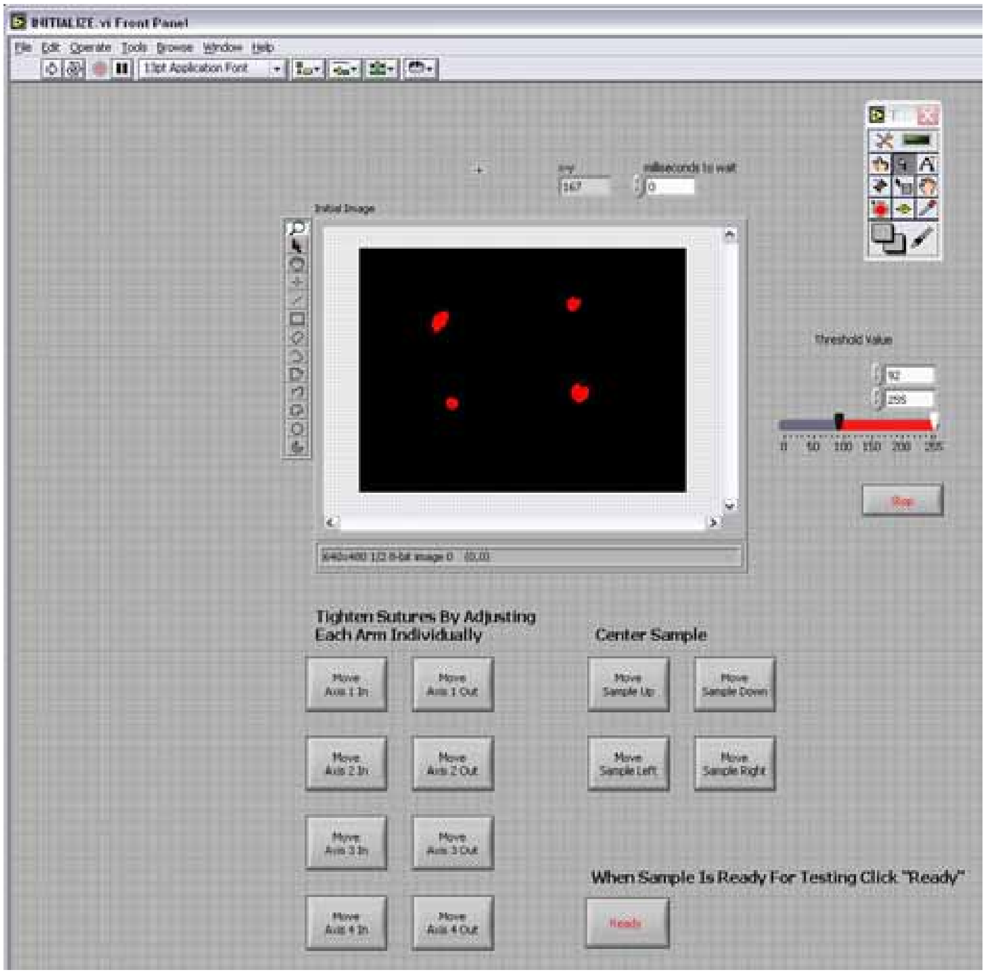

Figure 57. Initialize.VI
Buttons include: move X positive axis in, move X positive axis out,
move X negative axis in, move X negative axis out,
move Y positive axis in, move Y positive axis out,
move Y negative axis in, move Y negative axis out, move sample right,
move sample left, move sample up, and move sample down.

These controls can be used to tighten and center the sample before testing. Once the sample is ready for testing, there is a stop button that ends the program.

5.2.2 FINAL.VI

The second program is called FINAL.VI and this performs the biaxial stretch test and where both stress and strain experienced in the sample is measured. The FINAL.VI interface contains two main inputs for the user, which control the strain applied to the sample. The first is the percent strain, which is input as how far to stretch the sample in relation to its original dimensions. For example, if the user wanted to stretch the sample 10%, they would enter 0.1 into the percent strain input. The second is the rate of stretching, which is input as how fast the sample is stretched (in s^{-1}). If the user wanted the 10% strain to be completed in one second, they would enter 0.1 into the strain rate input.

5.2.3 Image Acquisition (IMAQ)

IMAQ is again needed to monitor the sample's movement during stretching. The camera obtains a threshold image similar to the threshold image in the INITIALIZE.VI This threshold image is again displayed on the interface in real-time and shows the user the locations of the graphite markers as they are stretched.

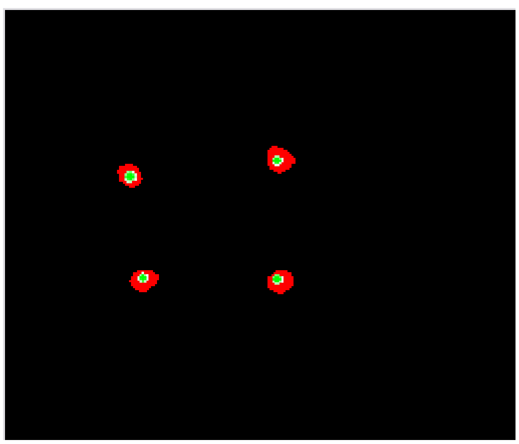

Figure 58. Centroids on Graphite Markers
Threshold image calculates the centroids of markers through particle analysis and are continually tracked during stretching

The displacement measurements of the markers are then used to calculate the average strain, which is then plotted on a strain vs. time graph. This process is performed in a while loop, and continually graphs the average strain in real-time throughout the stretching of the sample.

5.2.4 Transducer Data Acquisition

Data must also be obtained from the two torque transducers in order to measure the stress applied to the sample during stretching. Data is gathered from the NI SC-2345 Signal Conditioning Board, which obtains the force measured by the transducers. The FINAL.VI interface contains inputs for the user that are used to determine the stress.

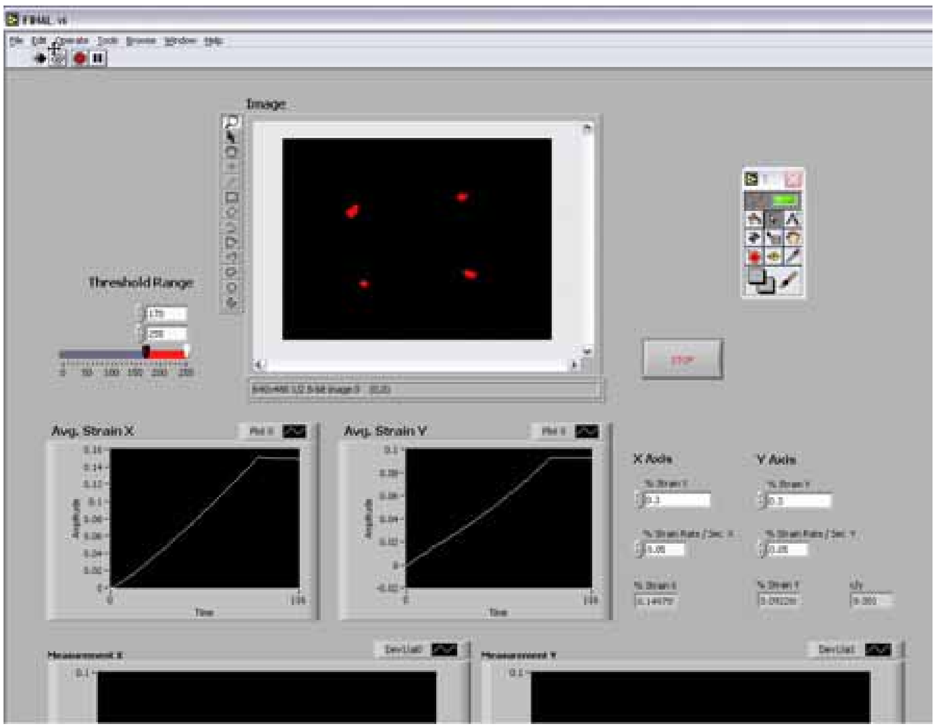

Figure 59. FINAL.VI
Inputs include width of sample in both axes, thickness of sample, and
Length of arm attached to transducer

These inputs then calculate the average stress in the sample according to the force, which is being applied. This process is also performed in a while loop, and continually graphs the average stress in real-time during stretching. This graph is displayed to the user on the interface.

5.2.5 Required Inputs for INITIALIZE.VI and FINAL.VI

The two LabVIEW programs provide easy to use interfaces for the user. Table 1 lists the required inputs and outputs for both the INITIALIZE.vi and the FINAL.vi.

INITIALIZE.vi		FINAL.vi	
Input	Output	Input	Output
Threshold range	Threshold image	Percent strain	Threshold image
Axis jog buttons		Rate of stretching	Stress v. time graph
		Sample length	Strain v. time graph
		Sample width	
		Sample thickness	
		Length of arm	
		Threshold range	

Figure 60. Inputs and outputs for VI
This compares the inputs and outputs of the INITIALIZE.vi and FINAL.vi in our LabVIEW program.

All of the obtained data is then saved to an excel spreadsheet for further analysis.

Test Data

	A	B	C	D	E	F	G	H	I	J	K	L	M
1	Time	%Strain X	%Strain Y	1-X	1-Y	2-X	2-Y	3-X	3-Y	4-X	4-Y	Stress X (Voltage)	
2	0.173	0	0	416.0432	157.9514	185.2736	189.646	427.3345	329.6571	207.3038	349.9439	-0.00398	
3	0.295	-0.00009	-0.00066	416.0545	157.9019	185.3031	189.6827	427.3661	329.461	207.3599	349.9086	-0.00398	
4	0.357	-0.00155	-0.0009	416.0833	158.5215	185.5206	190.111	427.3031	329.9812	207.7633	350.355	-0.00383	
5	0.422	-0.00254	-0.00183	415.9539	158.935	185.5733	190.5946	427.0136	330.3215	207.7411	350.6042	-0.00363	
6	0.491	-0.00457	-0.0034	415.5756	159.504	185.7454	190.7868	426.7343	330.4856	207.8225	350.6805	-0.00355	
7	0.556	-0.00562	-0.0043	415.5807	159.6774	185.9024	191.2433	426.4873	330.687	207.8979	350.8108	-0.00343	
8	0.623	-0.00699	-0.00564	415.2872	160.0559	185.9745	191.417	426.2487	330.753	207.9132	350.8503	-0.00322	
9	0.69	-0.00835	-0.00658	415.0515	160.4201	185.9309	191.6763	425.6965	330.968	207.7811	350.9468	-0.00307	
10	0.758	-0.00957	-0.00728	414.8223	160.6791	185.99	191.8941	425.396	331.1762	207.7433	350.9851	-0.00301	
11	0.824	-0.01093	-0.00826	414.688	160.8747	186.1166	192.1266	425.1591	331.2014	207.8559	351.0601	-0.00288	
12	0.889	-0.01196	-0.00985	414.4105	161.3711	186.0358	192.4092	424.7685	331.4413	207.7327	351.0721	-0.00274	
13	0.958	-0.0131	-0.01085	414.0825	161.6064	185.9355	192.6533	424.3424	331.5136	207.5958	351.1467	-0.00257	
14	1.026	-0.01484	-0.01224	413.8189	162.0499	186.0331	192.7612	423.9524	331.5595	207.6276	351.1922	-0.00251	
15	1.09	-0.01543	-0.01297	413.8158	162.15	186.2472	192.9343	424	331.5939	207.7229	351.1867	-0.00235	
16	1.159	-0.01656	-0.01368	413.7734	162.408	186.3271	193.1744	423.7407	331.8424	207.8524	351.2018	-0.00222	
17	1.224	-0.01779	-0.01554	413.2995	162.7865	186.1119	193.4157	423.2221	331.8678	207.6311	351.1799	-0.00208	
18	1.292	-0.01857	-0.016	413.1877	162.8817	186.1391	193.4986	422.9439	331.8895	207.5646	351.1832	-0.00203	
19	1.362	-0.01989	-0.01738	412.9818	163.1558	186.1847	193.6306	422.6906	331.9299	207.6536	351.0904	-0.00184	
20	1.43	-0.02015	-0.01809	412.862	163.3047	186.0987	193.7518	422.5908	331.9525	207.6364	351.103	-0.0018	
21	1.492	-0.02152	-0.01917	412.6016	163.4948	186.0275	193.9146	422.1015	332.0051	207.5779	351.0419	-0.00167	
22	1.576	-0.02221	-0.02064	412.4139	163.8021	185.952	194.0335	421.7757	332.024	207.4518	350.9639	-0.00158	
23	1.664	-0.02327	-0.02175	412.112	164.099	185.9325	194.1924	421.5672	332.0655	207.4373	351.0092	-0.00146	
24	1.725	-0.02427	-0.0228	412	164.282	185.9006	194.3487	421.3247	332.0361	207.5627	351.0275	-0.0014	
25	1.79	-0.02465	-0.02339	411.9031	164.3927	185.8059	194.4459	421.062	332.0499	207.4691	351.0278	-0.00132	
26	1.859	-0.02522	-0.02483	411.5596	164.7332	185.7098	194.5203	420.7743	332.1129	207.1934	350.9003	-0.00114	
27	1.924	-0.02637	-0.02538	411.0812	164.8613	185.3443	194.6467	420.2232	332.1678	207.0481	350.9189	-0.00109	
28	1.998	-0.02619	-0.02653	410.3658	165	184.5416	194.9274	419.4722	332.1805	206.3025	350.9414	-0.00107	

Test Data

Figure 61. Data in Excel Spreadsheet
Stress and strain data taken at real-time for each axis

After testing, the user can reset all input settings and vary the parameters depending on the results. APPENDIX I explains the step by step procedure for running the LabVIEW program. The program can be easily modified in the future to accommodate new needs or testing methods as described in the Recommendations section of this paper.

6.0 Discussion

The entire device was designed with versatility in mind. Every component on the device can be replaced by the same or similar components. For this reason, components were not permanently welded on to the device, but are all attached securely to the device. The software is also very versatile and additional programming can be added at any time should the user choose to remodel the software.

The device had a simple method of attaching the sample with the use of fishing hooks. These hooks were placed on a pivoting mechanism, which was crucial to distribute the forces evenly on the sample. This modified design resulted in very low friction forces and allowed the user to easily wrap the sutures around the pulleys.

The shape of the bath chamber allowed us to reduce the overall size of the device. There was also less solution in the chamber, which required less physiological solution. The smaller size also reduced the heating time for the physiological solution to reach 37ºC (with a simple controller unit with a steady state relay to heat the base of the chamber).

One of the sections, which was completed with few difficulties, was the framework. Because of our decision to use the specialized aluminum extrusions, the fabrication and assembly time was greatly reduced. Users are also able to make very quick adjustments by loosening various bolts.

The motion system was a very simple design. A stepper motor was mounted to a threaded rail. Each rail has a theoretical travel of 25 microns, although the system will never reach this accuracy.

A unique component of the device is the force measurement system required to calculate the stress. Using torque transducers, the problem of finding submergible linear transducers, was eliminated. The arm, which extends from the transducer to the bath, translates the force to a torque. We can also adjust the range of forces it can measure by changing the length of the arm.

The displacement measurement components consisted of a vision system with a camera mounted above the sample. The camera obtains images of the markers on the center of the sample and tracks their centroid movements. The centroid displacements are then converted into lengths, which then allow the device to calculate the strain.

Overall, the user interface is relatively simple. There is an initialization program to set up the sample for testing: proper tensioning, thresholding, and centering. A second program is used to actually test the sample. The user inputs the necessary parameters and the device pulls to the designated strain. Once the test is complete, the device will save the data into a spreadsheet file where the user can analyze the data.

7.0 Recommendations

After nine months of design, construction, and testing, this team has created a working planar biaxial test device for soft compliant tissues. However due to time constraints, few design elements were not completed. This includes installing limit switches and allowing the stress to be plotted in real-time.

Since there are stop buttons on the device and stop encoders in the program, limit switches are not vital. However, if installed, they can prevent the possibility of the force mechanism colliding into the machine mount ends. This just provides an additional safety factor for the user so the device could be run without constant monitoring.

The device is programmed to have the stress measurements gathered during the entire stretch of the sample. Upon completion of the test, all stress experienced by the sample is displayed on a graph in the interface. Further work should include programming the stress measurements to be gathered and displayed in real-time.

Other programming recommendations include allowing the user to test samples using force control rather than displacement control. The system, as it stands now, only allows the user to input the strain desired and the strain rate. A few modifications to the existing code could allow the user to input force or stress rather than strain. Another testing method would be cyclic testing. This involves the sample being stretched and relaxed over a certain number of cycles. Additions to the back panel of LabVIEW would allow for the interface to include a 'number of cycles' input for the user.

The LabVIEW program we designed could also be simplified combine the INITIALIZE.vi and FINAL.vi to one VI. An improvement in the vision loop speed is also another programming recommendation. This would include making the loop run faster as well as cleaning the programming window to be in the order that the program runs.

Further testing of the device should be done on various samples to be able to compare data, analyze accuracy, and prove that sample attachment does not harm the sample. Since the design and construction took a great deal of time, only latex samples were tested. Future research in sample attachment could be done to find another suitable method for connecting the sample to the device.

Further testing could also lead to analysis of the time scale for the stress and strain data. Tests were never performed to identify the number of points per collection while acquiring the stress and strain data. There may be more programming needed in this aspect to ensure that the stress and strain data are on the same time scale and match up.

Finally, if the user wanted, all of the aluminum parts could be anodize to prevent rust or corrosion. However, tests would be needed to ensure that all of the parts could still connect after anodization. This would include that all rails could still slide into place, bolts and screws could be tightened properly, and the size of the device does not increase significantly so as not to fit on a laboratory bench top.

References

MQP 2004-2005

1. Arbogast, K.B., et al., A high-frequency shear device for testing soft biological tissues. *J Biomech*, 1997. **30**(7): p. 757-9.
2. Brouwer, I., et al., Measuring in vivo animal soft tissue properties for haptic modeling in surgical simulation. *Stud Health Technol Inform*, 2001. **81**: p. 69-74.
3. Chew, P.H., F.C. Yin, and S.L. Zeger, Biaxial stress-strain properties of canine pericardium. *J Mol Cell Cardiol*, 1986. **18**(6): p. 567-78.
4. Cummings, C.L., et al., Properties of engineered vascular constructs made from collagen, fibrin, and collagen-fibrin mixtures. *Biomaterials*, 2004. **25**(17): p. 3699-706.
5. Demer, L.L. and F.C. Yin, Passive biaxial mechanical properties of isolated canine myocardium. *J Physiol*, 1983. **339**: p. 615-30.
6. Downs, J., et al., An improved video-based computer tracking system for soft biomaterials testing. *IEEE Trans Biomed Eng*, 1990. **37**(9): p. 903-7.
7. Feng, Z., et al., Investigation on the mechanical properties of contracted collagen gels as a scaffold for tissue engineering. *Artif Organs*, 2003. **27**(1): p. 84-91.
8. Flynn, D.M., et al., A finite element based method to determine the properties of planar soft tissue. *J Biomech Eng*, 1998. **120**(2): p. 202-10.
9. Gloeckner, D.C., et al., Mechanical evaluation and design of a multilayered collagenous repair biomaterial. *J Biomed Mater Res*, 2000. **52**(2): p. 365-73.
10. Hoffman, A.H. and P. Grigg, A method for measuring strains in soft tissue. *J Biomech*, 1984. **17**(10): p. 795-800.
11. Hsu, F., Liu, Alex, Downs John, Rigamonti Daniele, Humphrey Jay D., A triplane Video-based experimental system for studying axisymmetrically inflated biomembranes. *IEEE Trans Biomed Eng,* 1995. **42**(5): p. 442-450.
12. Humphrey, J.D., D.L. Vawter, and R.P. Vito, Quantification of strains in biaxially tested soft tissues. *J Biomech*, 1987. **20**(1): p. 59-65.
13. Humphrey, J.D. and F.C. Yin, Biomechanical experiments on excised myocardium: theoretical considerations. *J Biomech*, 1989. **22**(4): p. 377-83.
14. Jun, J.H., et al., Effect of thermal damage and biaxial loading on the optical properties of a collagenous tissue. *J Biomech Eng*, 2003. **125**(4): p. 540-8.
15. Lafrance, H., et al., Study of the tensile properties of living skin equivalents. *Biomed Mater Eng*, 1995. **5**(4): p. 195-208.
16. Langdon, S.E., et al., Biaxial mechanical/structural effects of equibiaxial strain during crosslinking of bovine pericardial xenograft materials. *Biomaterials*, 1999. **20**(2): p. 137-53.
17. Lanir, Y., Constitutive equations for fibrous connective tissues. *J Biomech,* 1983. **16**(1): p. 1-12.
18. Lanir, Y., *Handbook of bioengineering*, ed. B. Sun, Halston, Jim, Warren, Nancy. 1987: McGraw-Hill.
19. Lanir, Y. and Y.C. Fung, Two-dimensional mechanical properties of rabbit skin. I. Experimental system. *J Biomech*, 1974. **7**(1): p. 29-34.

20. Lanir, Y. and Y.C. Fung, Two-dimensional mechanical properties of rabbit skin. II. Experimental results. *J Biomech*, 1974. **7**(2): p. 171-82.
21. Lepetit, J., et al., A simple cryogenic holder for tensile testing of soft biological tissues. *J Biomech*, 2004. **37**(4): p. 557-62.
22. Liu X. and James, R.D., Stability of Fiber Networks Under Biaxial Stretching, *ASME Journal of Applied Mechanics,* 1995. 62: p.398-406.
23. Makinde, A., L Thibodeau, and K.W. Neale, Development of an Apparatus for Biaxial Testing Using Cruciform Specimens. *Experimental Mechanics*, 1992. **32**: p. 138-144.
24. Mansour, J.M., et al., A method for obtaining repeatable measurements of the tensile properties of skin at low strain. *J Biomech*, 1993. **26**(2): p. 211-6.
25. Maurel, W., *3-D Modeling of the Human Upper Limb Including the Biomechanics of Joints, Muscles and Soft Tissues, PhD. Thesis No. 1906, Ecole PlytechniqueFederale de Lausanne*, 1998.
26. May-Newman, K. and F.C. Yin, Biaxial mechanical behavior of excised porcine mitral valve leaflets. *Am J Physiol*, 1995. **269**(4 Pt 2): p. H1319-27.
27. Miller, K., How to test very soft biological tissues in extension? *J Biomech*, 2001. **34**(5): p. 651-7.
28. Nielsen, P.M., P.J. Hunter, and B.H. Smaill, Biaxial testing of membrane biomaterials: testing equipment and procedures. *J Biomech Eng,* 1991. **113**(3): p. 295-300.
29. Olansen, J., Rosow, Eric, *Virtual bio-instrumentation: biomedical, clinical, and healthcare applications in LabVIEW*. 2002, Upper Saddle River, NJ: Prentice Hall.
30. Optics, E.I., *Optics and Optical Instruments Catalog*. 2004, USA. pp. 203-204, 238-239.
31. Oxlund, H., J. Manschot, and A. Viidik, The role of elastin in the mechanical properties of skin. *J Biomech*, 1988. **21**(3): p. 213-8.
32. Pereira, J.M., J.M. Mansour, and B.R. Davis, Dynamic measurement of the viscoelastic properties of skin. *J Biomech*, 1991. **24**(2): p. 157-62.
33. Reihsner, R., B. Balogh, and E.J. Menzel, Two-dimensional elastic properties of human skin in terms of an incremental model at the in vivo configuration. *Med Eng Phys*, 1995. **17**(4): p. 304-13.
34. Roeder, B.A., et al., Tensile mechanical properties of three-dimensional type I collagen extracellular matrices with varied microstructure. *J Biomech Eng*, 2002. **124**(2): p. 214-22.
35. Sacks, M.S., A method for planar biaxial mechanical testing that includes in-plane shear. *J Biomech Eng*, 1999. **121**(5): p. 551-5.
36. Sacks, M.S. and C.J. Chuong, Orthotropic mechanical properties of chemically treated bovine pericardium. *Ann Biomed Eng*, 1998. **26**(5): p. 892-902.
37. Tezcaner, A.H., Vasif, Soft tissue engineering with ophthalmological applications, *Tissue Engineering and biodegradable equivalents: Scientific and Clinical Applications*. 2002, Marcel Dekker Inc. p. 545-548.
38. van Noort, R.B., M.M., Greaney, M.G., Irvin, T, *A new in vitro method for the measurement of mechanical strength of abdominal wounds in laboratory animals.*
39. Veronda, D.R. and R.A. Westmann, Mechanical characterization of skin-finite deformations. *J Biomech*, 1970. **3**(1): p. 111-24.

40. Vito, R.P., The mechanical properties of soft tissues--I: a mechanical system for bi-axial testing. *J Biomech*, 1980. **13**(11): p. 947-50.

Website References

41. *Burn Incident and Treatment in the US: 2000 Fact Sheet,* American Burn Association, November 2004, retrieved from, http://www.ameriburn.org/pub/BurnIncidenceFactSheet.htm

42. *Planar-Biaxial Soft Tissue Test System,* Instron, September 2004, retrieved from www.instron.com

43. *DC motor*, Hyperphysics, September 2004, retrieved from http://hyperphysics.phy-astr.gsu.edu/hbase/magnetic/mothow.html

44. *DC stepper motor,* Advanced Micro System, Inc. September 2004, retrieved from http://www.ams2000.com/stepping101.html#introduction

45. *Stepper Motor,* Images SI Inc, September 2004, retrieved from http://www.imagesco.com/articles/picstepper/02.html

46. *Servo motor,* Arrick Robotics, September 2004, retrieved from www.robotics.com/motors.html

47. Dawson, Brett, *Pneumatic/hydraulic motor,* Team DaVinci Robotics, September 2004, retrieved from http://www.teamdavinci.com/understanding_pneumatics.htm

48. *Linear actuators*, Ultra Motion, October 2004, retrieved from, http://www.ultramotion.com/products/bug/php

49. National Instruments, October 2004, retrieved from www.nationalinstruments.com

APPENDIX A: Standard Graphs for All Living Tissues [25]

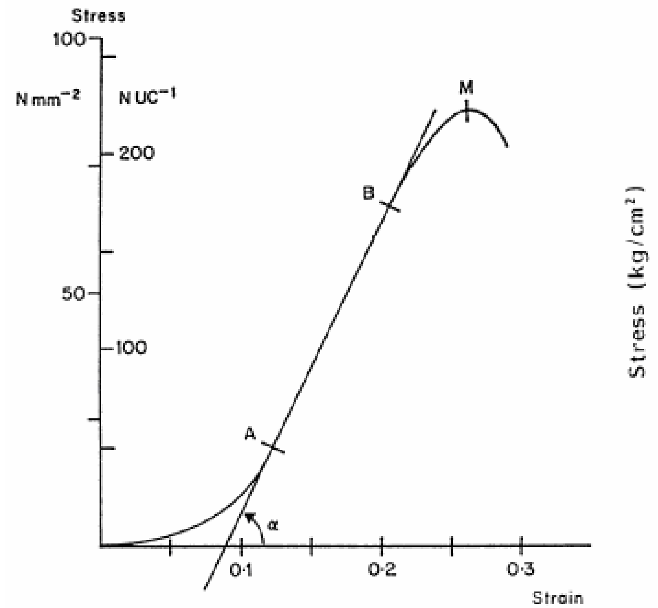

(Viidik 80)

Fig. 4.13. Load-extension curve

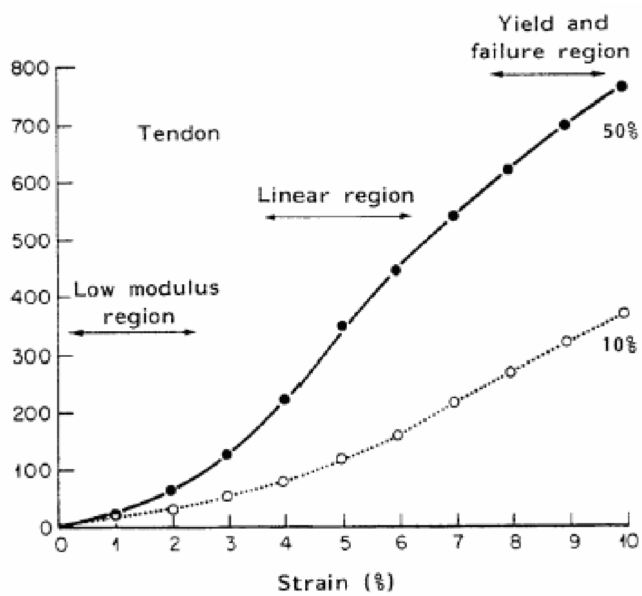

(Birk 91)

Fig. 4.14. Influence of the train rate

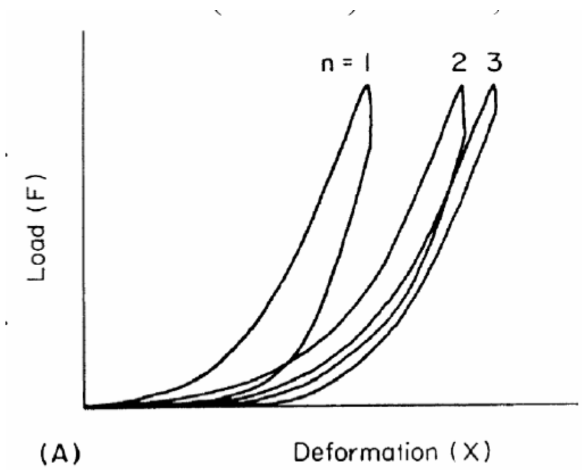

Fig. 4.16. Preconditioning (Viidik 73)

Viscoelastic Behaviors

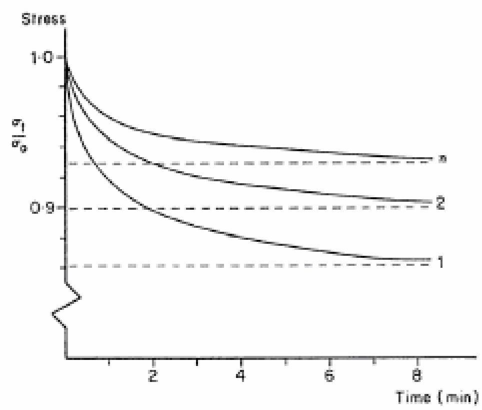

a) stress-relaxation (Viidik 80)

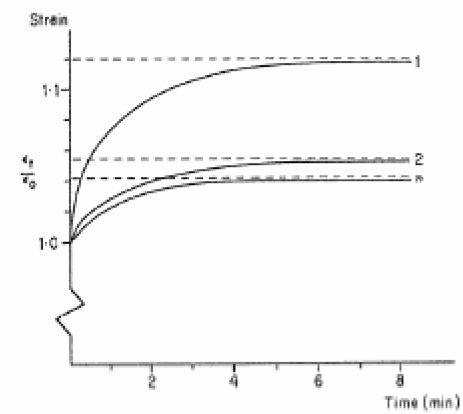

b) creep (Viidik 80)

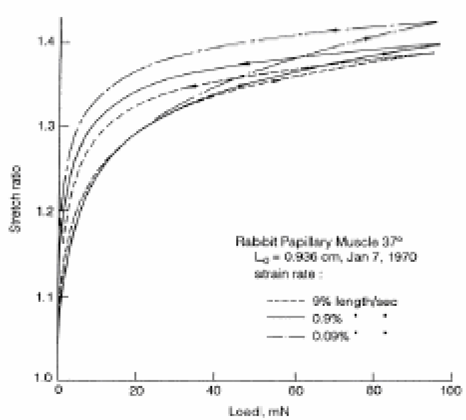

c) hysteresis (Fung 72)

APPENDIX B: The Objective Tree

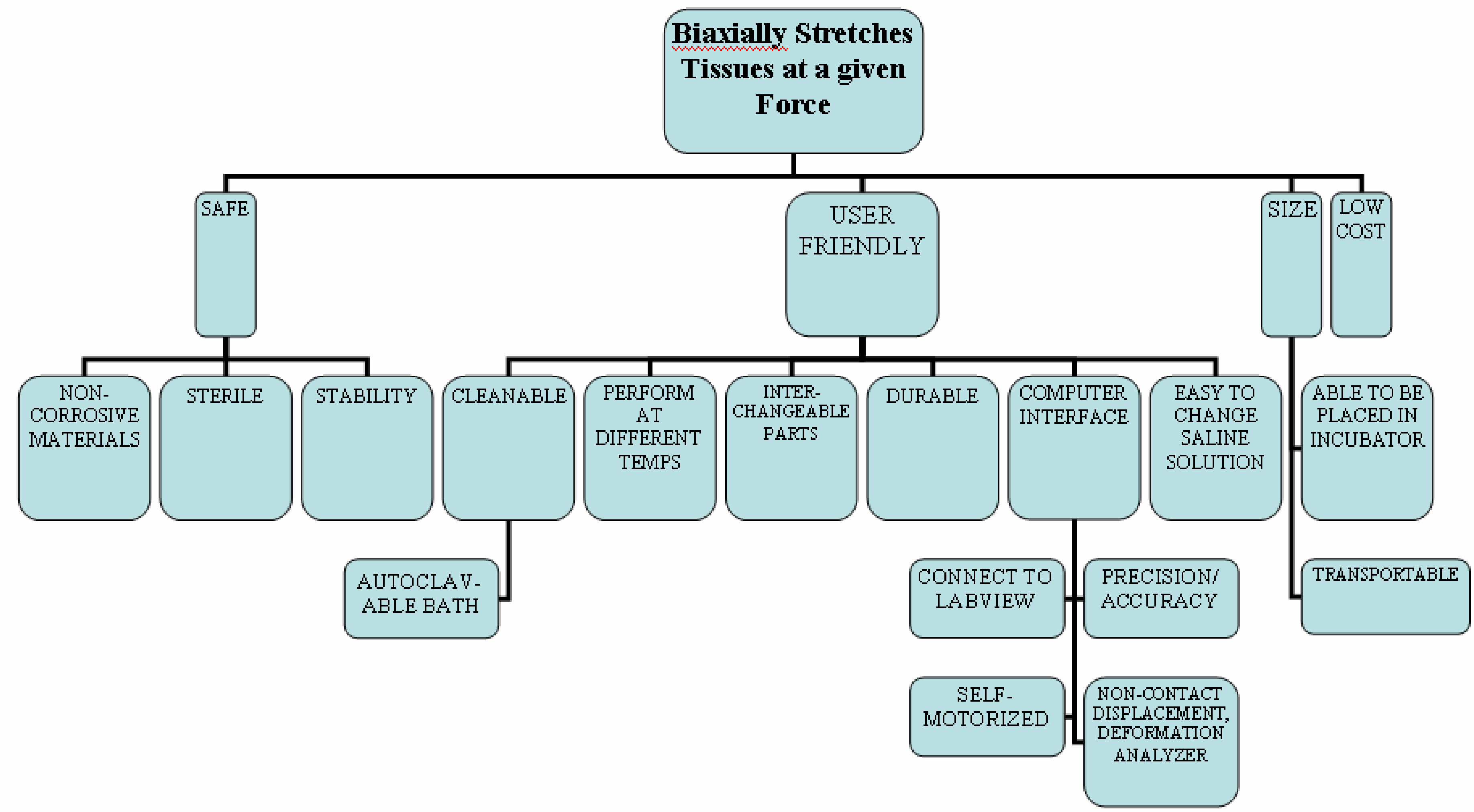

APPENDIX C: Pair-wise Comparison Chart

The purpose of these charts is to rate the importance of our objectives based on what our client wants.

Instructions:

- **Compare column to row**
- **If the objective in the column is higher on the objective list than the row place a 1 in the square**
- **If the objective in the column is lower on the objective list than the row place a 0 in the square**
- **If the objectives are of equal importance place a ½ in each box.**
- **The total number of points will be placed in the TOTAL column (these will be tallied by row)**

Main Objectives

	BIOCOMPATIBILITY	PERFORMANCE	SIZE	LOW COST	TOTAL
BIOCOMPATIBILITY	---	0	.5	.5	0
PERFORMANCE	0	--------------------------------	1	1	2
SIZE	0.5	1	---------------	0	1.5
LOW COST	0.5	1	0	------------	1.5

Secondary Objectives

	PRECISION / ACCURACY	USER FRIENDLY	SELF MOTORIZED	NON-CONTACT DISPLACEMENT ANALYZER	PERFORM AT DIFF. TEMPS.	NON-CORROSIVE MATERIALS	STERILE	TRANSPORTABLE	PLACED IN INCUBATOR	DURABLE	LOW COST	TOTAL
PRECISION / ACCURACY	------------------------	1	1	.5	1	1	1	1	1	1	1	9.5
USER FRIENDLY	1	-----------------------	0	0	.5	0	1	1	1	1	0	5.5
SELF MOTORIZED	1	0	-------------------------------	.5	1	1	1	1	1	1	1	8.5
NON-CONTACT DISPLACEMENT ANALYZER	.5	0	.5	---	1	1	1	1	1	1	1	8
PERFORM AT DIFF. TEMPS.	1	.5	1	0	------------------------	0	1	1	1	1	0	6.5
NON-CORROSIVE MATERIALS	1	0	1	1	0	----------------------------	1	1	1	1	1	8
STERILE	1	1	1	1	1	1	------------------------	0	.5	0	0	6.5
TRANSPORTABLE	1	1	1	1	1	1	0	---	1	1	0	8
PLACED IN INCUBATOR	1	1	1	1	1	1	.5	1	---------------------------	.5	0	8
DURABLE	1	1	1	1	1	1	0	1	.5	-------------------------	0	7.5
LOW COST	1	0	1	0	0	1	0	0	0	0	-------------	3

APPENDIX D-1: National Instruments (Series Comparison)

(www.nationalinstruments.com)

Feature	7330 Series	7340 Series	7350 Series
Maximum Number of Axes	4	2,4	2,4,6,8
Servo Control	-	•	•
Closed loop stepper control	•	•	•
Linear Interpolation	•	•	•
Configurable auxiliary DIO	•	•	•
RTSI	•	•	•
S-curve	•	•	•
Configurable Move complete criteria	•	•	•
Software limits	•	•	•
High speed capture	•	•	•
Blending	•	•	•
Upgradeable firmware	•	•	•
NI Motion Software API	•	•	•
Circular, spherical, and helical interpolation	•	•	•
Contouring	-	•	•
Electronic Gearing	-	•	•
On-board programming functionality	-	•	•
Static Friction compensation	-	•	•
Sinusoidal Commutation	-	-	•
Buffered Breakpoints	-	-	•
4 MHz Periodic Breakpoints	-	-	•
Buffered High Speed Capture	-	-	•
Number of axes per 62.5 microsecond PID rate	1	1	2
Static PWM outputs	2	2	2
DIO Lines	32	32	64
Digital to analog converter	-	16 bit	16 bit
Analog to digital converter	12 bit	12 bit	16 bit
Maximum Step output rate	4 MHz	4 MHz	8 MHz
Encoder rate	20 MHz	20 MHz	20 MHz

APPENDIX D-2: National Instruments (Low Cost Motion Control)

(www.ni.com)

NI PCI-7332

- Firmware you can upgrade
- Quadrature encoder or analog feedback
- RTSI bus for powerful synchronization with other NI measurement products
- Linear interpolation for coordinated, multiaxis motion control
- Four 12-bit ADCs with ±10 V range

NI PXI-7334

- Quadrature encoder or analog feedback
- PXI trigger bus for powerful synchronization with other NI measurement products
- 3D linear interpolation for coordinated, multiaxis motion control
- Four 12-bit ADCs with ±10 V range
- Firmware you can upgrade

NI PCI-7334

- Firmware you can upgrade
- 4-axis stepper motor control board
- Quadrature encoder or analog feedback
- RTSI Bus for powerful synchronization with other NI measurement products
- 3D linear interpolation for coordinated, multiaxis motion control
- Four 12-bit ADCs with ±10 V range

APPENDIX D-3: Precision MicroControl Corp Motion Control

(www.pmccorp.com)

Features of Multiflex PCI 1040	
•	4 axes of pulse control (stepper or pulsed servo) in an economical half-length PCI card
•	Available with 4 optional encoders - providing up to 4 axes of closed-loop control
•	Multi-axis point-to-point & coordinated motion
•	Trapezoidal, S-curve and parabolic profiles
•	5 MHz pulse outputs for high-speed microstepping
•	20 million encoder counts/sec for high speed and resolution
•	Open and closed-loop stepper control
•	1 KHz closed-loop update rate each axis
•	On-the-fly trajectory and direction changes
•	Eight 14-bit analog inputs (option)
•	On-board multi-tasking and programmable interrupts free host PC for other tasks
•	Consistent real-time behavior: Peak performance is maintained no matter which features are enabled
•	Dedicated high-speed I/O (capture & compare)
•	All I/O signals conveniently available via high-density VHDCI-SCSI connectors on bracket
•	All I/O signals are differential or complementary twisted-pairs for superior noise immunity
•	Fully programmable in C/C++, VB, Delphi, LabVIEW or easy-to-use command language
•	Comprehensive and powerful software **API** for the ultimate in high-level programming flexibility
•	Includes Motion Integrator™ suite of graphical installation, tuning and diagnostic programs at no extra charge

APPENDIX D-4: Galil Motion Control

(www.galilmc.com)

DMC-1842

- Accepts up to 12 MHz encoder frequencies for servos and 3 MHz for steppers
- Advanced PID compensation with Velocity and Acceleration feedforward, integration limits, notch filter and low-pass filter. Sample times to 62.5 microseconds per axis
- Modes of motion include jogging, point-to-point positioning, contouring, linear and circular interpolation, electronic gearing and ECAM
- Multitasking for concurrent execution of up to eight application programs
- Non-volatile memory for application programs, variables and arrays
- Home input and forward and reverse limits accepted for every axis
- 8 Uncommitted inputs and 8 outputs
- Expanision for 64 I/O available with DB-14064
- High speed position latch and output compare
- Sinusoidal commutation for brushless servo motors
- High-density shielded cable minimizes EMI
- Custom hardware and firmware options available
- Ceramic Motor Option allows precise control for all Ceramic Motors.
- Connects directly to AMP-19540 4-axis drive for cost-effective, multi-axis controller/drive solution. Drives brush or brushless servos up to 500 Watts each

DMC-2143

- Ethernet connectivity : 10Base-T
- One RS232 port up to 19.2kb
- Ethernet supports multiple masters and multiple slaves allowing communication with multiple computers and I/O devices
- Supports Modbus protocol for communication with I/O devices
- Accepts up to 12 MHz encoder frequencies for servos and 3 MHz for steppers
- Advanced PID compensation with Velocity and Acceleration feedforward, integration limits, notch filter and low-pass filter. Sample times to 62.5 microseconds per axis
- Modes of motion include jogging, point-to-point positioning, contouring, linear and circular interpolation, electronic gearing and ECAM
- Multitasking for concurrent execution of up to eight application programs
- Non-volatile memory for application programs, variables and arrays
- Dual encoders, home input and forward and reverse limits accepted for every axis
- 8 TTL uncommitted inputs and 8 outputs for 1- through 4-axis models; 16 inputs and 16 outputs for 5- through 8-axis models
- Add 8 analog inputs and 40 digital I/O with DB-28040
- Connects to Galil's IOC-7007 Intelligent I/O controller for additional analog and digital I/O on the Ethernet
- High speed position latch and output compare for each axis
- Sinusoidal commutation for brushless servo motors
- 1-4 axes card: 4.25" x 7.0"
5-8 axes card: 4.25" x 10.75"
- DIN-Rail mount option
- Accepts +5V, +/-12V DC inputs; DC-to-DC converter option for single 18V to 72V DC input
- DMC-21x2 uses 100-pin SCSI connector for each set of 4 axes
DMC-21x3 uses 96-pin DIN connector for each set of 4 axes

- Custom hardware and firmware options available
- Ceramic Motor Option allows precise control for all Ceramic Motors.

SDM-20640 (motor drive)

- Connects to Galil DMC-18xx PCI bus motion controller to provide a complete controller/drive solution with minimal wiring
- 18V to 80V dc; 7 Amps continuous, 10 Amps peak per axis
- Drives four servo motors up to 500 Watts each
- Configurable for driving brush or brushless motors
- High-bandwidth PWM drives with 60 kHz switching frequency
- Compact 6.8" x 8.75" x 1" metal enclosure
- Provides 15-pin Hi-density D-sub connectors for X,Y,Z and W axes
- Connects to DMC-18xx PCI controller with single 100-pin SCSI cable
- Shunt Regulator option is available

APPENDIX E: Calculations Loads for Force Transducers

Calculations of maximum loads for the force transducers

Circular shape

- According to our background research, skin can withstand up to 20 N/m
- We are assuming the tissue sample size to be in a circular shape with a diameter of 2.5 cm. Catherine worked in Professor Pins's laboratory over the summer 2004. She made circular collagen samples by drying the collagen gel in the hood on circular shaped polymer mold. The diameter was approximately 2.5 cm.

Therefore $d := 2.5\text{cm}$

Circumference of circle

$C := \pi d \quad C = 0.079\text{m}$

Because this is a biaxial system, we divided the circumference into 4 sections

$C2 := \frac{C}{4} \qquad \frac{C}{4} = 0.02\text{m} \qquad \sigma := 20\frac{\text{N}}{\text{m}}$

Force per section = $F := C2 \cdot \sigma \qquad F = 0.393\text{N} \qquad G := 9.81\frac{\text{m}}{\text{s}^2}$

Load = $L := \frac{F}{G} \qquad L = 0.04\text{kg}$ Convert to grams = **40 g**

Cruciate form

- Main concern about this sample shape is determining the dimensions.
- To figure this out, we decided to take the longest distance within the cross-shaped form, which is from one corner to the opposite corner (diameter).

$d = 0.025\text{m}$

We then decided to concentrate on one edge of the cruciform. The center of diameter is the radius.

radius = $r := \frac{d}{2} \qquad r = 0.013\text{m}$

This gives us an isosceles triangle (two sides are equal lengths). We need to find the base of that triangle.
To find the angle (angle α) between the two equal sides, we divided 360 degrees by 8 (because there are 8 sections).

$\alpha := 45$ degrees

Now divide angle α in half $\phi := \alpha \div 2 \qquad \phi := 22.5$ degrees

z = half of base

$z := \sin(22.5)\, r$

$z := .4784 \cdot cm$

base = $b := z \cdot 2 \quad b = 9.568 \times 10^{-3} m$

To also verify our calculations for the base length, we use the LAW OF COSINE equation.

$$A^2 + B^2 - 2 \cdot A \cdot B \cdot \cos(\alpha) =$$

Our answer was0.9153 cm, which is similar.
However, we chose to use 0.9567 cm because it is safer to assume a larger number.

So to find the load...

$F1 := \sigma \cdot b \quad F1 = 0.191N$

$L1 := F1 \div G \quad L1 = 0.02kg$ Convert to grams = **20 g**

Our conclusion...

Using the circular sample, our range for the transducer needs to be higher. It would work out best to have the range from 0 grams to 50 grams.

Using the cruciate form, our range for the transducer can be 0 grams to 30 grams.

More Calculations based on Literature Review

Reference : Feng, Z., et al., *Investigation on the mechanical properties of contracted collagen gels as a scaffold for tissue engineering.* Artif Organs, 2003. ***27*** (1) : p. 84-91.

Data taken from pg. 88, Figure 6

These are contracted collagen gels and are tested uniaxially. The dimensions of the sample are 9 mm x 5 mm with the thickness of 0.3 mm.
The collagen concentration is 1.67 mg/ml.

Taking the data from the "4 weeks" results for ultimate stress, it is approximately 235 kPa for apparent stress. (This is apparent stress because the width and thickness decreases under preconditioning.)

Converting kPa to N/m² ......

$$\frac{235000\,\mathrm{Pa}\cdot 1\mathrm{N}}{\mathrm{Pa}\cdot \mathrm{m}^2} = 2.35\times 10^5\,\frac{\mathrm{N}}{\mathrm{m}^2} \qquad \sigma := 235000\frac{\mathrm{N}}{\mathrm{m}^2}$$

The cross sectional area of the sample is....

$$t := 0.0003\mathrm{m} \qquad w := .005\mathrm{m}$$

$$A := t\cdot w \qquad A = 1.5\times 10^{-6}\,\mathrm{m}^2$$

$$F := \sigma\cdot A \qquad F = 0.353\mathrm{N}$$

$$L := \frac{F}{G} \qquad L = 0.036\mathrm{kg}$$

Convert to grams = **36 g**

Reference : Roeder, B.A., et al., *Tensile mechanical properties of three-dimensional type I collagen extracellular matrices with varied microstructure.* J Biomech Eng, 2002. **124** (2) : p. 214-22.

Materials used: Type I collagen,neutralized in 10 x phosphate buffer saline at 37 degrees C temperature chambers. The collagen concentration varied to 0.3, 1.0, 2.0, and 3.0 mg/ml, which effected the mechanical properties.

Dimensions :

$l := 0.01m \qquad w := 0.004m \qquad t := 0.0018m$

Cross sectional Area:

$A := w \cdot t \qquad A = 7.2 \times 10^{-6} m^2$

In the article, there was a graph with data for a representation of what the stress-strain relationship is for a sample with collagen concentration of 0.2 mg/ml. The failure stress was at 6.5 kPa.

6.5 kPa = 6500 Pa $\qquad 6500Pa \cdot 1 \frac{N}{Pa \cdot m^2} = 6.5 \times 10^3 \frac{N}{m^2}$

$\sigma := 6500 \frac{N}{m^2}$

$F := \sigma \cdot A \qquad F = 0.047N$

$L := F \div G \qquad L = 4.771 \times 10^{-3} kg$

Convert to grams = 4.77 g

*This is a representative data for a collagen sample with a collagen concentration of 2 mg/ml.

For a collagen matrix with a concentration of 0.3 mg/mL and a pH of 7.4:

0.5 kPa (looking at figure 10 for failure stress):

$$0.5 \text{ kPa} \times \frac{1000 \text{ Pa}}{1 \text{ kPa}} = 500 \text{ Pa} \times 1 \text{ (N/m}^2\text{)/1 (Pa)} = 500 \text{ N/m}^2$$

By using the same area as before (7×10^{-6} m^2):

$$500 \times \frac{\;}{m^2} \times 7 \times 10 \;\; m = 3.5 \times 10 \;\; N$$

To solve for weight:

$$\frac{0.0035 N}{9.81 \frac{m}{s^2}} = 3.568 \times 10^{-4} kg$$

Converting to grams:

$$3.568 \times 10^{-4} kg \times \frac{1000 gm}{1 kg} = 0.357 gm$$

For a collagen concentration of 1.0 mg/mL and a pH of 7.4:

$$4 \text{ kPa} \times \frac{1000 \text{ Pa}}{1 \text{ kPa}} = 4000 \text{ Pa} \times \frac{1 \text{ N/m}^2}{1 \text{ Pa}} = 4000 \text{ N/m}^2$$

$$4000 \frac{N}{m^2} \times 7 \times 10^{-6} m^2 = 0.028 N$$

Converting to mass:

$$\frac{0.028 N}{9.81 \frac{m}{s^2}} = 2.854 \times 10^{-3} kg$$

Converting to grams:

$$2.854 \times 10^{-3} kg \frac{1000 gm}{1 kg} = 2.854 gm \quad \text{for 1.0 mg/mL}$$

For a collagen concentration of 2mg/mL and a pH of 7.4:

$$6\text{ kPa} \times \frac{1000\text{ Pa}}{1\text{ kPa}} \times \frac{1\text{ N/m}^2}{1\text{ Pa}} = 6000\text{ N/m}^2$$

$$6000\frac{\text{N}}{\text{m}^2} \times 7 \times 10^{-6}\text{m}^2 = 0.042\text{N}$$

Converting to mass:

$$\frac{0.042\text{N}}{9.81\frac{\text{m}}{\text{s}^2}} = 4.281 \times 10^{-3}\text{kg}$$

Converting to grams:

$$4.281 \times 10^{-3}\text{kg} \cdot \frac{1000\text{gm}}{1\text{kg}} = 4.281\text{gm}$$ for 2mg/mL

For a collagen concentration of 3mg/mL and a pH of 7.4:

$$9\text{ kPa} \times \frac{1000\text{ Pa}}{1\text{ kPa}} = 9000\text{ Pa} \times \frac{1\text{ N/m}^2}{1\text{ Pa}} = 9000\text{ N/m}^2$$

$$9000\frac{\text{N}}{\text{m}^2} \times 7 \times 10^{-6}\text{m}^2 = 0.063\text{N}$$

To convert to mass:

$$\frac{0.063\text{N}}{9.81\frac{\text{m}}{\text{s}^2}} = 6.422 \times 10^{-3}\text{kg}$$

$$0.006422\text{kg} \times \frac{1000\text{gm}}{1\text{kg}} = 6.422\text{gm}$$ for 3mg/mL

From looking at Figure 11, the higher the pH value (more basic), then the higher the failure stress. The conclusion is: the higher the collagen concentration the higher the load needs to be.

Reference : Properties of Engineered Vascular Constructs made from collagen, fibrin, and collagen-fibrin mixtures. Authors: Christopher L. Cummings, Debby Gaulitta, Robert M. Norem. Biomaterials (article in press)

Material : Pure collagen, collagen-fibrin, pure fibrin

ASSUME : Thickness = 0.5mm

$t := 0.5\text{mm}\cdot\frac{1\text{m}}{1000\text{mm}} \qquad t = 5\times 10^{-4}\,\text{m}$

using our example base: 0.009567m

$\text{Area} := A$

$b := 0.009567\text{m} \qquad A := t\cdot b$

$A = 4.784\times 10^{-6}\,\text{m}^2$

For Pure Collagen:
using bovine type I collagen in gel formation

At 2mg/mL the Ultimate Tensile Stress can be calculated by:

$$37\ \text{kPa} \times \frac{1000\ \text{Pa}}{1\ \text{kPa}} \times \frac{1\ \text{N/m}^2}{1\ \text{Pa}} = 37000\ \text{N/m}^2$$

$$37000\cdot\frac{\text{N}}{\text{m}^2}\times 5\times 10^{-6}\,\text{m}^2 = 0.185\text{N}$$

To convert to mass:

$$\frac{0.185\text{N}}{9.81\,\frac{\text{m}}{\text{s}^2}} = 0.01886\text{kg}$$

Converting to grams:

$$0.01886\text{kg}\times\frac{1000\text{gm}}{1\text{kg}} = 18.86\text{gm}$$

At 4 mg/ML the Ultimate Tensile Stress can be calculated by:

$$20 \text{ kPa} \times \frac{1000 \text{ Pa}}{1 \text{ kPa}} \times \frac{1 \text{ N/m}^2}{1 \text{ Pa}} = 20000 \text{ N/m}^2$$

$$20000\frac{\text{N}}{\text{m}^2} \times 5 \times 10^{-6}\text{m}^2 = 0.1\text{N}$$

To convert to mass:

$$\frac{0.1\text{N}}{9.81\frac{\text{m}}{\text{s}^2}} = 0.010194\text{kg}$$

To convert to grams:

$$0.010194\text{kg} \times \frac{1000\text{gm}}{1\text{kg}} = 10.194\text{gm}$$

Determining the RIGHT force transducer

It is critical to figure out which force transducer will fit in our design system.

After deciding to order the force transducer from FUTEK, we had to calculate some numbers to determine which load cells to order. The measurements came in in-oz.

$$1\,g\cdot cm\cdot 2.54\frac{in}{1\,cm} = 2.54\,g\cdot in$$

$$2.54g\cdot in\frac{lb}{454g} = 0.09\,in\cdot oz$$

Load $\quad L := 0.09in\cdot oz$

The diamter of the transducer is 50 mm so the radius is 25 mm.

The calculations based on literature review portrays a range from 0.3 g to 40 g. Therefore, to be safe, we decided to use the load cell of 50 g for the force transducer.

If we assume to have a distance of 4 cm between the water and the force transducer to get the maximum load....

$d := 4cm \qquad L := 50g$

$$Lmax := d\cdot L \qquad Lmax = 200\,g\cdot cm$$

$$Lmax\cdot 2.54\cdot\frac{in}{cm}\cdot\frac{lb}{454\cdot g} = 17.903in\cdot oz$$

Rounding the Lmax to 18 in-oz, this tells us that we do not need a load greater than 20 in-oz.

APPENDIX F-1: Plexiglas® Thermal Conduction

Aluminum Thermal Conductivity = k3

$$q := 90W \qquad k_3 := 250\frac{W}{m \cdot K} \qquad A := 36in^2$$

$$s := 0.25in \qquad T_3 := \begin{pmatrix} 323K \\ 333K \\ 343K \\ 350K \\ 353K \\ 363K \end{pmatrix}$$

$$T_2 := -\left(\frac{q \cdot s}{k_3 \cdot A}\right) + T_3 \qquad T_2 = \begin{pmatrix} 322.902 \\ 332.902 \\ 342.902 \\ 349.902 \\ 352.902 \\ 362.902 \end{pmatrix} K$$

Saline Thermal Conductivity = k1

$$q := 90W \qquad k_1 := 0.7\frac{W}{m \cdot K} \qquad A := 36in^2$$

$$T_0 := 310K \qquad s := 1 \cdot mm$$

$$T_1 := \left(\frac{q \cdot s}{k_1 \cdot A}\right) + T_0 \qquad T_1 = 315.536K$$

Plexiglas Thermal Conductivity = k2

$$q := 90W \qquad k_2 := 0.18\frac{W}{m \cdot K} \qquad A := 36in^2$$

$$s := \frac{\left[\left(T_2 - T_1\right) \cdot k_2 \cdot A\right]}{q} \qquad s = \begin{pmatrix} 0.342 \\ 0.807 \\ 1.271 \\ 1.596 \\ 1.736 \\ 2.2 \end{pmatrix} mm$$

$0.0625in = 1.587mm$

$350 - 273 = 77$

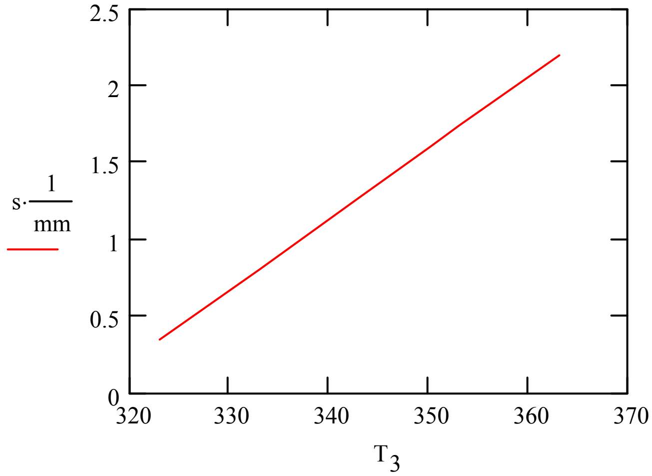

The temperature of the outside of the aluminum plate will have to be approximately 77 C to maintain a temperture of 37 C in the saline solution.

APPENDIX F-2: Mylar Thermal Conduction

Calculations for heat transfer using Mylar instead of Plexiglass

$T_o := 310.15K \qquad q := 90W \qquad Area := 36 \cdot in^2 \qquad Area = 0.023m^2$

Saline Thickness = Ss $\qquad S_s := 1 \cdot mm \qquad S_s = 1 \times 10^{-3} m$

Saline Thermal Conductivity = ks $\qquad k_s := 0.7 \cdot \frac{W}{m \cdot K}$

Mylar Thickness = Sm $\qquad S_m := 0.1 \cdot mm \qquad S_m = 1 \times 10^{-4} m$

Mylar Thermal Conductivity = km $\qquad k_m := 0.155 \cdot \frac{W}{m \cdot K}$

Aluminum Thickness = Sa $\qquad S_a := 0.25 \cdot in \qquad S_a = 6.35 \times 10^{-3} m$

Aluminum Thermal Conductivity = ka $\qquad k_a := 250 \cdot \frac{W}{m \cdot K}$

Heat through saline:

$$T_1 := \frac{(q \cdot S_s)}{k_s \cdot Area} + T_o \qquad T_1 = 315.686K$$

Heating through mylar:

$$T_2 := \frac{S_m \cdot q}{k_m \cdot Area} + T_1 \qquad T_2 = 318.186K$$

Heating through aluminum

$$T_3 := \frac{S_a \cdot q}{k_a \cdot Area} + T_2 \qquad T_3 = 318.284K$$

$$318.284 - 273 = 45.284$$

$T_3 := 45.3 \cdot C$

The bath will only need to go up to
45.3 C to get the sample
area at body temperature of 37 C.

APPENDIX G-1: Pivot Mechanism

Component Required:
- Vee Jewel Assembly
- Vee Jewel Bearings
- Vee Jewel Pivots

Fabricated Components:
- Pulley Frame
- Pulley
- Short Arm

- Vee Jewels and Teflon purchased from Smallparts.com
- Pivot Mechanism should be machined from Lexan, not Acrylic
- For plastic: Plastics Unlimited Inc. in Worcester
- For metal: Peterson Steel corporation in Worcester

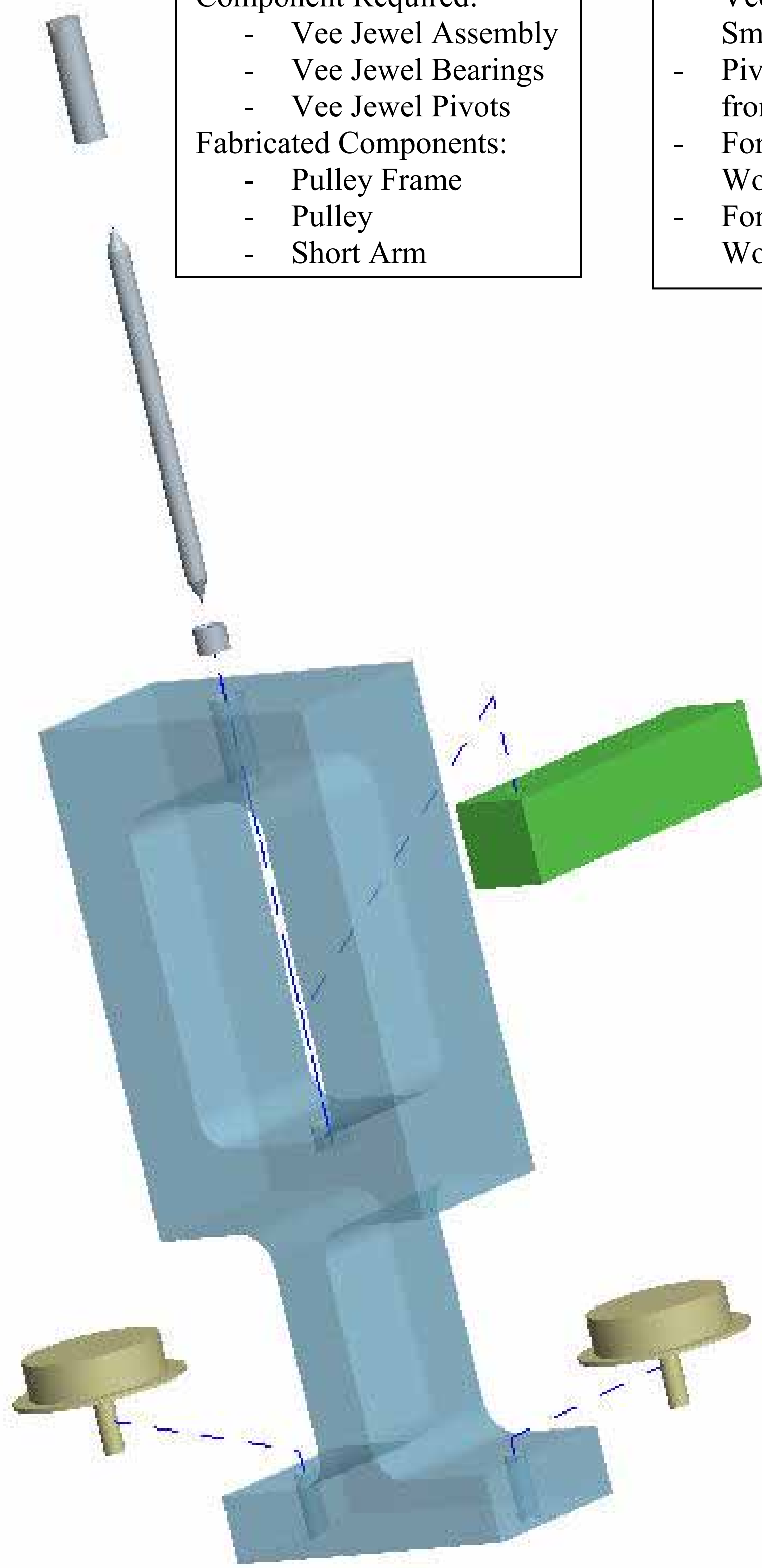

APPENDIX G-2: Bearings - Vee Jewel Assembly

BEARINGS - Vee Jewel Assembly

http://www.smallparts.com/products/descriptions/vja%2dhst.cfm

Set in Brass, Vee Jewel Assemblies are screw mounted. Spring loaded assemblies are recommended in an environment of shock and vibration. The Beryllium Copper spring acts as a shock absorber and permits the jewel and pivot to move without breaking and then return to its normal position. Non-spring loaded screw mounted assemblies are typically used in a more stable environment. Pivot not included.

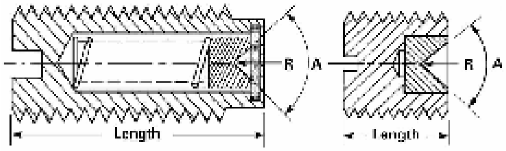

BRASS

Part No.	Angle (A)	Dimensions in Inches			Screw Size	Price	
		Radius (R)	Length	Vee Depth		Each	5
VJA-1	80/85°	.003/.004	0.172	0.015/0.020	#2-80 UNS-3A (rigid)	7.00	26.25
VJA-3	80/85°	.003/.004	0.175	0.015/0.020	#2-80 UNS-3A (spring loaded)	7.00	26.25
VJA-5	80/85°	.003/.004	0.250	0.015/0.020	#5-40 UNC-2 (rigid)	8.00	30.00
VJA-7	85/95°	.008/.012	0.750	0.025/0.030	#10-32 (spring loaded)	12.00	45.00

Also available on the **Small Parts, Inc** Line: Stainless Steel Vee Jewels and Vee Jewel Sapphire Bearings .

TAPS FOR VEE JEWEL ASSEMBLY — High Speed Steel

Part No.	Size/Thread	Flutes	Price	
			Each	5
HST-0280	2-80 NS	3	40.10	180.35
HST-0540	5-40 NC	3	5.60	25.50
HST-1032	10-32 NF	4	4.35	19.70

VJA-1 selected

BEARINGS - Vee Jewel, Sapphire

http://www.smallparts.com/products/descriptions/vj.cfm

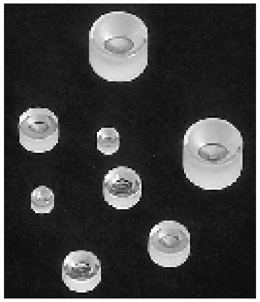

Synthetic sapphires are next to diamonds in hardness which makes these highly polished bearings scratch and shock resistant. They also have a long wear life, and are highly resistant to heat, corrosion and distortion. In addition, sapphire bearings are nonmagnetic, dielectrically strong and provide good shaft end support and freedom of motion. They are especially well suited for use in delicate instruments such as ammeters, voltmeters, compasses and precision indicator devices.

The jewel radius should be 2.5 to 3 times the pivot radius. In general, the greater the ratio between jewel and pivot, the greater the sensitivity and pivot roll. The contact area of the pivot should be highly polished and a finish of 2 to 3 micro-inch on the pivot radius is recommended.

Properties

Melting Point	3722°F (2050°C)
Specific Gravity	3.98
Scratch Hardness (Mohs' Scale)	9
Compressive Strength	300,000 psi at 25°C (77° F)
Thermal Conductivity	100°C=.06 cal cm./sec ° C cm^2

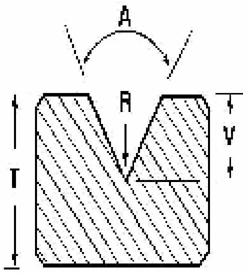

VJ-0469 selected

Synthetic Sapphire

Part No.	Angle (A)	Dimensions in Inches: O.D.	Thickness (T)	Vee Depth (V)	Radius (R)	Price: Each	5
VJ-0469	75/85°	.0469/.0472	.0374/.0394	.0138/.0177	.0020/.00331	$8.55	$35.50
VJ-0787	85/95°	.0787/.0791	.0433/.0453	.0250/.0300	.0080/.0120	$6.00	$23.90
VJ-0800	85/95°	.0800/.0803	.0450/.0500	.0200/.0300	.0080/.0120	$9.25	$38.45
VJ-1244	90/95°	.1244/.1256	.0880/.0930	.0450/.0550	.0059/.0099	$14.00	$52.50

STAINLESS STEEL VEE JEWEL PIVOTS

http://www.smallparts.com/products/descriptions/vjpx.cfm

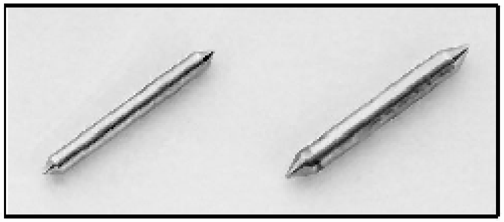

These double-pointed pivots are used in conjunction with Vee Jewel and Vee Jewel Assemblies found under part numbers VJ, VJA, HST. To keep friction at a minimum, the radius in the pit of the Vee of the Jewel should be approximately three times larger than the radius of the pivot (3:1 ratio).

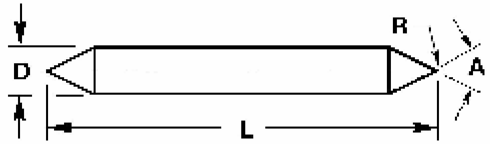

STAINLESS STEEL VEE JEWEL PIVOTS

Part No.	Dimensions in Inches				Price	
	R Radius	D Diameter	L Length	A Angle	Each	5
VJPX-1D	0.00098-0.00012	0.0156-0.0160	0.485-0.495	50°	3.65	14.95
VJPX-2D	0.00069-0.00089	0.0397-0.0403	0.365-0.375	70°	2.60	10.70
VJPX-7D	0.002-0.004	0.0496-0.0501	0.395-0.405	53°	3.70	15.35

Also available on the **Small Parts, Inc** Line:
Vee Jewel Sapphire Bearings, Brass Vee Jewel Bearings & High Speed Tap for Vee Jewel Assembly.

PIVOT	VEE JEWEL	PIVOT	ASSEMBLY
VPJX-1D	VJ-0469	VJPX-1D	VJA-1 VJA-3
VPJX-2D	VJ-0469	VJPX-2D	VJA-5
VJPX-7D	VJ-0787 VJ-0800 VJ-1244	VJPX-7D	VJA-7

VJPX-1D selected

APPENDIX G-3: Dimensions of Pulley Frame

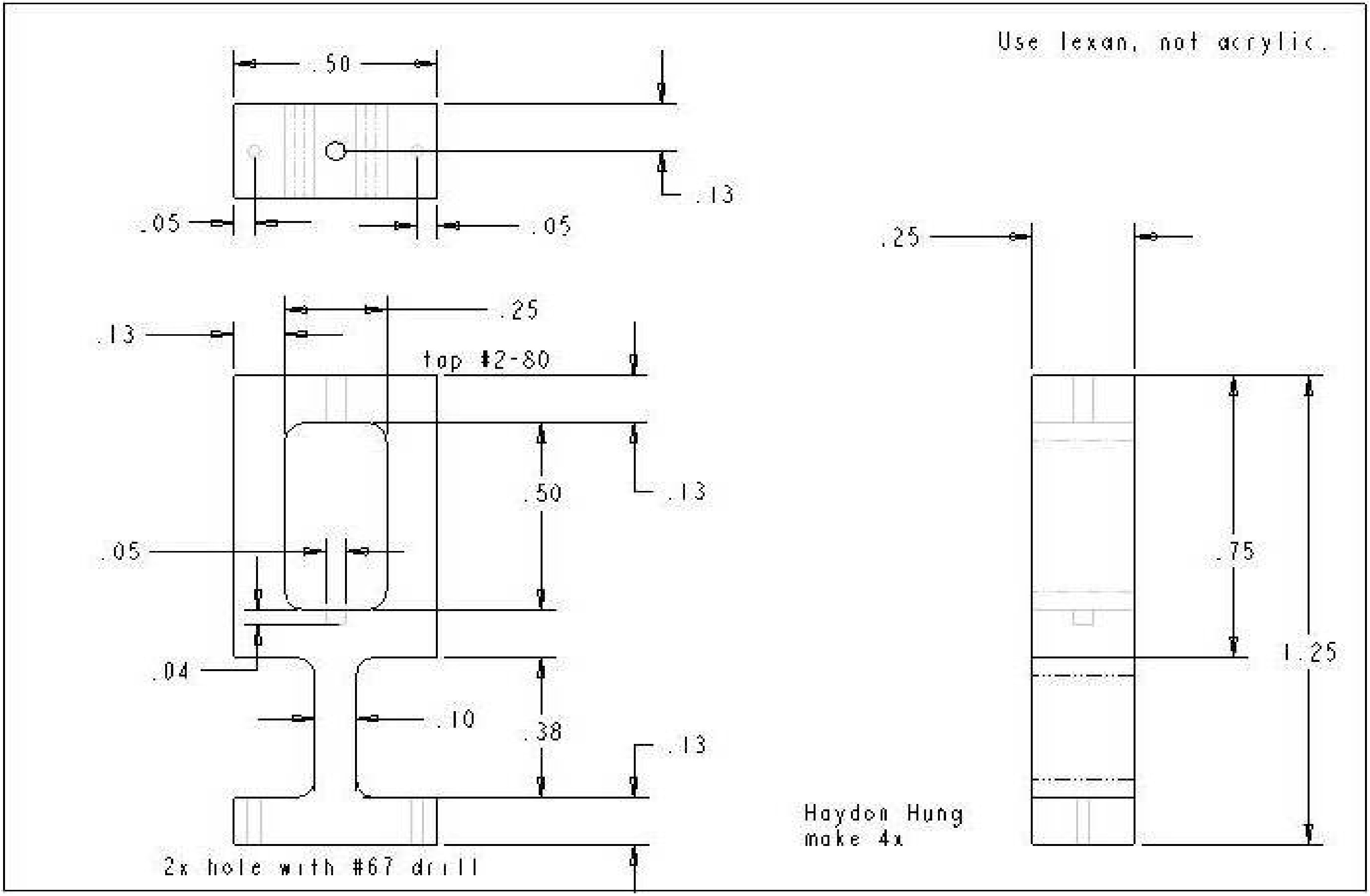

APPENDIX G-4: Dimensions of Pulley

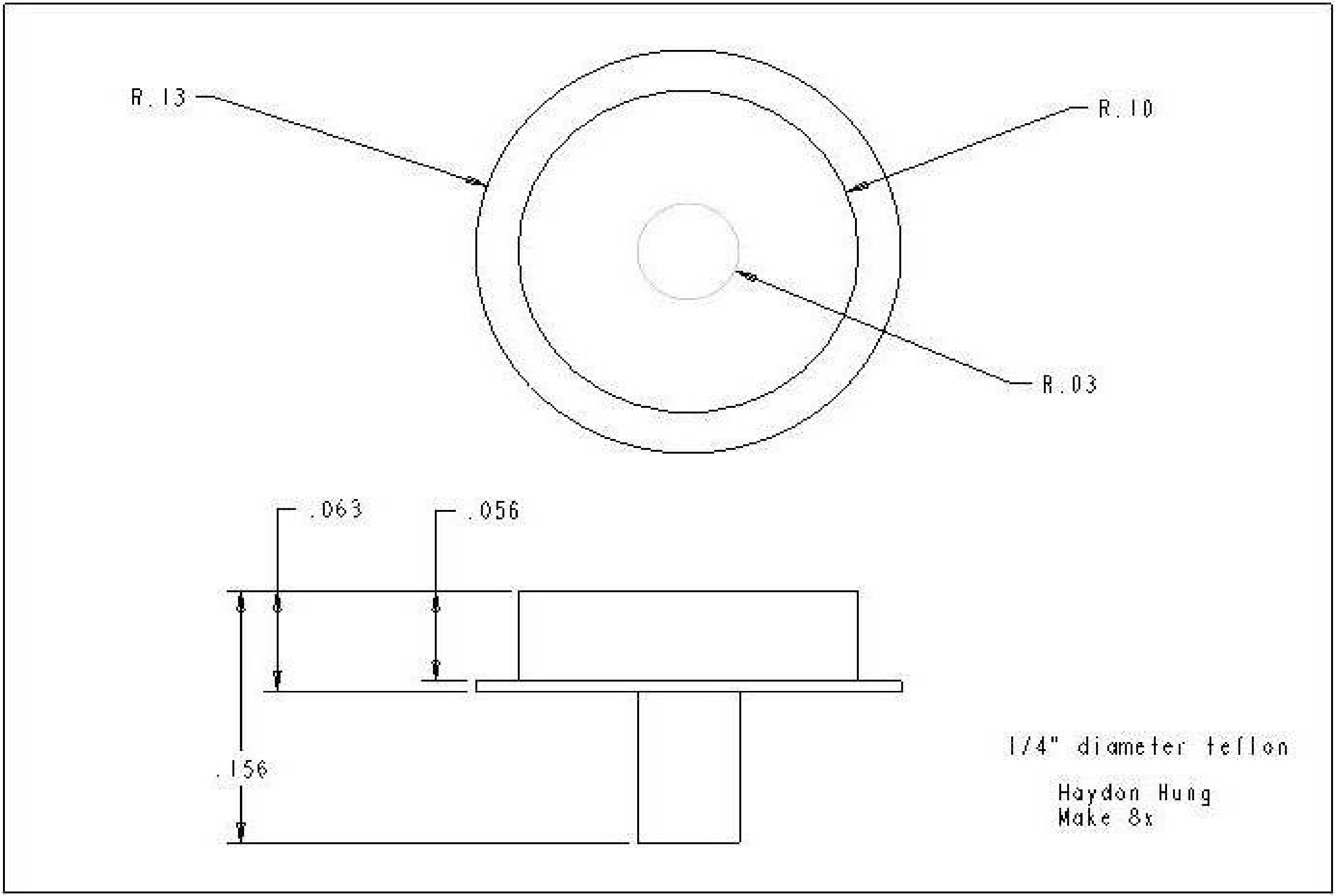

APPENDIX G-5: Assembly of Bath Chamber

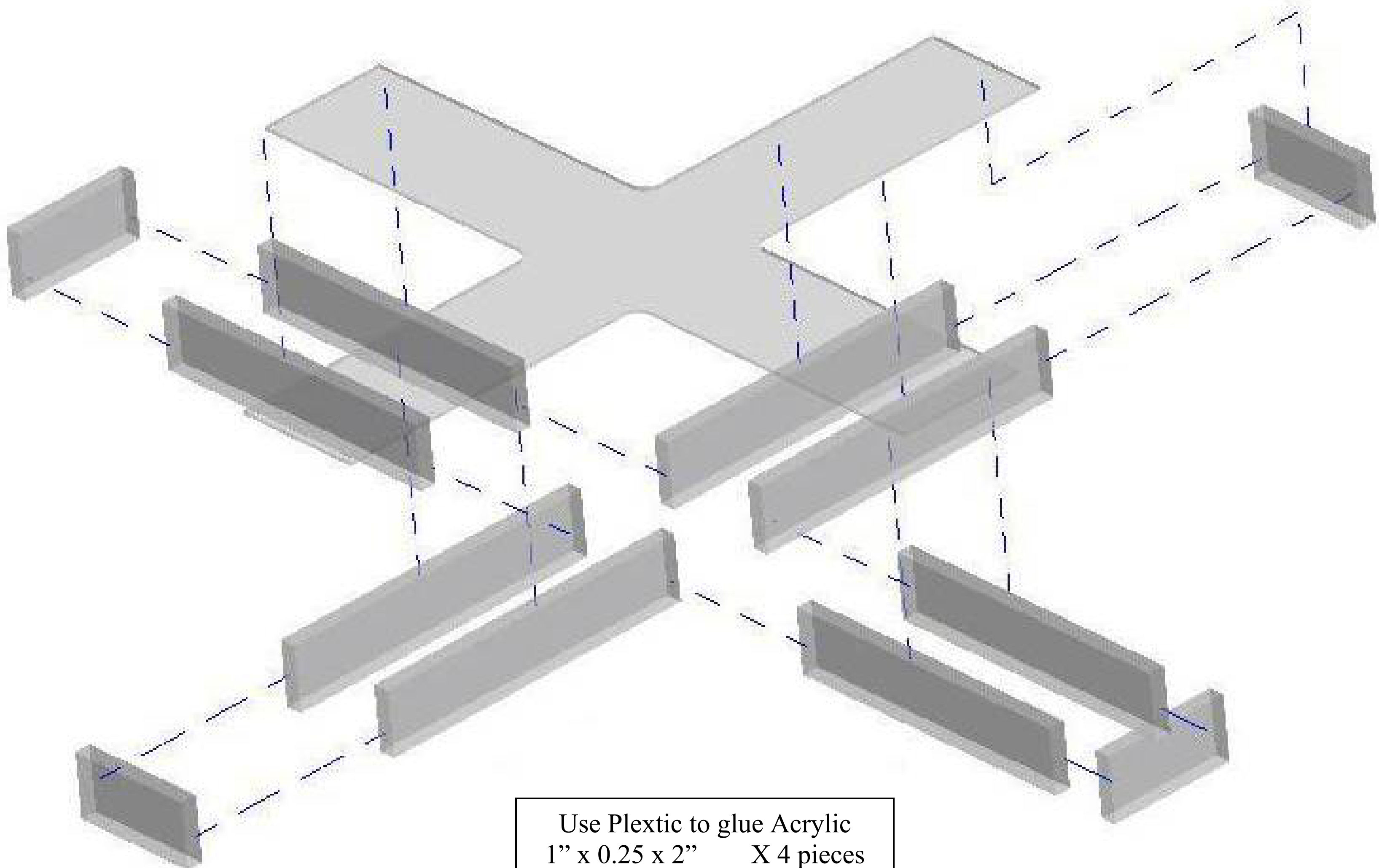

Use Plextic to glue Acrylic	
1" x 0.25 x 2"	X 4 pieces
1" x 0.25 x 4.75"	X 4 pieces
1" x 0.25 x 5"	X 4 pieces

APPENDIX G-6: Dimensions of Chamber Base

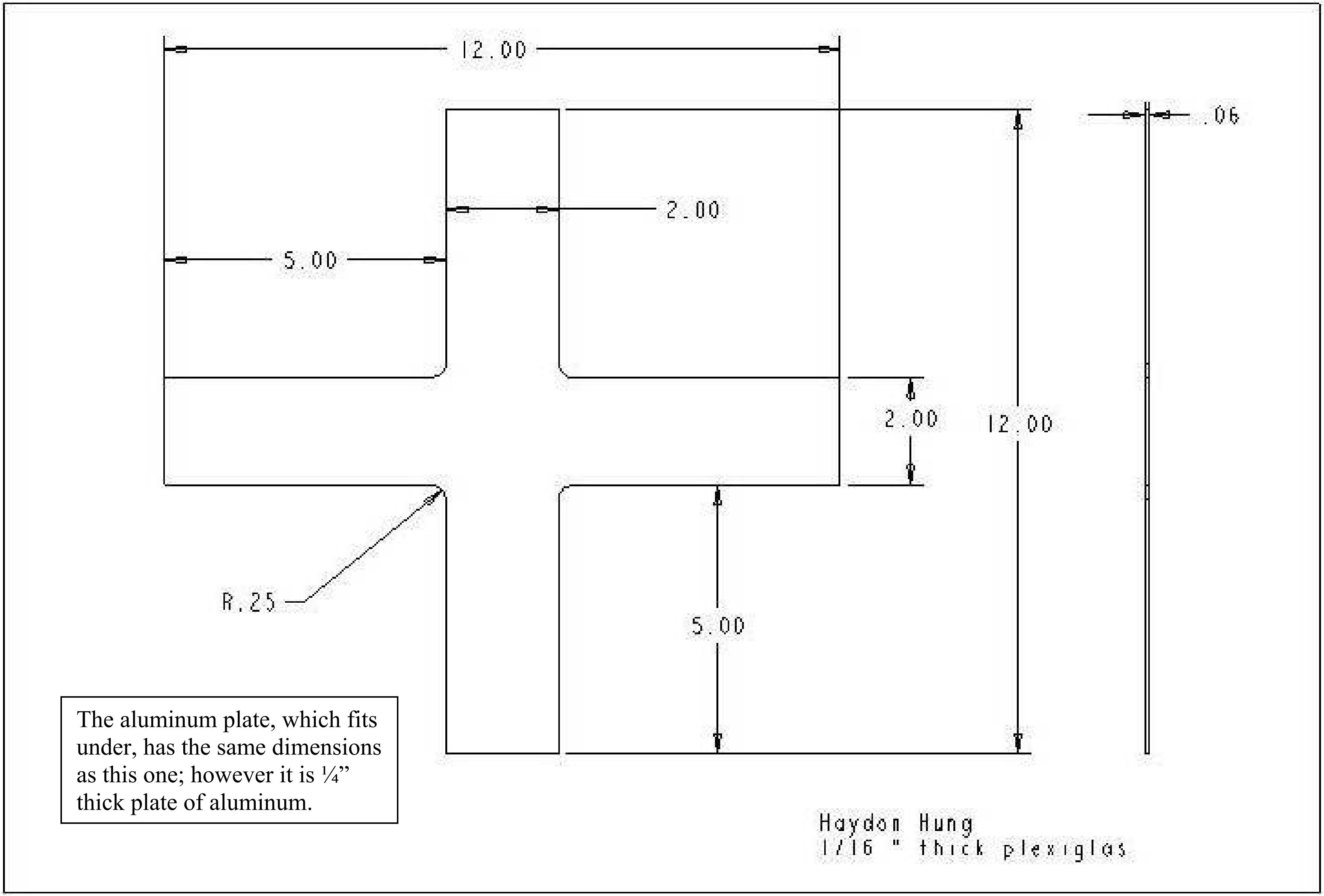

The aluminum plate, which fits under, has the same dimensions as this one; however it is ¼" thick plate of aluminum.

APPENDIX G-7: Dimensions of Framework Pieces

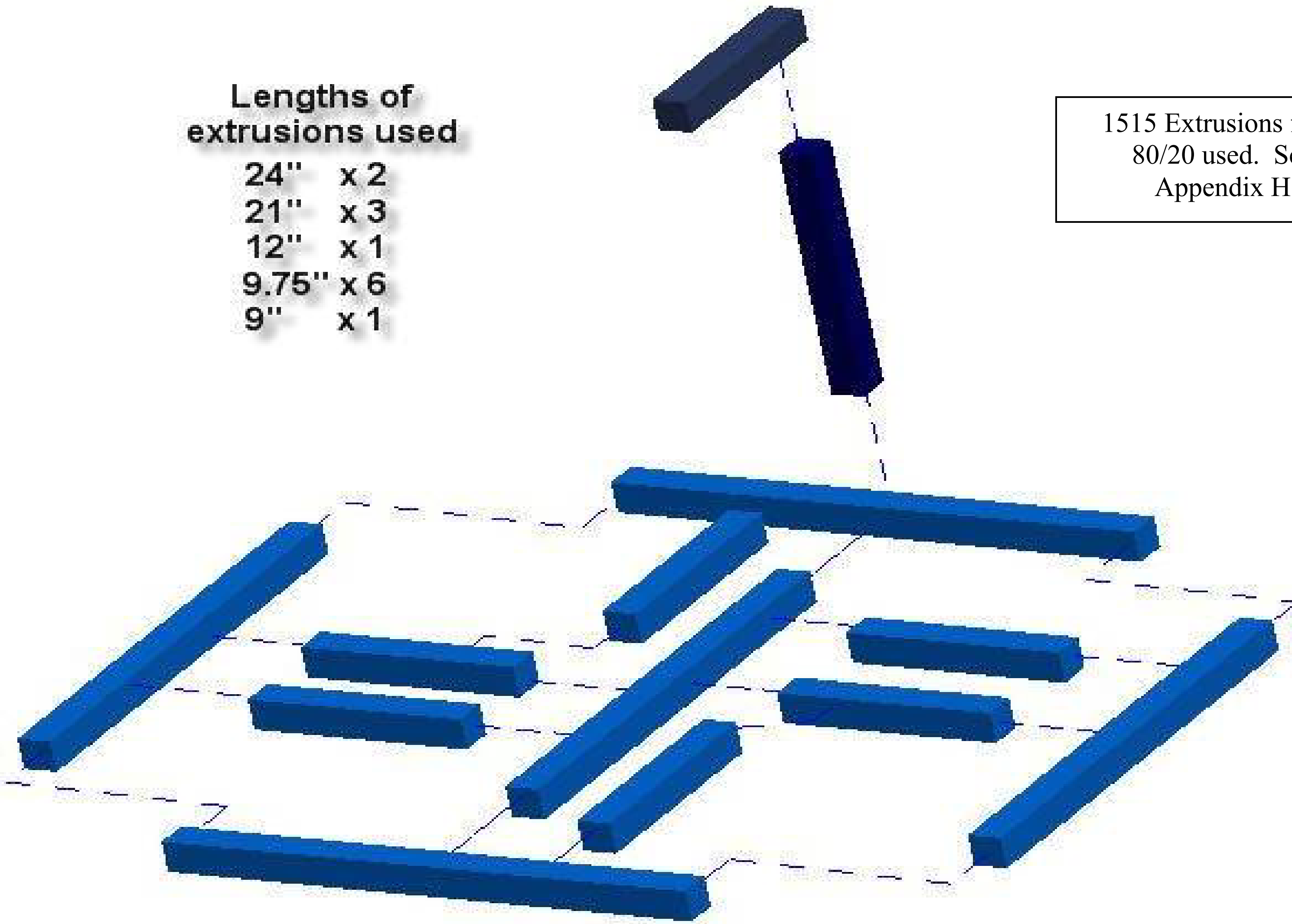

1515 Extrusions from 80/20 used. See Appendix H

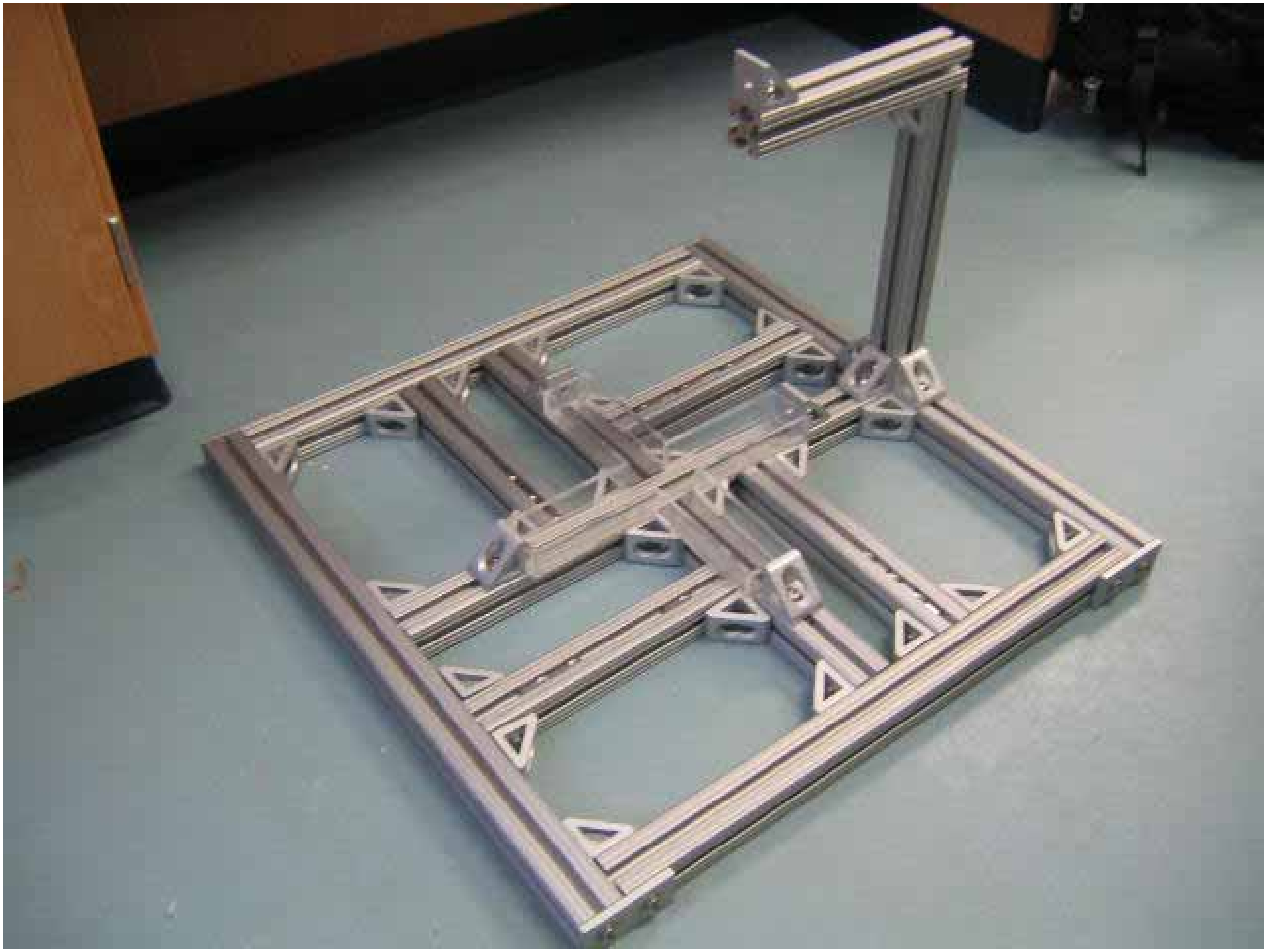

APPENDIX G-8: CAD Drawings of Motor Mounts

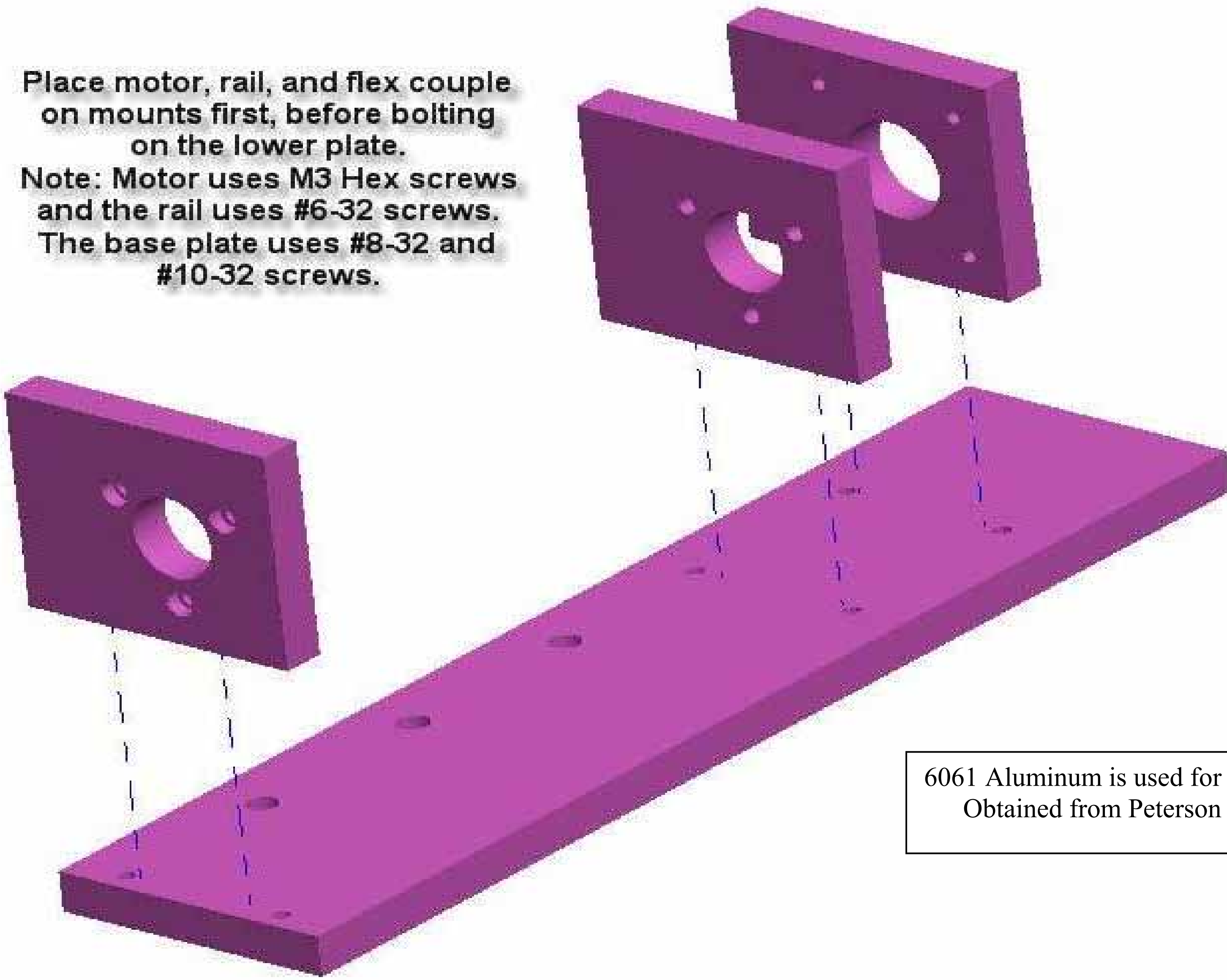

6061 Aluminum is used for all parts.
Obtained from Peterson Steel

APPENDIX G-9: Dimensions for Motor Plates

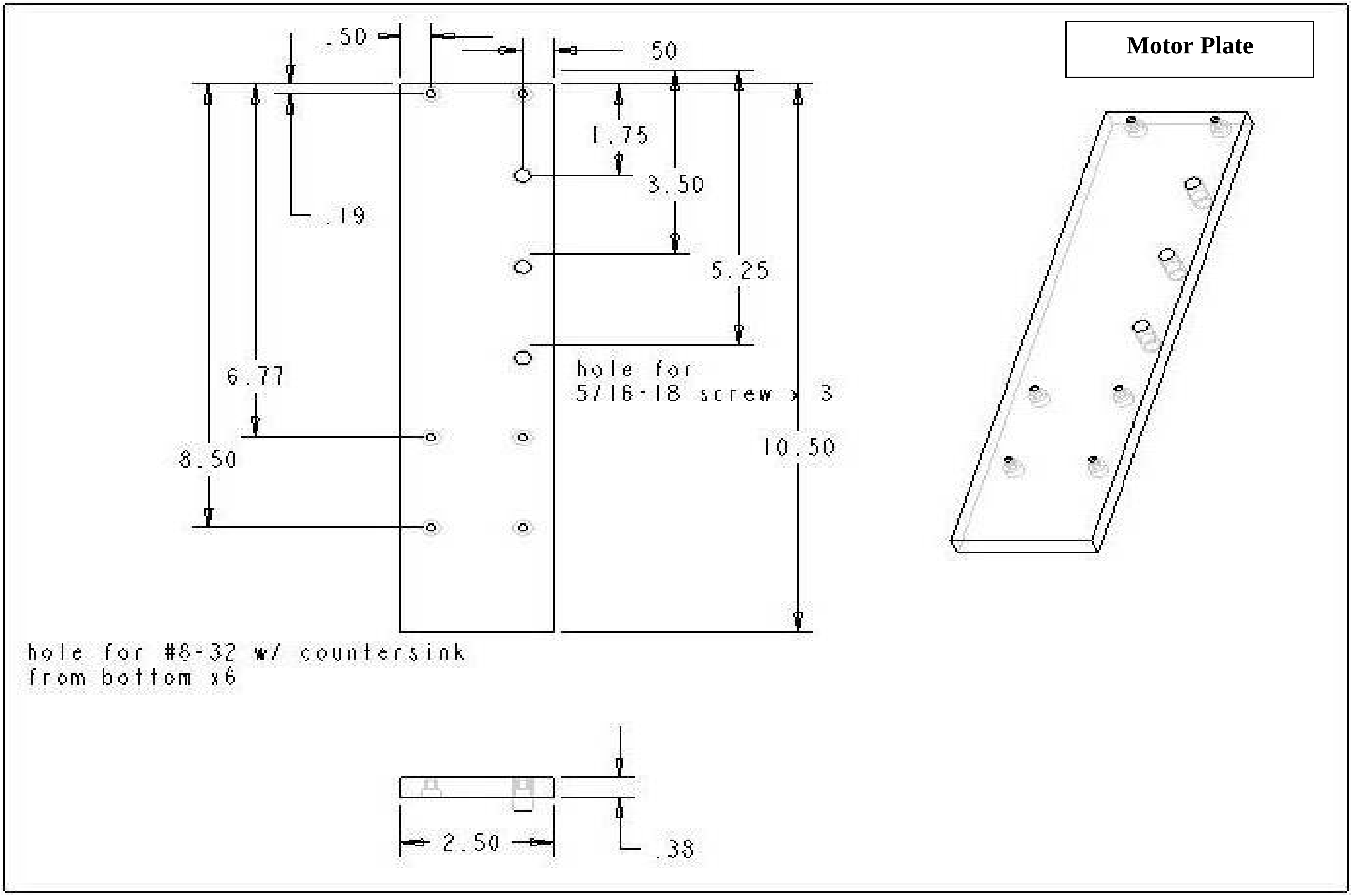

Motor Plate 1

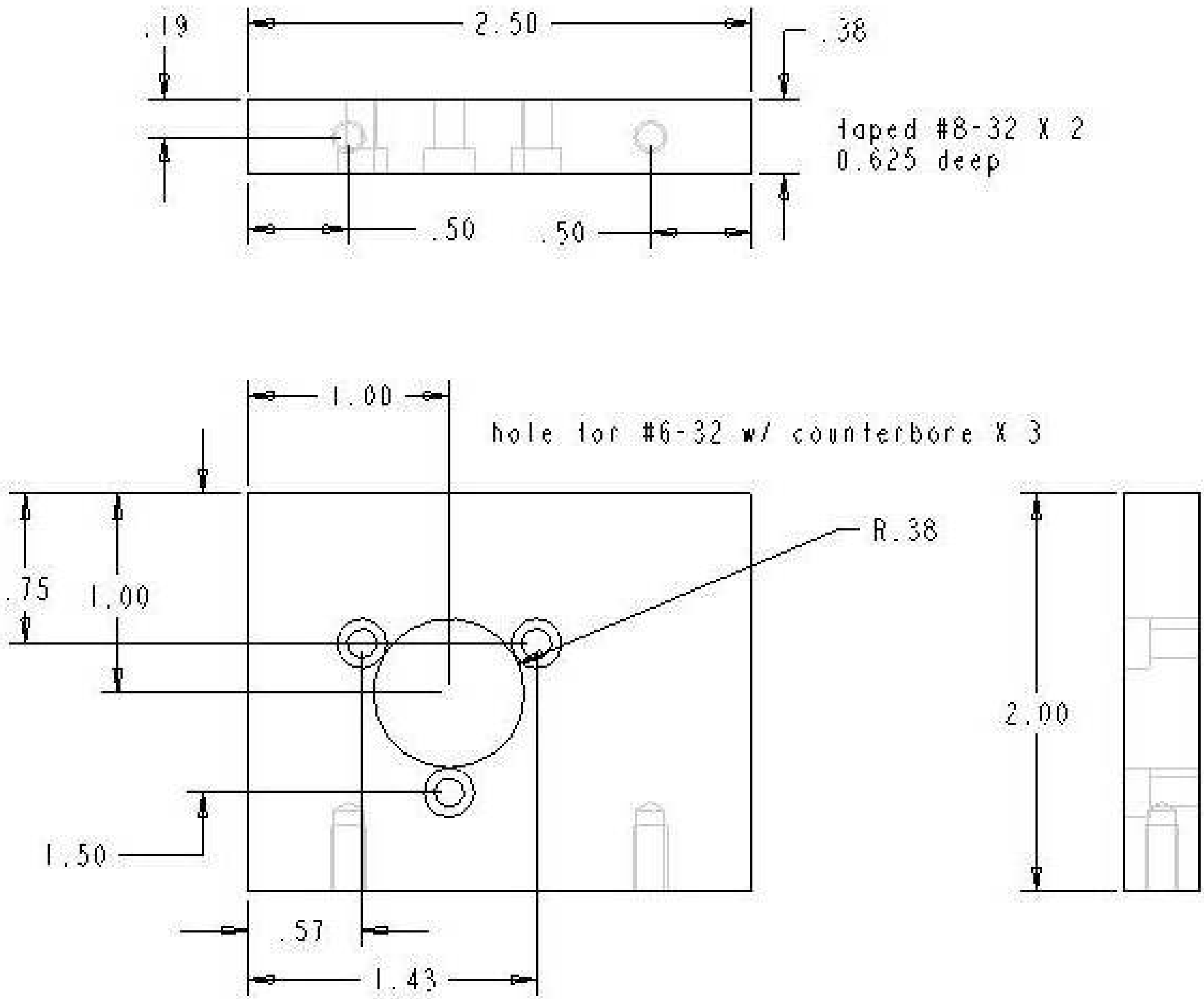

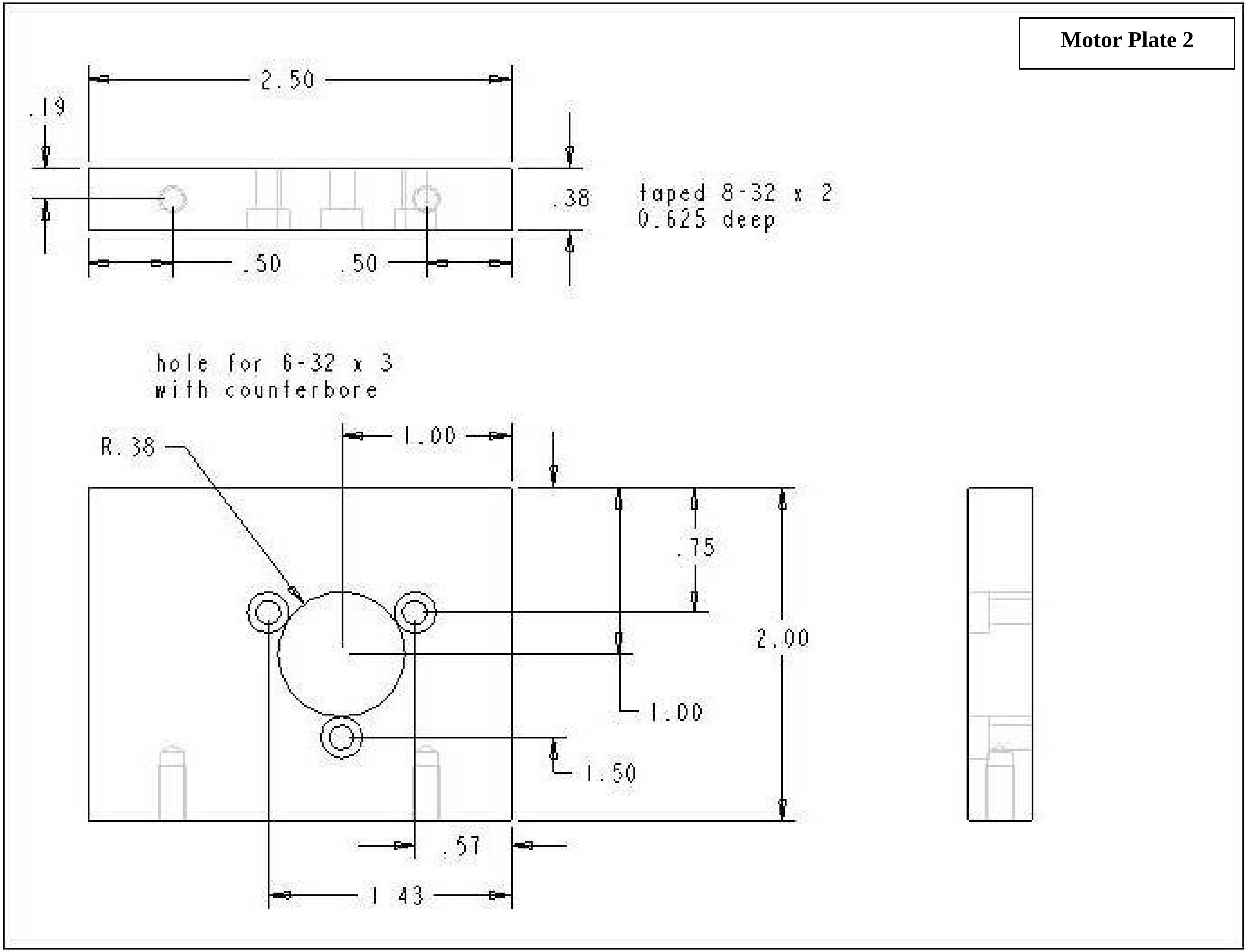
Motor Plate 2
2.50
.19
.38
taped 8-32 x 2
0.625 deep
.50
.50
hole for 6-32 x 3
with counterbore
R.38
1.00
.75
2.00
1.00
1.50
.57
1.43

Motor Plate 3

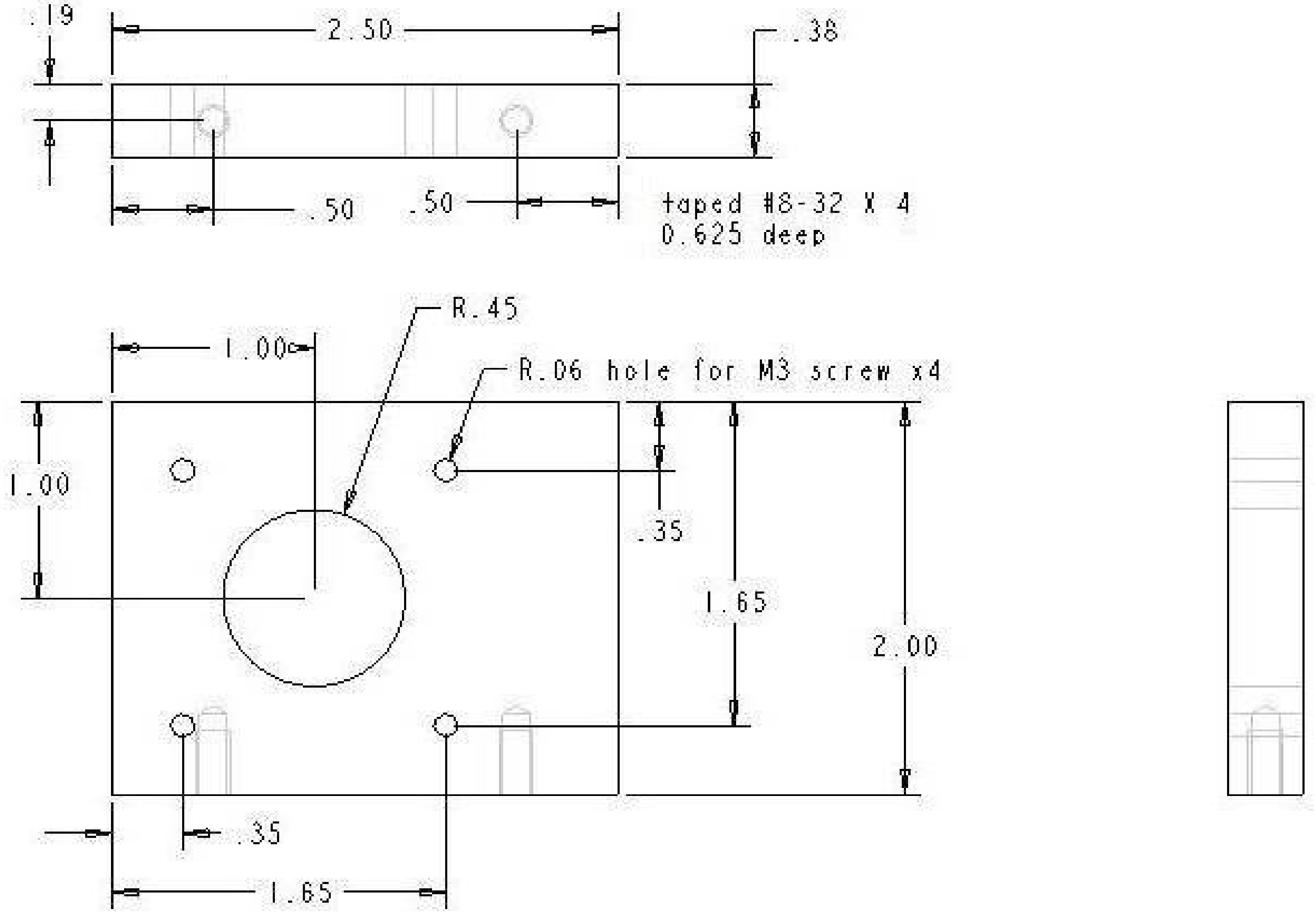

APPENDIX G-10: CAD Drawings of Transducer Mounts

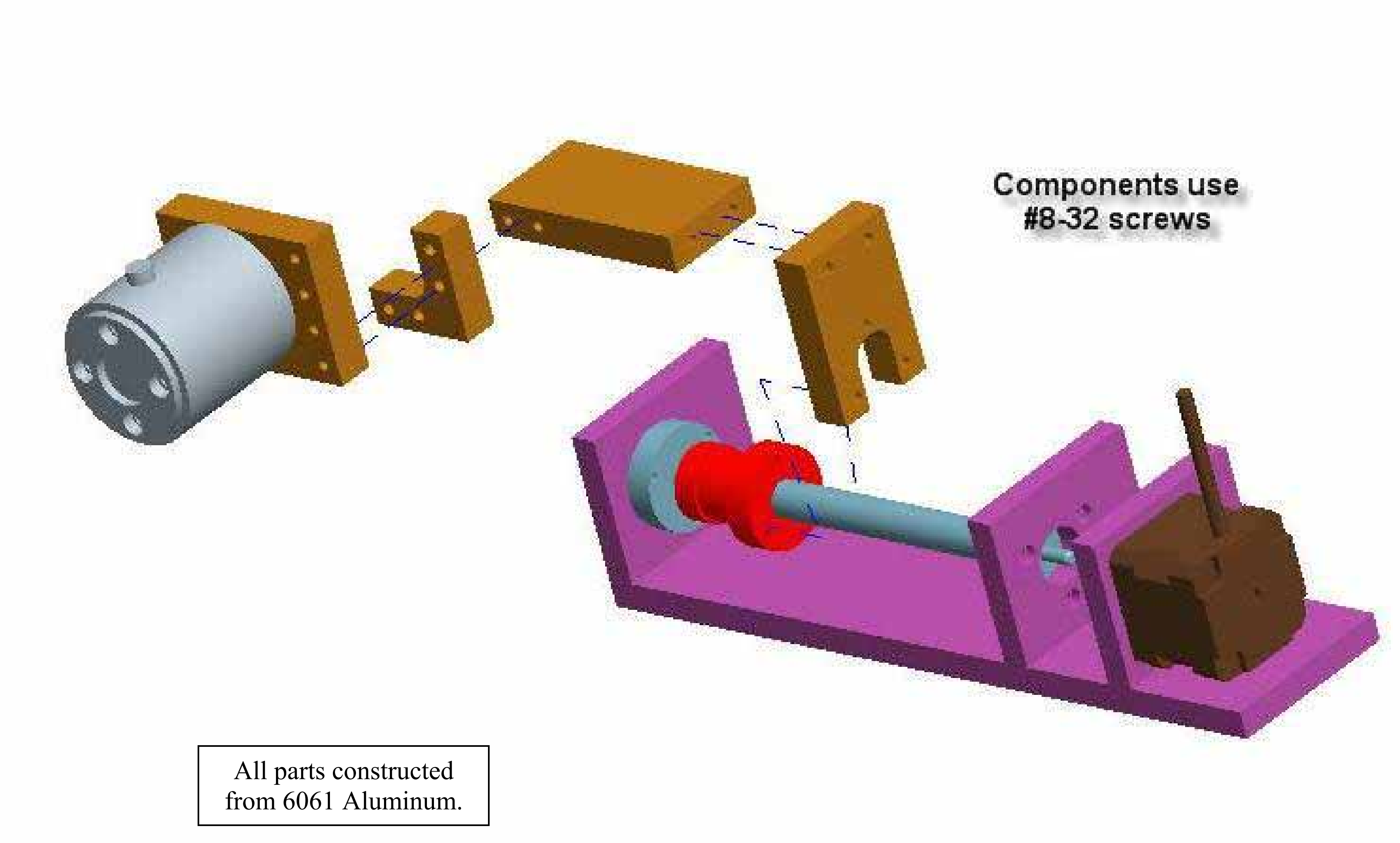

APPENDIX G-11: Dimensions of Transducer Mounts

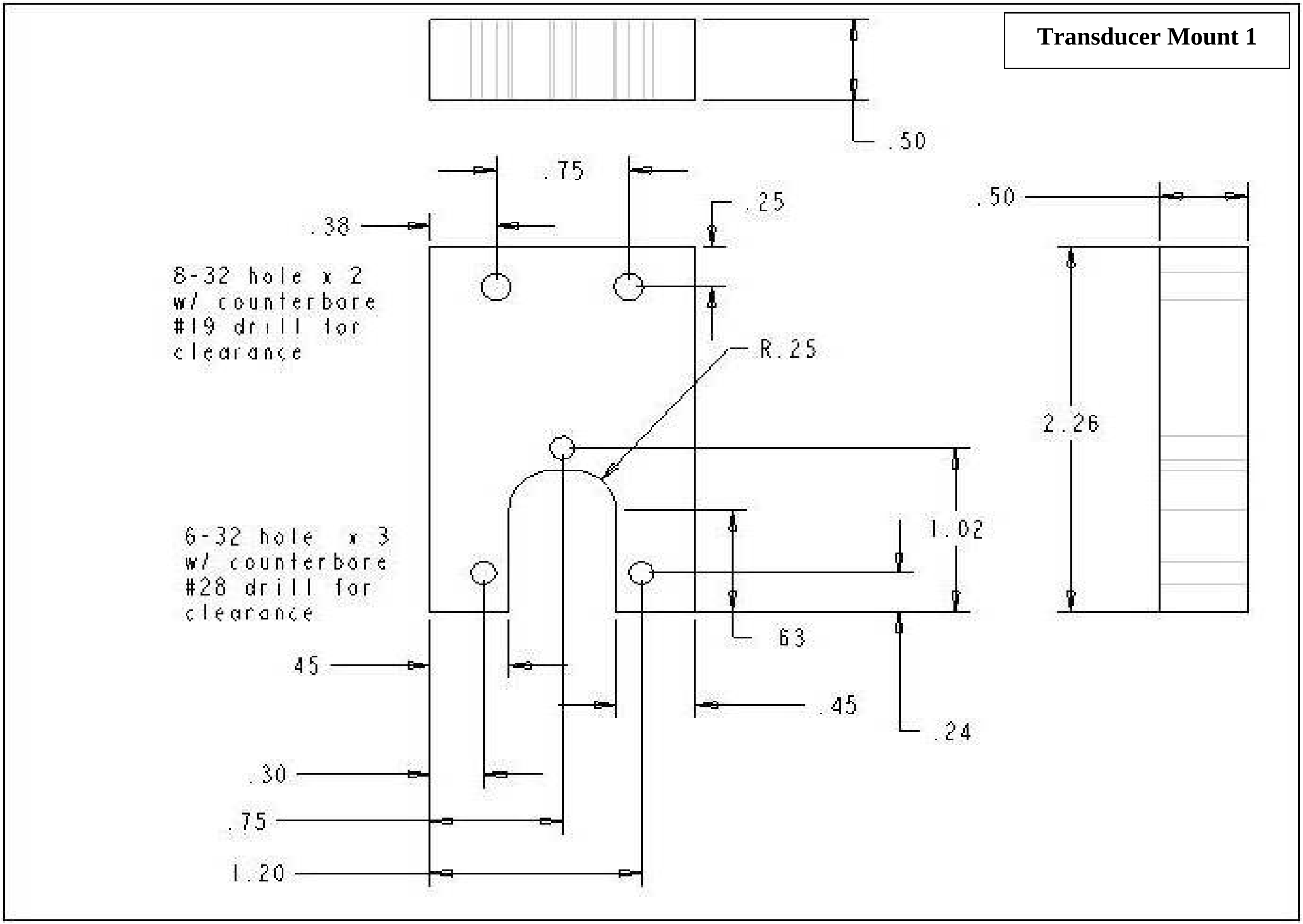

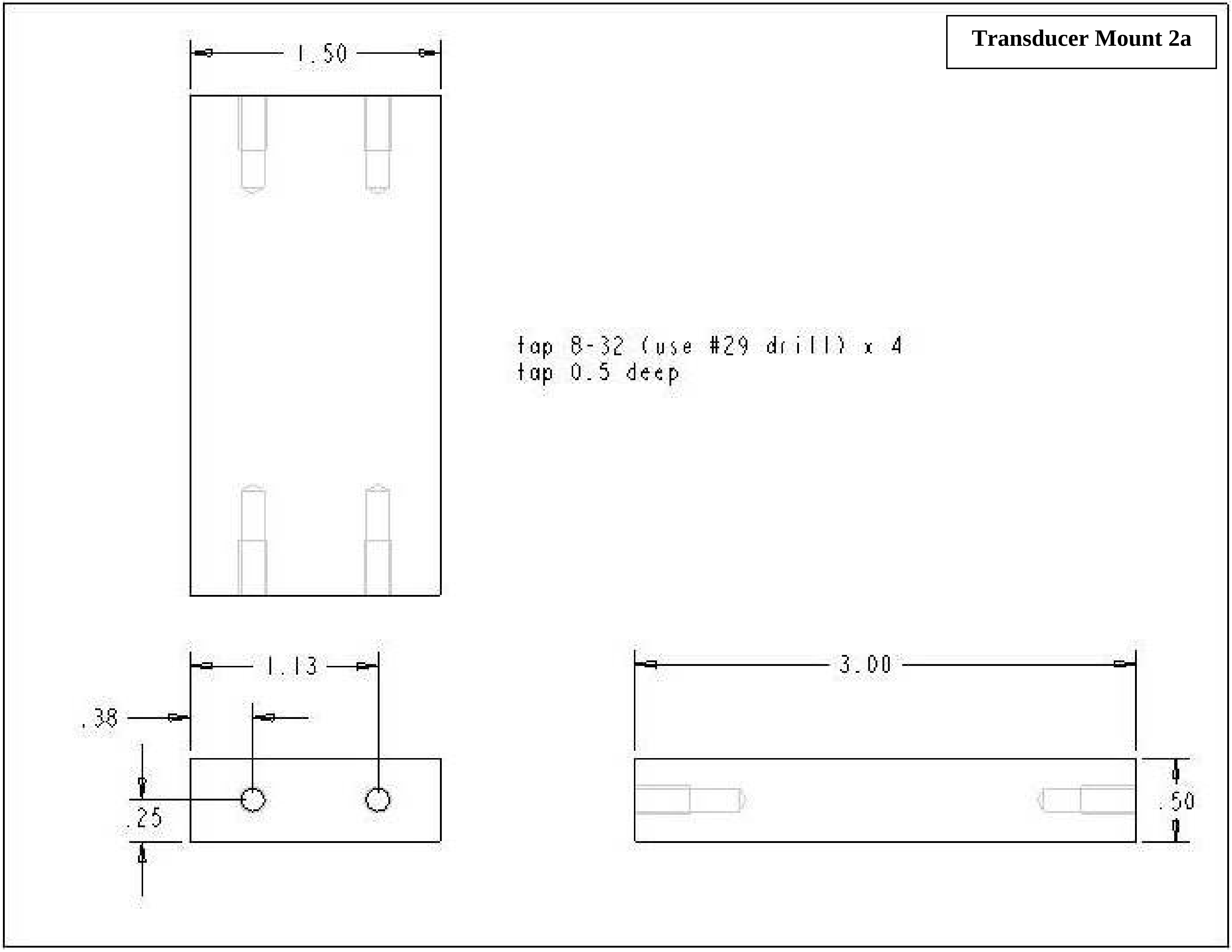
Transducer Mount 2a
1.50
tap 8-32 (use #29 drill) x 4
tap 0.5 deep
1.13
.38
.25
3.00
.50

Transducer Mount 2b
See arm section

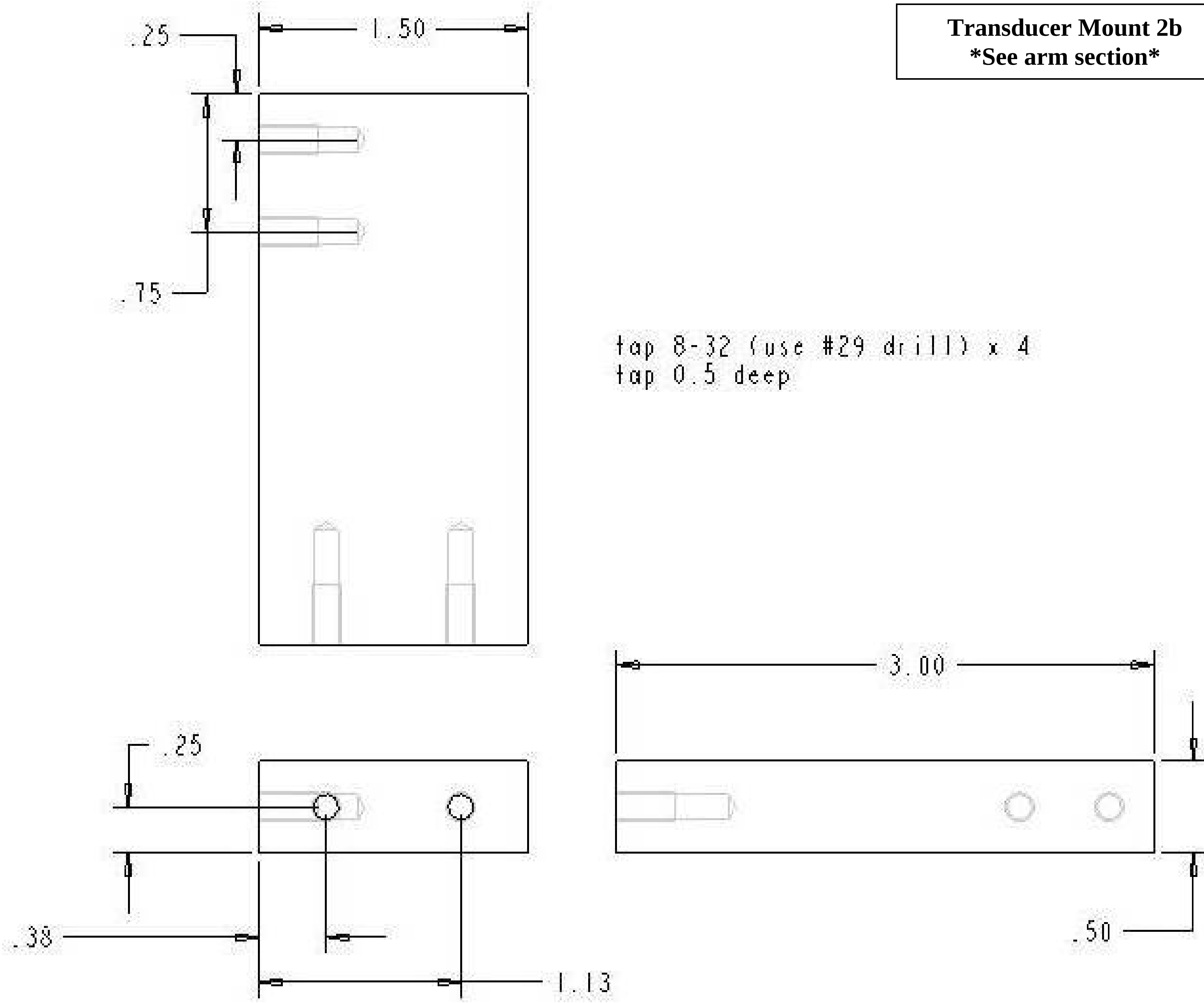

Transducer Mount 3

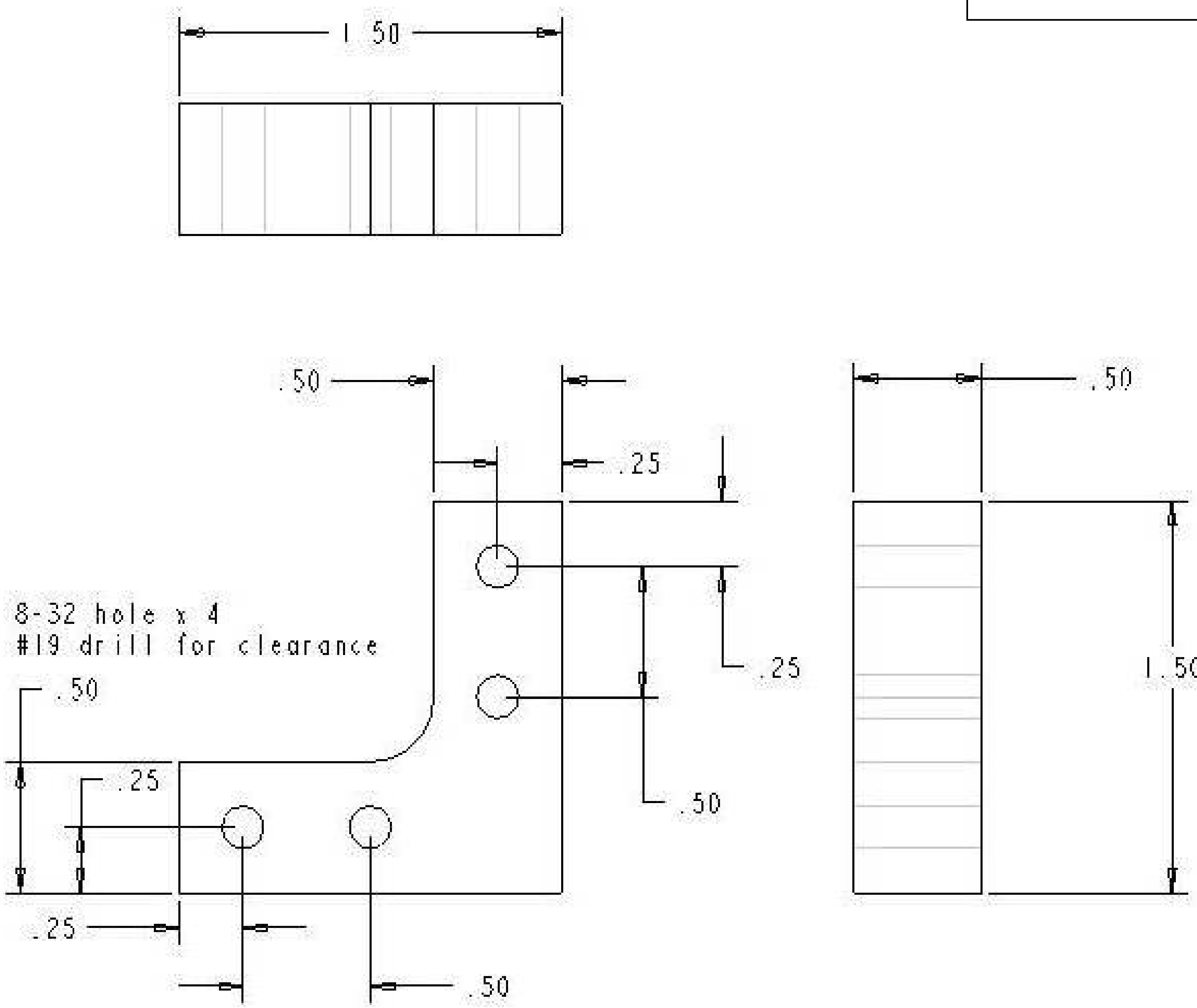

Transducer Mount 4

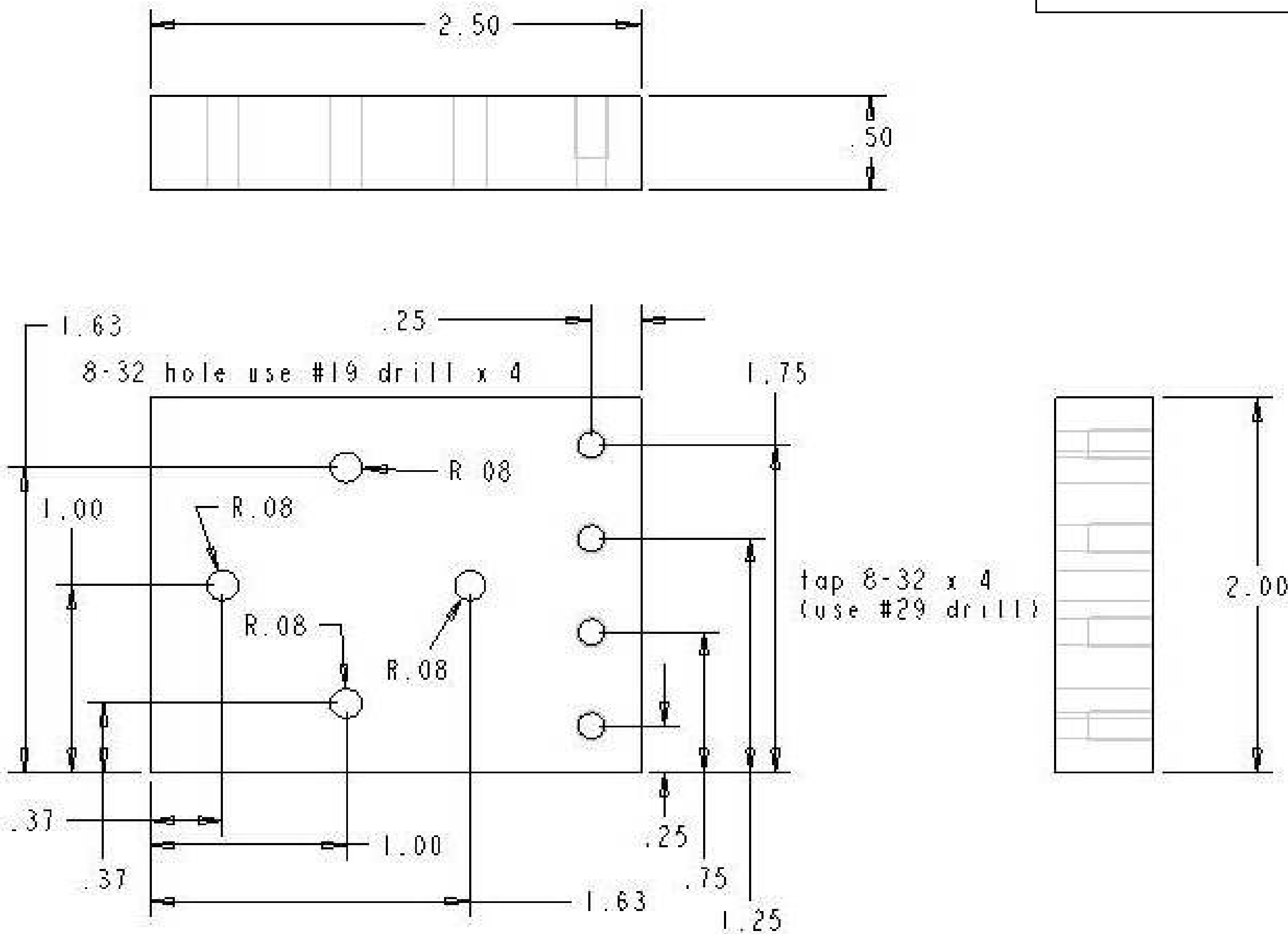

APPENDIX G-12: CAD Drawings for Assembly of Motors and Transducers

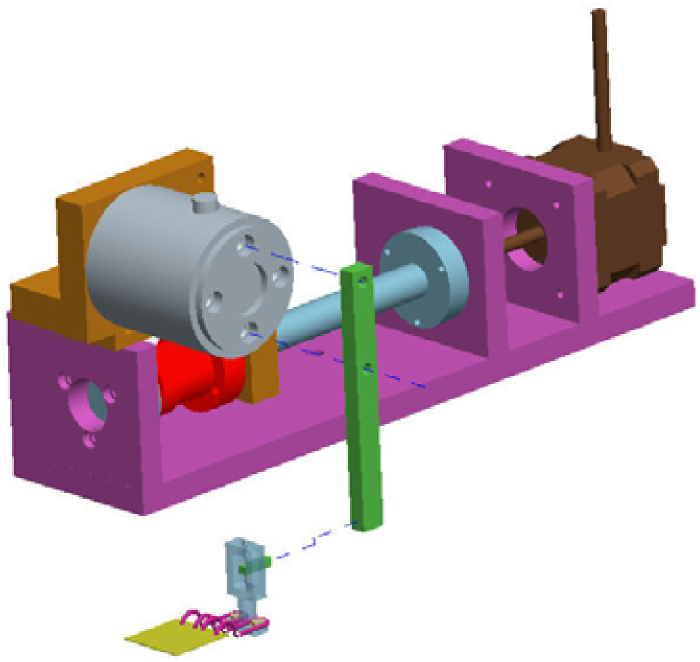

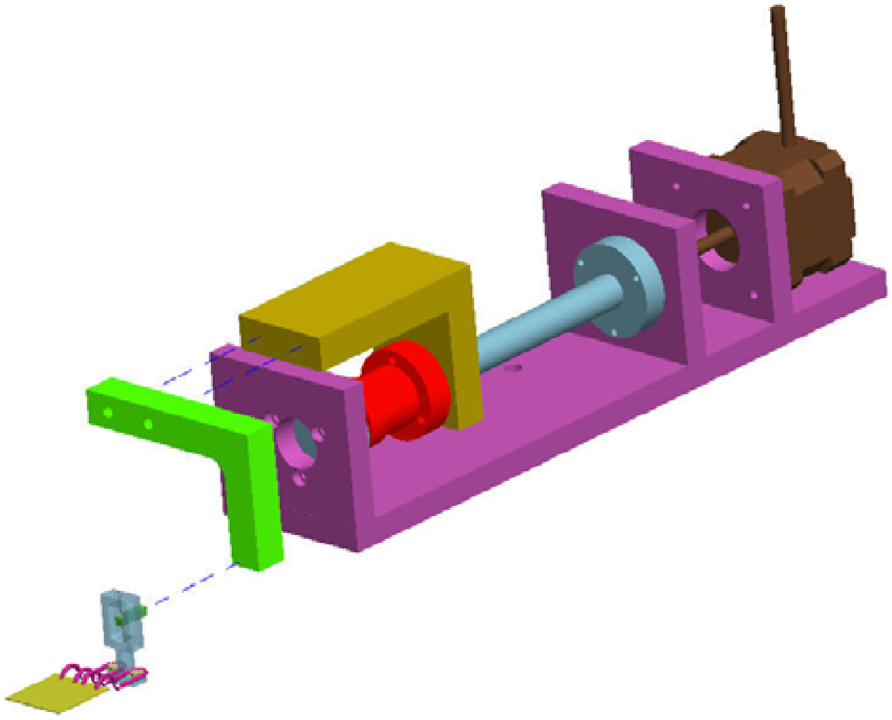

This configuration uses:

- Transducer Mount 1
- Transducer Mount 2a
- Transducer Mount 3
- Transducer Mount 4
- Arm

The short arm from the Pivot Mechanism is glued to each arm. Both arms constructed from plastic.

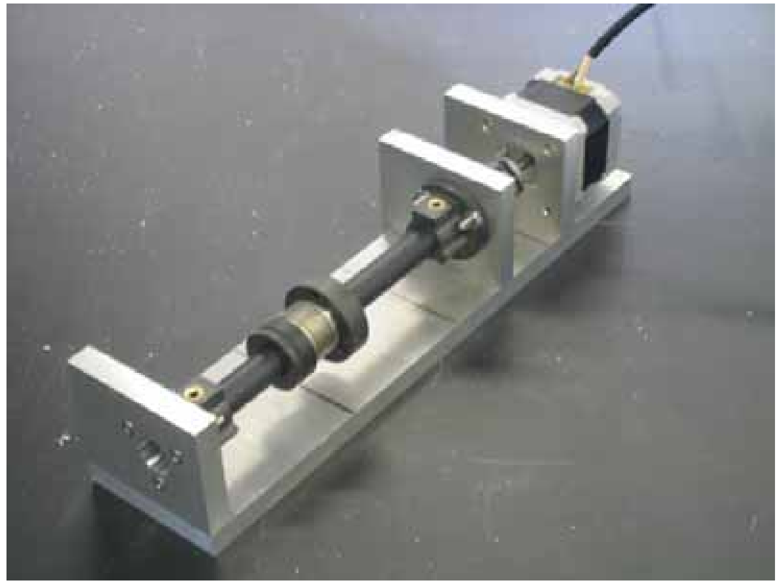

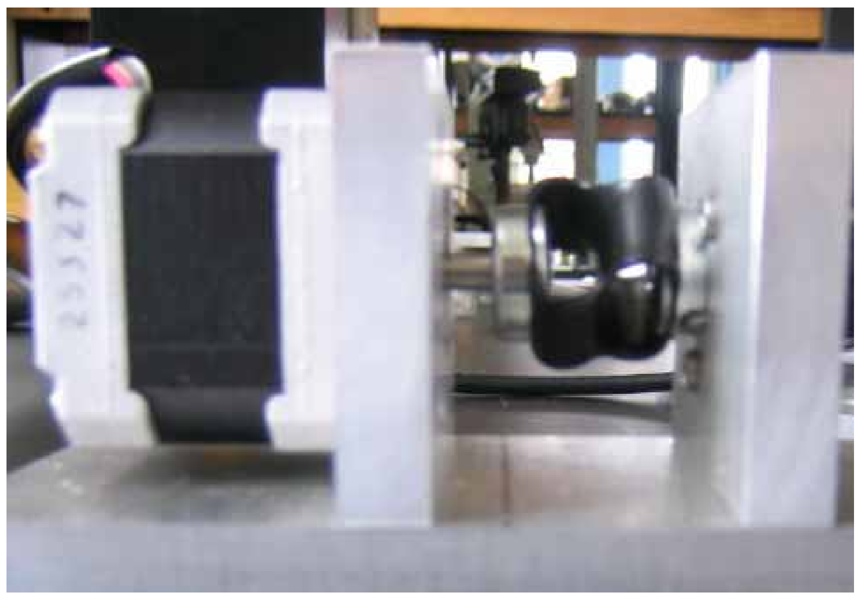

APPENDIX G-13: Dimensions of Arm

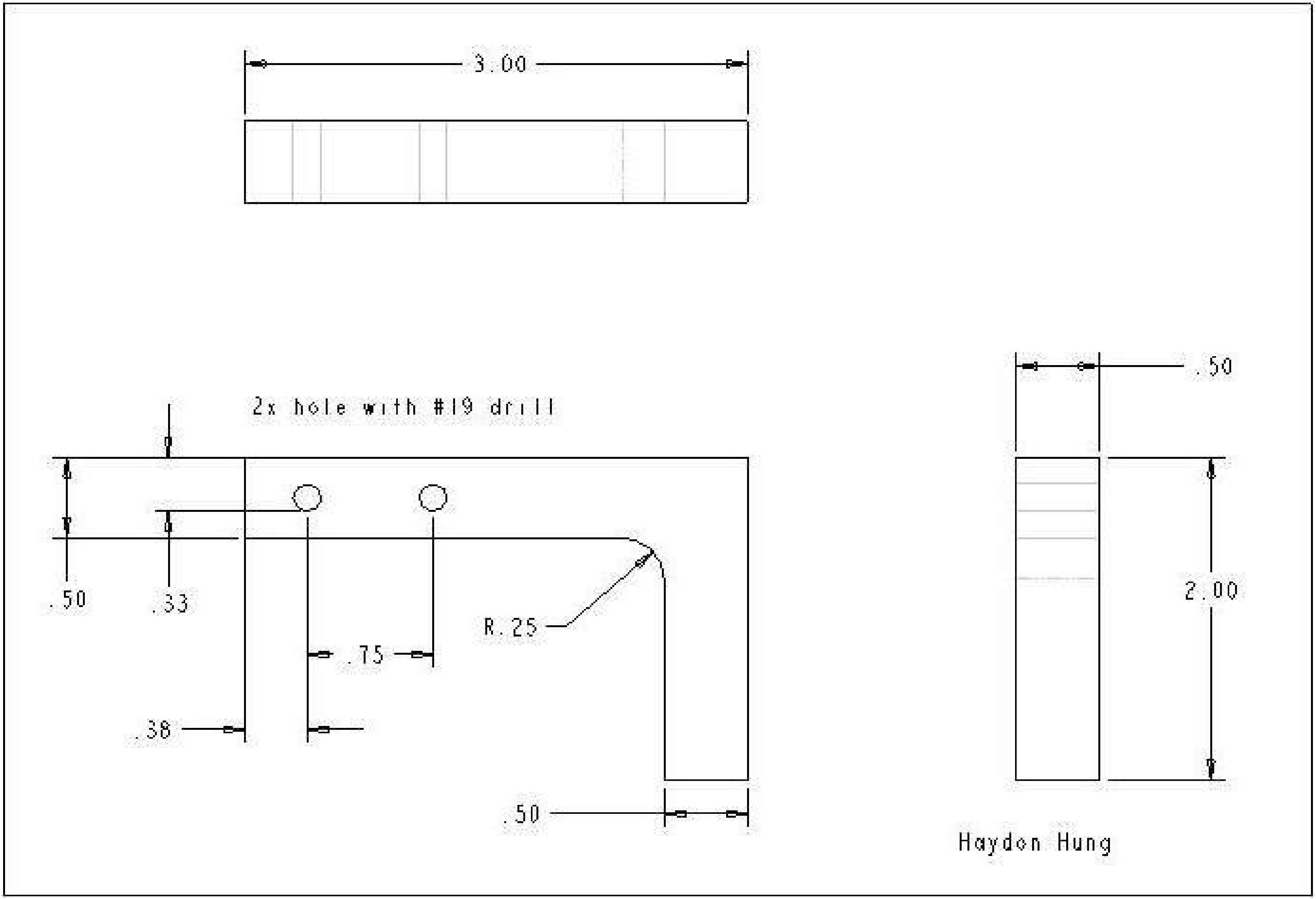

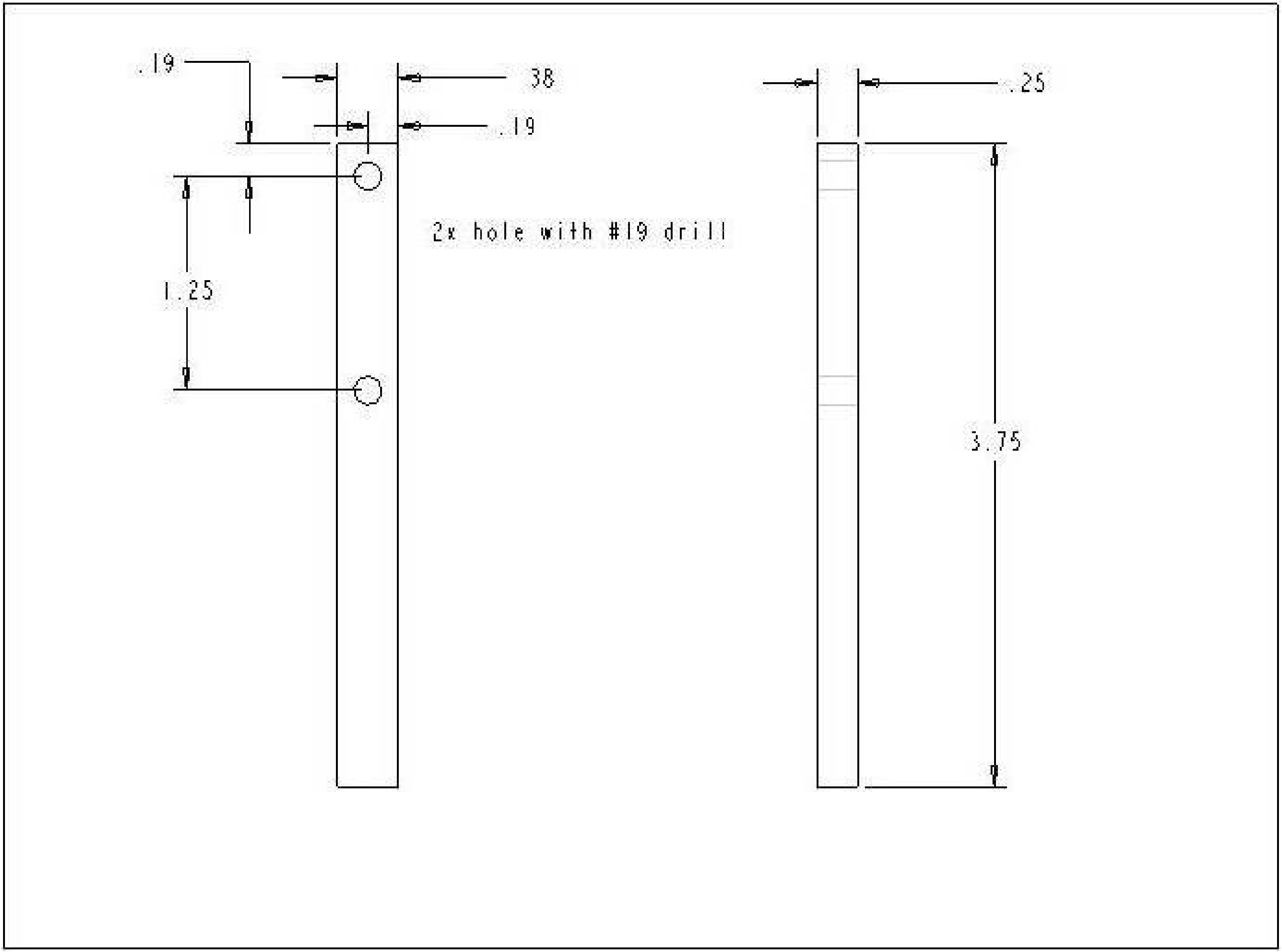
.19
.38
.19
.25
2x hole with #19 drill
1.25
3.75

APPENDIX H: Excel Sheet with Part Number, Description, Company, and Price

Parts List			
Part Number	**Description**	**Company**	**Price**
Bath Chamber			
CNI 3223	PID controller, temperature/procss with 2 control outputs	Omega Engineering	195.00
XC-20-K24	Kapton insulated thermocouple wire	Omega Engineering	24.00
KH-104/10	Kapton insulated flexible heaters (1 x 4 in), 10 W/in^2	Omega Engineering	31.00
Framework			
1515	Aluminum extrusions, 242"	Air Incorporated	121.00
4332	2 Hole gusset triangle bracket	Air Incorporated	4.05
4307	2 Hole joining strip	Air Incorporated	3.25
3630	Stainless 5/16 - 18-3 nut/bolt assembly	Air Incorporated	1.05
2367	Foot mounting plate	Air Incorporated	15.75
2207	Anti-vibration feet	Air Incorporated	14.55
Motion			
AM17-44-3MT	Stepper motor, size 17	Advanced Micro Systems	48.00
A 5Z 7-10606	Flexible Couple, bore size: 0.188", overall length: 1.1875"	Sterling Instruments	16.00
SRZ4005Tx6"	Kerk rail, lead pitch, 0.05, 6" travel	Kerk Motion Products Inc.	81.90
SR4000ES	End support for 4000 series	Kerk Motion Products Inc.	7.50
778417-01	PCI 7334 Low cost stepper motion controller	National Instruments	850.50
777936-01	MID 7604, 4-axis integrated stepper driver power (115V)	National Instruments	1975.50
186380-02	SHC68-C68-S 68 pin, VHDCI, 2m	National Instruments	135.00
Force Measurement			
FSH00270	TFF40, 20 oz-in, reaction torque sensor with center through hole	Futek	950.00
777459-37	Signal conditioning module, SCC-SG24, 2-channel, full bridge, 10 V excitation	National Instruments	265.50
777458-02	Signal conditioning carrier, SC-2345, hinged lid, universal AC)	National Instruments	220.50
779066-01	PCI 6221 M series multifunction DAQ, two 16 bit analog outputs	National Instruments	427.50
192061-01	SHC68-68 EPM Noise rejecting, shielded cable	National Instruments	85.50
Displacement Measurment			
Y55-698	Sony SC-ST50 analog/monochrome camera	Edmunds Optic	750.00
778838-01	PCI 1405 Single channel color/monochrome image acquisition	National Instruments	535.50
183882-02	IMAQ-BNC-1 analog camera cable, 2m	National Instruments	45.00

APPENDIX H-1: AM Series Stepper Motors

AMS

Precision Step Motor Control and Drive Products
ADVANCED MICRO SYSTEMS, INC.

AM SERIES STEP MOTORS

ADVANCED MICRO SYSTEMS offers a variety of high performance, 2 phase hybrid step motors. All motors are industry standard 1.8° (200 steps per revolution), full-step angle construction. Optional .9° (400 steps per revolution), full-step angle motors are also available. Each step motor is carefully constructed with permanently lubricated ball bearings for extended service life.

All AMS step motors are bipolar drive compatible. NEMA sizes 23, 34 and 42 motors can be wired with a parallel winding (standard) or in series for specific application requirements and come equipped with a convenient ten foot shielded cable.

MOTOR FEATURES

- ***Rotational angle of the motor rotor is directly proportional to the number of input step pulses for movement in full, half and microstep operations.***
- ***Precise and repeatable position sequencing, in open or closed loop applications.***
- ***Complete range of speed and torque characteristics.***
- ***Low-cost, high quality alternative to expensive pneumatic, hydraulic and servo motor designs.***

ENCODER FEEDBACK

Most AMS step motors may be ordered with shaft encoders. High resolution encoders operate in conjunction with the "EFB" electronics available in the MAX microstep controller/driver family. Benefits include dynamic stall detection and position maintenance capability. The EFB suffix includes assembled encoder and interface cables.

- ***50 to 500 lines per/rev, 500 standard***
- ***Quadrature output for 2000 ppr.***
- ***Index pulse used with homing***
- ***-40 to 100° (C) operating temperature***
- ***Adds less than 3/4" to motor length***

MOTOR SPECIFICATIONS (add **-EFB** suffix for motor with encoder)

Model Number	Parallel Winding				Series Winding				Holding Torque oz/in	Resistance per Phase Rm (ohms)	Inductance Per Phase MH @ 1000Hz	Rotor Inertia oz/in - Sec²	NEMA Frame Size
	1 Phase Energized		2 Phases Energized		1 Phase Energized		2 Phases Energized						
	Volts	Amps	Volts	Amps	Volts	Amps	Volts	Amps					
AM17-44-3MT	N/A	N/A	N/A	N/A	7.00	1.1	5.30	.85	44	6.20	16.00	.0004	17
AM23-72-1	3.56	5.6	2.52	4.0	4.78	2.8	3.38	2.0	72	.63	1.44	.0017	23
AM23-150-2	4.30	5.6	3.04	4.0	6.14	2.8	4.34	2.0	150	.76	2.54	.0033	23
AM23-210-3	5.09	5.6	3.60	4.0	7.83	2.8	6.54	2.0	210	.90	3.63	.0050	23
AM34-235-1	3.68	5.6	2.60	4.0	6.62	2.8	4.68	2.0	235	.65	5.10	.0091	34
AM34-420-2	4.64	5.6	3.28	4.0	8.54	2.8	6.04	2.0	420	.86	8.30	.0170	34
AM34-620-3	5.37	5.6	3.80	4.0	9.84	2.8	6.96	2.0	620	.95	11.20	.0265	34
AM42-810-2	5.26	5.6	3.72	4.0	10.50	2.8	7.40	2.0	810	.74	14.00	.0550	42
AM42-1440-3	6.78	5.6	4.80	4.0	13.60	2.8	9.60	2.0	1440	1.20	28.00	.1140	42

STEP MOTORS

Frame Size17

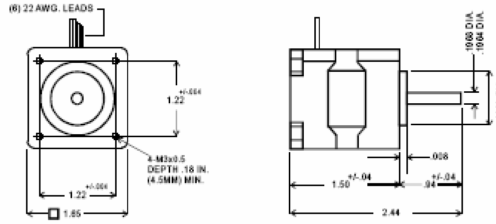

Dimensions= Inches
Mounting Hardware= millimeters

Model Number	Weight Ounces	No. of Leads	Lead Length	Motor Length
AM17-44-3MT	9.52	6	12 In.	2.44 In.

Frame Size 23

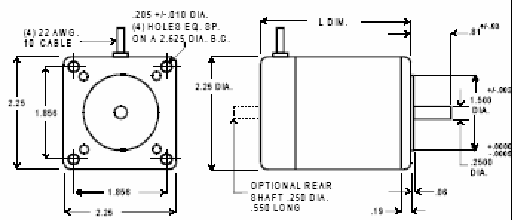

Model Number	Weight Ounces	No. of Leads	Lead Length	L Dim. Inches
AM23-72-1	19.0	4	10 Ft.	2.00
AM23-150-2	24.0	4	10 Ft.	3.00
AM23-210-3	47.0	4	10 Ft.	4.00

Frame Size 34

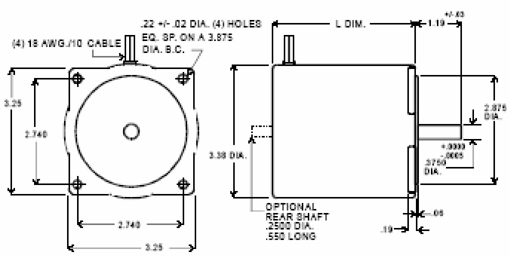

Model Number	Weight Ounces	No. of Leads	Lead Length	L Dim. Inches
AM34-235-1	48.0	4	10 Ft.	2.44
AM34-420-2	80.0	4	10 Ft.	3.70
AM34-620-3	121.0	4	10 Ft.	5.06

Frame Size 42

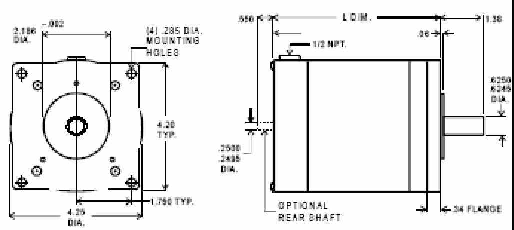

Model Number	Weight Ounces	No. of Leads	Lead Length	L Dim. Inches
AM42-810-2	216.0	4	10 Ft.	5.39
AM42-1440-3	320.0	4	10 Ft.	7.56

Wire Lead Color Codes

AM17-44-3MT

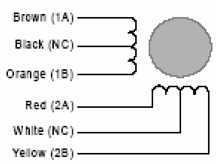

Note: Black and white wires are not connected (isolate and tie back).

AM23, 34, and 42 Series Motors*

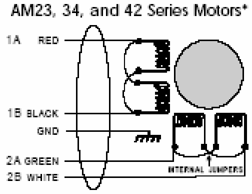

*Parallel winding configurations are standard. Optional series windings are available on most models.

Encoder Dimensions (inches)

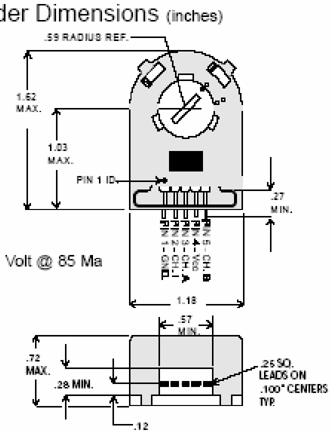

Power- 5 Volt @ 85 Ma

APPENDIX H-2: Universal Joints

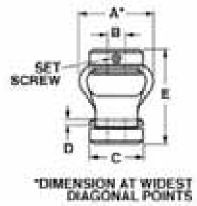

13 parts found

Part Number	Bore Size Inch	Overall Length inch	Mat'l(body)	Mat'l (hubs)	Major Diameter	Max. Speed rpm	Max. Torque in-lb	Angular Offset Degree	Paralle Offset Inch
	All	All	One option available	One option available	All	One option available	All	All	All
A 5Z 7-10606	0.188"	1.1875	Polyurethane	Steel, Zinc Plated	1.031	3600	3	10°	0.0
A 5Z 7-20808	0.25"	1.875	Polyurethane	Steel, Zinc Plated	1.813	3600	12	15°	0.1
A 5Z 7-10808	0.25"	1.1875	Polyurethane	Steel, Zinc Plated	1.031	3600	3	10°	0.0
A 5Z 7-21010	0.312"	1.875	Polyurethane	Steel, Zinc Plated	1.813	3600	12	15°	0.1
A 5Z 7-11010	0.312"	1.1875	Polyurethane	Steel, Zinc Plated	1.031	3600	3	10°	0.0
A 5Z 7-11212	0.375"	1.1875	Polyurethane	Steel, Zinc Plated	1.031	3600	3	10°	0.0
A 5Z 7-31212	0.375"	2.25	Polyurethane	Steel, Zinc Plated	2.063	3600	28	15°	0.1

APPENDIX H-3: Futek Torque Transducer

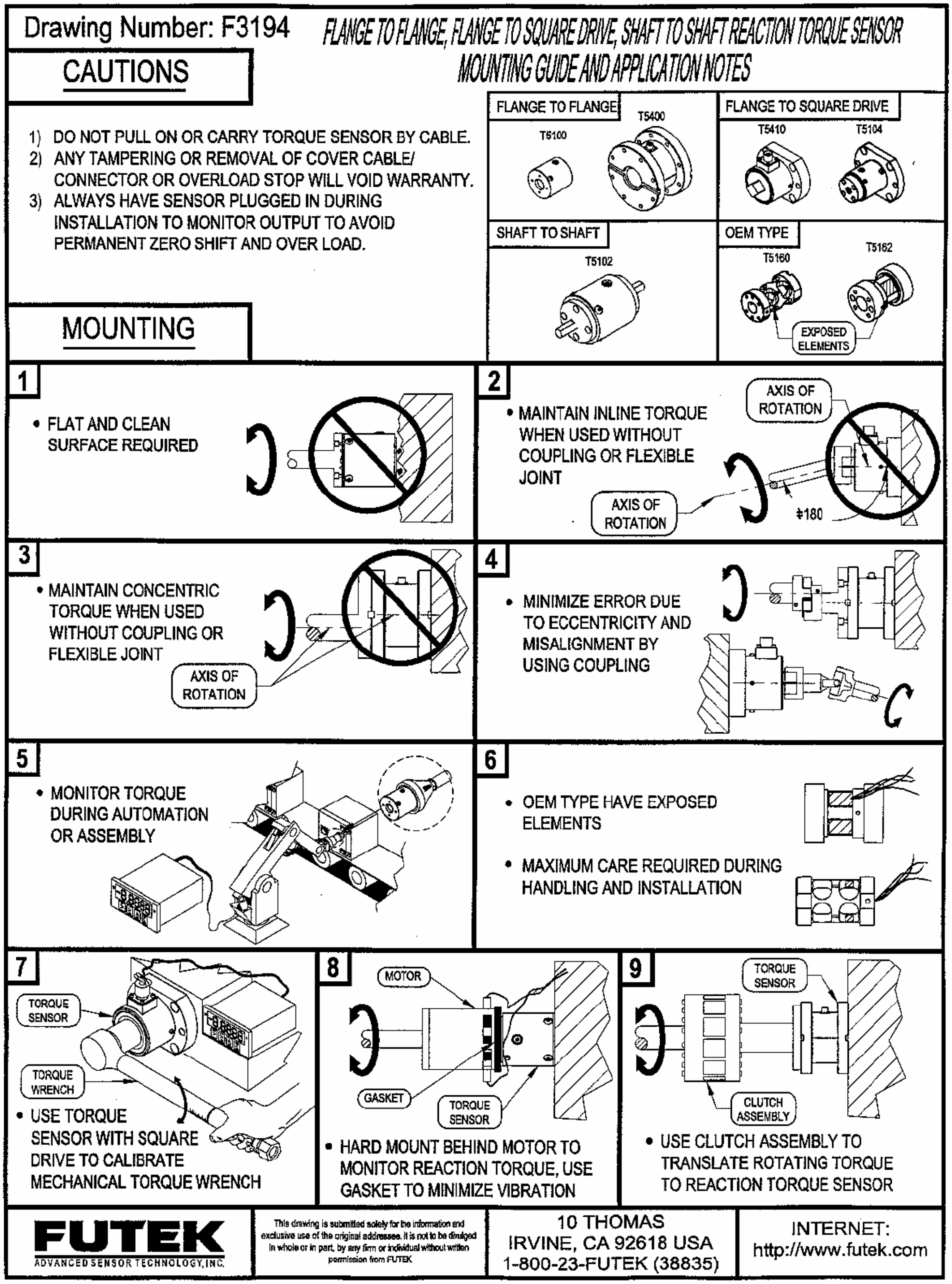

Drawing Number: F3194

FLANGE TO FLANGE, FLANGE TO SQUARE DRIVE, SHAFT TO SHAFT REACTION TORQUE SENSOR
MOUNTING GUIDE AND APPLICATION NOTES

CAUTIONS

1) DO NOT PULL ON OR CARRY TORQUE SENSOR BY CABLE.
2) ANY TAMPERING OR REMOVAL OF COVER CABLE/ CONNECTOR OR OVERLOAD STOP WILL VOID WARRANTY.
3) ALWAYS HAVE SENSOR PLUGGED IN DURING INSTALLATION TO MONITOR OUTPUT TO AVOID PERMANENT ZERO SHIFT AND OVER LOAD.

FLANGE TO FLANGE: T5100, T5400

FLANGE TO SQUARE DRIVE: T5410, T5104

SHAFT TO SHAFT: T5102

OEM TYPE: T5160, T5162, EXPOSED ELEMENTS

MOUNTING

1 • FLAT AND CLEAN SURFACE REQUIRED

2 • MAINTAIN INLINE TORQUE WHEN USED WITHOUT COUPLING OR FLEXIBLE JOINT
AXIS OF ROTATION
AXIS OF ROTATION
±180

3 • MAINTAIN CONCENTRIC TORQUE WHEN USED WITHOUT COUPLING OR FLEXIBLE JOINT
AXIS OF ROTATION

4 • MINIMIZE ERROR DUE TO ECCENTRICITY AND MISALIGNMENT BY USING COUPLING

5 • MONITOR TORQUE DURING AUTOMATION OR ASSEMBLY

6 • OEM TYPE HAVE EXPOSED ELEMENTS
• MAXIMUM CARE REQUIRED DURING HANDLING AND INSTALLATION

7 TORQUE SENSOR
TORQUE WRENCH
• USE TORQUE SENSOR WITH SQUARE DRIVE TO CALIBRATE MECHANICAL TORQUE WRENCH

8 MOTOR
GASKET
TORQUE SENSOR
• HARD MOUNT BEHIND MOTOR TO MONITOR REACTION TORQUE, USE GASKET TO MINIMIZE VIBRATION

9 TORQUE SENSOR
CLUTCH ASSEMBLY
• USE CLUTCH ASSEMBLY TO TRANSLATE ROTATING TORQUE TO REACTION TORQUE SENSOR

FUTEK ADVANCED SENSOR TECHNOLOGY, INC.

This drawing is submitted solely for the information and exclusive use of the original addressee. It is not to be divulged in whole or in part, by any firm or individual without written permission from FUTEK

10 THOMAS
IRVINE, CA 92618 USA
1-800-23-FUTEK (38835)

INTERNET:
http://www.futek.com

FUTEK MODEL TFF400

FLANGE TO FLANGE REACTION TORQUE SENSOR WITH BLIND CENTER

(Previously T5100/T5101)

Drawing Number: FI1133

INCH [mm] | R.O.= Rated Output

WIRING CODE (CC4)			
+Excitation	-Excitation	+Signal	-Signal
1	4	2	3

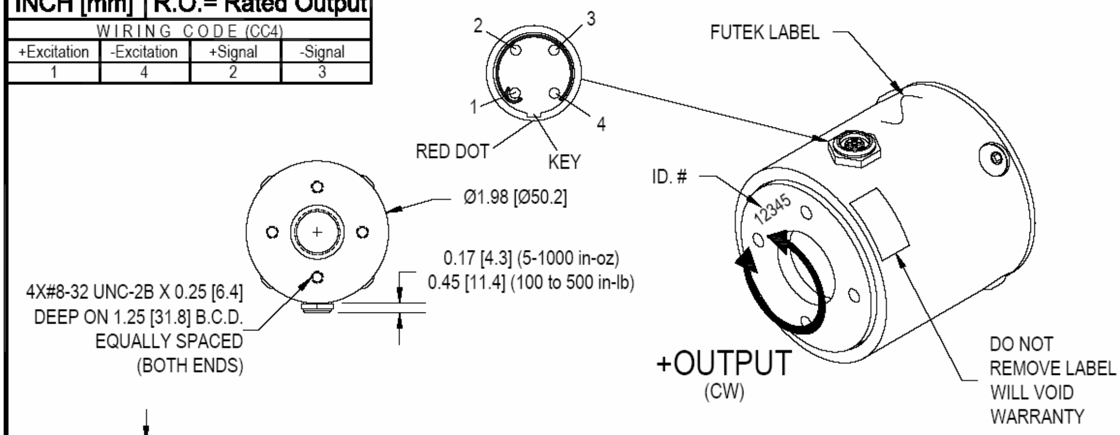

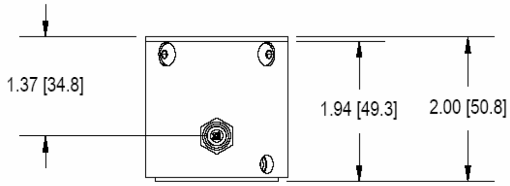

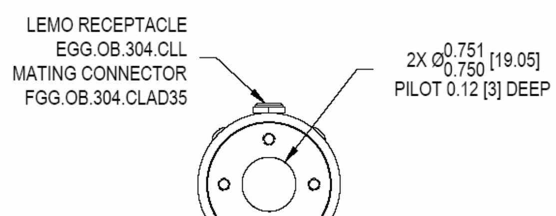

STK#	CAPACITY in-oz	Nm	TORSIONAL STIFFNESS in-oz/rad
FSH00268	5*	0.04	325
FSH00269	10*	0.08	700
FSH00270	20*	0.15	1600
FSH00271	50*	0.37	3500
FSH00272	100*	0.75	7300
FSH00273	160*	1.2	11000
FSH00274	400*	3.0	30000
FSH00275	1000	7.5	71000
FSH00276	100 in-lb	12	77000 in-lb/rad
FSH00277	200 in-lb	24	95000 in-lb/rad
FSH00278	500 in-lb	60	199000 in-lb/rad

* WITH OVERLOAD PROTECTION
FOR HIGHER CAPACITIES REFER TO MODELS TFF600-750 AND TDF600-675

SPECIFICATIONS:

RATED OUTPUT	1.5 mV/V nom. (5 in-oz) 2 mV/V nom. (10 in-oz to 500 in-lb)
SAFE OVERLOAD	300% (5 to 400 in-oz) 150% (1000 in-oz to 500 in-lb)
ZERO BALANCE	±1% of R.O.
EXCITATION (VDC OR VAC)	18 MAX
BRIDGE RESISTANCE	350 Ω nom. (5 to 1000 in-oz) 700 Ω nom. (100 to 500 in-lb)
NONLINEARITY	±0.2% of R.O.
HYSTERESIS	±0.2% of R.O.
NONREPEATABILITY	±0.05% of R.O.
TEMP. SHIFT ZERO	±0.002% of R.O./°F [0.0036% of R.O./°C]
TEMP. SHIFT SPAN	±0.002% of LOAD/°F [0.0036% of LOAD/°C]
COMPENSATED TEMP.	60 to 160°F [15 to 72°F]
OPERATING TEMP.	-60 to 200°F [-50 to 93°C]
WEIGHT	9 oz [250 g]
MATERIAL	ALUMINUM

CONNECTOR: 4 Pin LEMO Receptacle (EGG.OB.304.CLL)
ACCESSORIES AND RELATED INSTRUMENTS AVAILABLE

CALIBRATION (STD)	5 pt. CW; 60KΩ SHUNT CAL. VALUE (5 to 1000 in-oz) 100K Ω SHUNT CAL. VALUE (100 to 500 in-lb) 5 pt. CCW CALIBRATION (OPTIONAL)
CALIBRATION TEST EXCITATION	10 VDC

MCP00549 - OPTIONAL MOUNTING PLATE

MATERIAL: Aluminum, Clear Anodized

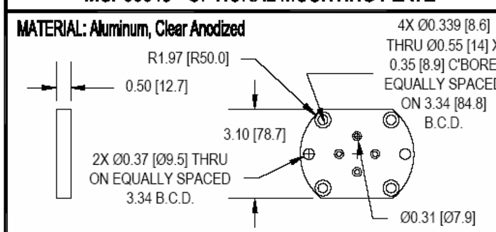

OPTIONAL 1/4" & 3/8" SQUARE ADAPTER

MATERIAL: Aluminum, Clear Anodized

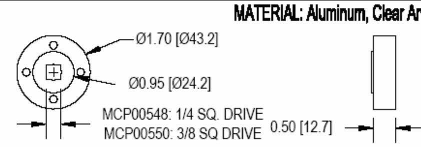

FUTEK
ADVANCED SENSOR TECHNOLOGY, INC.

10 THOMAS
IRVINE, CA 92618 USA
1-800-23-FUTEK (38835)

INTERNET:
http://www.futek.com

APPENDIX H-4: Kerk Screwrail Assemblies

SCREWRAIL ASSEMBLIES

Kerk Part #	Nominal Rail Diameter	Nominal Screw Diameter	Inch Lead **	Max. Drag Torque	Life at 1/4 Design Load x 10^6 (Non Anti-Backlash)	Torque to move load	Design Load	Screw Inertia	Equiv. Diameter* In line with slot	Equiv. Diameter* 90 degrees from slot
				oz.-in. (NM)	in. (cm)	oz.-in./lbs. (NM/kg)	lbs. (kg)	oz.-in. sec.^{2}/in. (NM sec.^{2}/mm)	in. (mm)	in. (mm)
SRA4005	1/2"	1/4"	0.050	2.0 (0.015)	150 to 200 (380 to 500)	0.5 (0.007)	25 (11)	0.3 x 10^{-5} (.8x10^{-4})	0.39 (9.9)	0.47 (11.9)
SRA4025			0.250	3.0 (0.020)		1.5 (0.023)				
SRA4050			0.500	4.0 (0.030)		2.5 (0.039)				
SRA4100			1.000	5.0 (0.040)		4.5 (0.070)				
SRA6010	3/4"	3/8"	0.100	3.0 (0.020)	180 to 280 (450 to 710)	1.0 (0.016)	50 (20)	1.5 x 10^{-5} (4.2x10^{-4})	0.60 (15.2)	0.72 (18.2)
SRA6020			0.200	4.0 (0.030)		1.5 (0.023)				
SRA6050			0.500	5.0 (0.040)		2.5 (0.039)				
SRA6100			1.000	6.0 (0.045)		4.5 (0.070)				
SRA8010	1"	1/2"	0.100	4.0 (0.030)	280 to 320 (710 to810)	1.0 (0.016)	100 (46)	5.2 x 10^{-5} (14.5x10^{-4})	0.81 (20.5)	0.97 (24.6)
SRA8020			0.200	5.0 (0.040)		1.5 (0.023)				
SRA8050			0.500	6.0 (0.045)		2.5 (0.039)				
SRA8100			1.000	8.0 (0.060)		4.5 (0.070)				
SRZ4005	1/2"	1/4"	0.050	3.0 (0.020)	75 to 100 (190 to 250)	0.5 (0.007)	25 (11)	.3x10^{-5} (.8x10^{-9})	0.39 (9.9)	0.47 (11.9)
SRZ4025			0.250	4.0 (0.030)		1.5 (0.023)				
SRZ4050			0.500	5.0 (0.040)		2.5 (0.039)				
SRZ4100			1.000	6.0 (0.045)		4.5 (0.070)				
SRZ6010	3/4"	3/8"	0.100	6.0 (0.045)	90 to 140 (230 to 350)	1.0 (0.016)	50 (23)	1.5x10^{-5} (4.2x10^{-9})	0.60 (15.2)	0.72 (15.2)
SRZ6020			0.200	6.5 (0.047)		1.5 (0.023)				
SRZ6050			0.500	7.0 (0.050)		2.5 (0.039)				
SRZ6100			1.000	7.5 (0.053)		4.5 (0.070)				
SRZ8010	1"	1/2"	0.100	8.0 (0.057)	140 to 150 (350 to 410)	1.0 (0.016)	100 (45)	5.2x10^{-5} (14.5x10^{-9})	0.81 (20.5)	0.97 (24.6)
SRZ8020			0.200	8.5 (0.060)		1.5 (0.023)				
SRZ8050			0.500	9.0 (0.064)		2.5 (0.039)				
SRZ8100			1.000	9.5 (0.067)		4.5 (0.070)				

* ScrewRail stiffness may be modeled using Classical Beam Deflection Theory with equivalent solid stainless steel beam of diameter given.
** Other leads available as custom orders.

HOW TO ORDER KERK SCREWRAILS

For ScrewRails with special journals, or nut, rail or screw modifications

Kerk will price and machine to your drawings and tolerances.
Order by your drawing or part number plus Kerk part number.

For standard configuration ScrewRails

Order by Kerk part number:

Example

SRA4025T X 12 = ScrewRail with a standard nut, 3 through-hole flange and 1/4 inch diameter screw (1/2 inch diameter rail) with .250 inch lead and a rail length of 12 inches.

Other options to be specified

Special nut, rail or screw modifications (Drawings required)
High lead accuracy - .0003, .0002, .0001 in./in. (mm/mm)
Left Hand (LH) or Right Hand/Left Hand (R/L) threads

For applications assistance or order entry, call your local Kerk representative or Kerk direct at 603-465-7227 Fax 603-465-3598.

SRA SERIES

Series	ØA	B	ØC	ØD	E	F	ØG	H(B.C.D.)	I	L1	L2
	in. (mm)	in. (mm)	in. (mm)	in. (mm)	in. (mm)	in. (mm)	in. (mm) MAX	in. (mm)	in. (mm)	in. (mm)	in. (mm)
4000 series	.491/.492 (12.472/12.496)	0.62 (15.75)	.1870/.1875 (4.750/4.762)	1.25 (31.8)	1.4 (36)	.38 (9.5)	0.8 (20.3)	1.03 (26.2)	0.140 (3.56)	0.26 (6.6)	0.36 (9.1)
6000 series	.741/.742 (18.822/18.846)	0.75 (19.05)	.2490/.2495 (6.325/6.337)	1.75 (44.5)	2.0 (51)	.50 (12.7)	1.20 (30.5)	1.48 (37.6)	0.173 (4.39)	0.38 (9.7)	0.70 (17.8)
8000 series	.991/.992 (25.172/25.196)	0.75 (19.05)	.2490/.2495 (6.325/6.337)	2.23 (56.7)	2.5 (64)	.63 (15.9)	1.60 (40.7)	1.92 (48.8)	0.200 (5.08)	0.48 (12.2)	0.77 (19.6)

NOTE: TOTAL TRAVEL = L - (L1 + L2 + E)

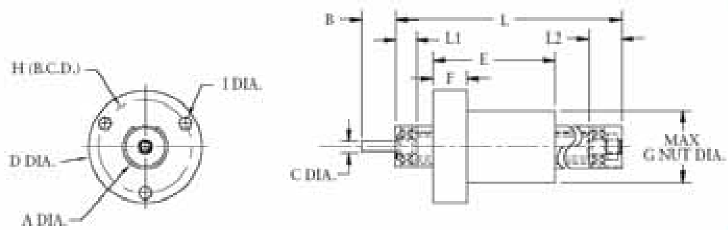

SRZ SERIES

SRZ Flange Option	ØA	B	ØC	ØD	E	F	ØG	H (B.C.D.)	I (Brass Inserts)	L1	L2
	in. (mm)	in. (mm)	in. (mm)	in. (mm)	in. (mm)	in. (mm)	in. (mm)	in. (mm)	in. (mm)	in. (mm)	in. (mm)
4000 series	.491/.492 (12.472/12.496)	0.62 (15.75)	.1870/.1875 (4.750/4.762)	1.31 (33.3)	1.4 (36)	.38 (9.5)	0.97 (24.7)	1.03 (26.2)	#6-32 *	0.26 (6.6)	0.36 (9.1)
6000 series	.741/.742 (18.822/18.846)	0.75 (19.05)	.2490/.2495 (6.325/6.337)	1.81 (46.0)	2.0 (51)	.50 (12.7)	1.38 (35.1)	1.48 (37.6)	#10-32 *	0.38 (9.7)	0.70 (17.8)
8000 series	.991/.992 (25.172/25.196)	0.75 (19.05)	.2490/.2495 (6.325/6.337)	2.30 (58.4)	2.5 (64)	.63 (15.9)	1.72 (43.7)	1.92 (48.8)	#10-32 *	0.48 (12.2)	0.77 (19.6)

*Metric threads as required

NOTE: TOTAL TRAVEL = L - (L1 + L2 + E)

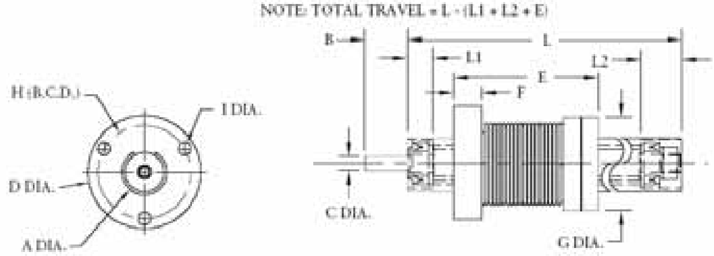

END SUPPORTS

As an additional option for all Kerk ScrewRails, standard End Supports offer the convenience of simple and compact mounting for the ScrewRail. The End Supports are designed to slide over the outside diameter of each end of the rail and "key" off the slot in the ScrewRail. The carbon reinforced polyacetal End Supports come standard with three hex nuts that are captured in the flange for easy assembly. The End Supports are also supplied with a brass threaded insert and a set screw to fasten to the outside diameter of the rail.

With the End Supports, the Kerk ScrewRail can be easily mounted to your assembly. However, if the End Supports are not utilized it is recommended to center the clamping force on each end at the L3 dimension as shown in the drawing below.

TYPICAL END SUPPORT STYLES

End Support	Part Number	Ø A'	Ø D'	F'	Ø H'	L3	L4	Q	R	S (Hex Nut)	T	U (Brass Insert)	Ø W	X	Y
		in. (mm)	in. (mm)	in. (mm)	in. (mm)	in. (mm)	in. (mm)	in. (mm)	in. (mm)	in. (mm)	in. (mm)	in. (mm)	in. (mm)	in. (mm)	in. (mm)
4000 series	SR4000ES	.624/.626 (15.85/15.90)	1.35 (34.3)	0.200 (5.08)	0.150 (3.81)	0.390 (9.91)	0.720 (18.29)	0.080 (2.03)	0.060 (1.52)	#6-32 *	1.03 (26.2)	#6-32	0.47 (12.0)	0.460 (11.68)	0.500 (12.70)
6000 series	SR6000ES	.749/.751 (19.03/19.08)	1.60 (40.6)	0.250 (6.35)	0.173 (4.39)	0.603 (15.32)	0.900 (22.86)	0.100 (2.54)	0.100 (2.54)	#8-32 *	1.31 (33.3)	#10-32	0.60 (15.3)	0.594 (15.09)	0.645 (16.38)
8000 series	SR8000ES	.999/1.001 (25.38/25.43)	2.20 (55.9)	0.375 (9.53)	0.200 (5.08)	0.920 (23.37)	1.200 (30.48)	0.125 (3.18)	0.175 (4.45)	#10-32 *	1.82 (46.2)	#10-32	0.82 (20.9)	0.800 (20.32)	0.820 (20.83)

*metric threads available upon request

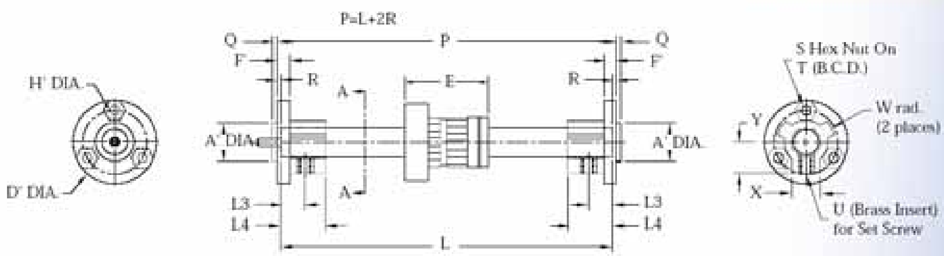

Dimensions E and L are referenced in the ScrewRail Dimensions section
Note: Total Travel=L-(E+2(L4))

View A-A

APPENDIX H-5: PID Controller

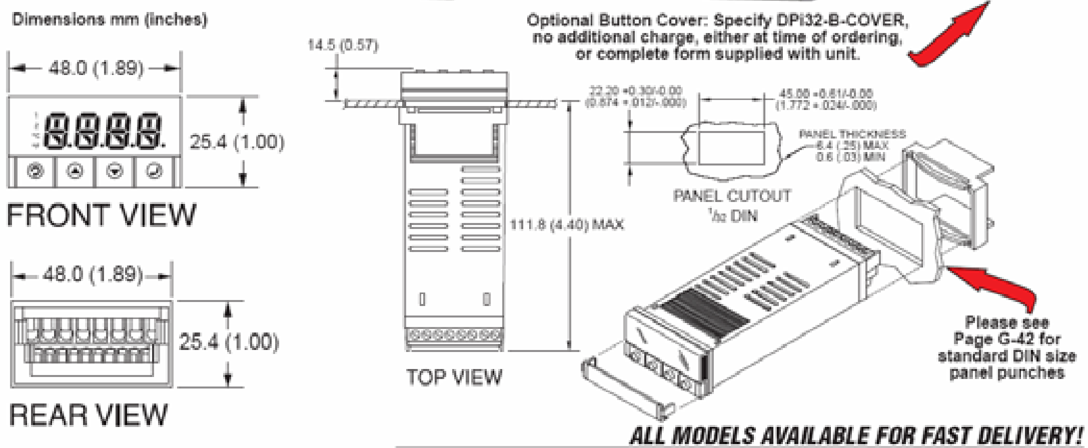

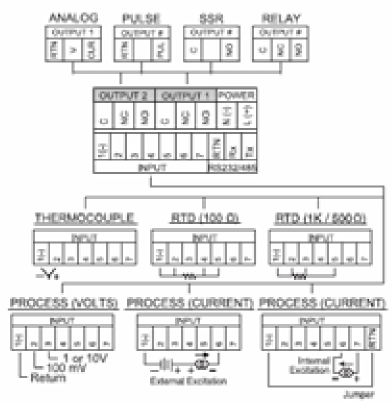

ALL MODELS AVAILABLE FOR FAST DELIVERY!

To Order (*Specify Model No.)				
Model Number			**Description**	**Price**
DPi32			Temperature/Process (Monitor only) ⅛ DIN	$150
DPiS32			Strain/Process (Monitor only) ⅛ DIN	195
CONTROL OUTPUTS #1 & 2 Direct (Cool) or Reverse (Heat) Acting				
CNi32	(*)	(*)	Temperature/Process with 2 Control Outputs	195
CNiS32	(*)	(*)	Strain/Process with 2 Control Outputs	240
	2	2	Two solid state relays (SSR's): 0.5 A @ 120/240 Vac continuous	N/C
	2	3	SSR and relay: Form "C" SPDT 3 A @ 120 Vac, 3 A @ 240 Vac	
	2	4	SSR and pulsed 10 Vdc @ 20 mA (for use with external SSR)	
	3	3	2 Relays: Form "C" SPDT 3 A @ 120 Vac, 3 A @ 240 Vac	
	4	2	Pulsed 10 Vdc @ 20 mA (for use with external SSR) and SSR	
	4	3	Pulsed 10 Vdc @ 20 mA (for use with external SSR) and relay: Form "C" SPDT 3 A @ 120 Vac, 3 A @ 240 Vac	
	4	4	Two pulsed 10 Vdc @ 20 mA (for use with external SSR)	
	5	2	Analog Output selectable as either control or retransmission of process value; 0 to 10 Vdc or 0 to 20 mA @ 500 ohm max. and SSR	
	5	3	Analog Output 0 to 10 Vdc or 0 to 20 mA @ 500 ohm max. and Relay	
	5	4	Analog Output 0 to 10 Vdc or 0 to 20 mA @ 500 ohm max., Pulse 10 Vdc	
			-AL Limit Alarm Version (Simplified Menu; No PID Control) *2	

*1 -DC, -C24 not available with Excitation. *2 Analog Output (Option 5) is not available with -AL units.

NETWORK OPTIONS		Price
-C24	Isolated RS-232 and R-485/422, 300 to 19.2k Baud *1	$60
EIS-2B	Industrial iServer Microserver™, serves 32 devices	195
POWER SUPPLY		
*	Standard power input: 90-240 Vac/dc, 50-400 Hz (no entry required)	N/C
-DC	12 to 36 Vac/dc, 24 Vac *1	25
FACTORY SETUP		
-FS	Factory Setup and Configuration (req. -C24 Serial Communication option)	N/C
SOFTWARE (REQUIRES NETWORK OPTION)		
OPC-SERVER LICENSE	OPC Server/Driver Software License	295

***Ordering Examples: CNi3222-C24**, ⅛ DIN PID Controller with two solid state relays for PID control and serial communications, both RS-232 and RS-485 $195 + 60 = **$255**.*
***DPi32**, ⅛ DIN Temperature/Process monitor, **$150**.*
***CNiS322-AL**, ⅛ DIN Strain/Process controller, limit alarm version with SSR output, **$240**.*

iServer

$195 See iDRN Series in Section N

The "iServer" is a DIN rail mounted device which can be a hub connecting up to 32 instruments to the Ethernet and Internet. The "iServer" is both a Web Server and an Ethernet-Serial bridge. To connect to the iServer, iSeries devices must feature the "C24" Serial Communications option.

P-20

APPENDIX H-6: Kapton Flexible Heaters

KAPTON INSULATED FLEXIBLE HEATERS

KH Series, Rectangular, 115 Volts

To Order *(Specify Model Number)*								
		Total wattage for Watt Density			Without PSA		With PSA	
Width, cm (")	Length, cm (")	2.5W/in²	5W/in²	10W/in²	Model No.	Price	Model No.	Price
2.5 (1)	7.6 (3)	—	—	30	**KH-103/(*)**	**$30**	**KH-103/(*)-P**	**n/a**
2.5 (1)	10 (4)	—	20	40	**KH-104/(*)**	**31**	**KH-104/(*)-P**	**$34**
2.5 (1)	7.6 (3)	—	25	50	**KH-105/(*)**	**31**	**KH-105/(*)-P**	**35**
2.5 (1)	15 (6)	15	30	60	**KH-106/(*)**	**32**	**KH-106/(*)-P**	**36**
2.5 (1)	13 (8)	20	40	80	**KH-108/(*)**	**34**	**KH-108/(*)-P**	**37**
2.5 (1)	25 (10)	25	50	100	**KH-110/(*)**	**36**	**KH-110/(*)-P**	**39**
2.5 (1)	30 (12)	30	60	120	**KH-112/(*)**	**37**	**KH-112/(*)-P**	**41**
5 (2)	5 (2)	—	20	40	**KH-202/(*)**	**30**	**KH-202/(*)-P**	**33**
5 (2)	7.6 (3)	15	30	60	**KH-203/(*)**	**32**	**KH-203/(*)-P**	**35**
5 (2)	10 (4)	20	40	80	**KH-204/(*)**	**33**	**KH-204/(*)-P**	**37**
5 (2)	13 (5)	25	50	100	**KH-205/(*)**	**35**	**KH-205/(*)-P**	**38**
5 (2)	15 (6)	30	60	120	**KH-206/(*)**	**36**	**KH-206/(*)-P**	**40**
5 (2)	20 (8)	40	80	160	**KH-208/(*)**	**39**	**KH-208/(*)-P**	**43**
5 (2)	25 (10)	50	100	200	**KH-210/(*)**	**42**	**KH-210/(*)-P**	**46**
5 (2)	30 (12)	60	120	240	**KH-212/(*)**	**45**	**KH-212/(*)-P**	**49**
7.6 (3)	7.6 (3)	22.5	45	90	**KH-303/(*)**	**34**	**KH-303/(*)-P**	**37**
7.6 (3)	10 (4)	30	60	120	**KH-304/(*)**	**36**	**KH-304/(*)-P**	**39**
7.6 (3)	13 (5)	37.5	75	150	**KH-305/(*)**	**38**	**KH-305/(*)-P**	**42**
7.6 (3)	15 (6)	45	90	180	**KH-306/(*)**	**40**	**KH-306/(*)-P**	**44**
7.6 (3)	20 (8)	60	120	240	**KH-308/(*)**	**44**	**KH-308/(*)-P**	**49**
7.6 (3)	25 (10)	75	150	300	**KH-310/(*)**	**48**	**KH-310/(*)-P**	**53**
7.6 (3)	30 (12)	90	180	360	**KH-312/(*)**	**53**	**KH-312/(*)-P**	**58**
10 (4)	10 (4)	40	80	160	**KH-404/(*)**	**38**	**KH-404/(*)-P**	**42**
10 (4)	13 (5)	50	100	200	**KH-405/(*)**	**41**	**KH-405/(*)-P**	**45**
10 (4)	15 (6)	60	120	240	**KH-406/(*)**	**44**	**KH-406/(*)-P**	**48**
10 (4)	20 (8)	80	160	320	**KH-408/(*)**	**49**	**KH-408/(*)-P**	**54**
10 (4)	25 (10)	100	200	400	**KH-410/(*)**	**55**	**KH-410/(*)-P**	**60**
10 (4)	30 (12)	120	240	480	**KH-412/(*)**	**60**	**KH-412/(*)-P**	**66**
13 (5)	13 (5)	62.5	125	250	**KH-505/(*)**	**45**	**KH-505/(*)-P**	**49**
13 (5)	15 (6)	75	150	300	**KH-506/(*)**	**48**	**KH-506/(*)-P**	**53**
13 (5)	20 (8)	100	200	400	**KH-508/(*)**	**55**	**KH-508/(*)-P**	**61**
13 (5)	25 (10)	125	250	500	**KH-510/(*)**	**62**	**KH-510/(*)-P**	**68**
13 (5)	30 (12)	150	300	600	**KH-512/(*)**	**69**	**KH-512/(*)-P**	**76**
15 (6)	15 (6)	90	180	360	**KH-606/(*)**	**52**	**KH-606/(*)-P**	**57**
15 (6)	20 (8)	120	240	480	**KH-608/(*)**	**60**	**KH-608/(*)-P**	**66**
15 (6)	25 (10)	150	300	600	**KH-610/(*)**	**68**	**KH-610/(*)-P**	**75**
15 (6)	30 (12)	180	360	720	**KH-612/(*)**	**77**	**KH-612/(*)-P**	**84**
20 (8)	20 (8)	160	320	640	**KH-808/(*)**	**62**	**KH-808/(*)-P**	**69**
20 (8)	25 (10)	200	400	800	**KH-810/(*)**	**71**	**KH-810/(*)-P**	**78**
20 (8)	30 (12)	240	480	960	**KH-812/(*)**	**80**	**KH-812/(*)-P**	**88**
25 (10)	25 (10)	250	500	1000	**KH-1010/(*)**	**74**	**KH-1010/(*)-P**	**81**
25 (10)	30 (12)	300	600	1200	**KH-1012/(*)**	**83**	**KH-1012/(*)-P**	**91**
30 (12)	30 (12)	360	720	1440	**KH-1212/(*)**	**89**	**KH-1212/(*)-P**	**96**

n/a = not availabe with PSA. *Comes with complete operator's manual.*

** Insert watt density: 2 for 2.5 W/in², 5 for 5 W/in² or 10 for 10W/in².*

*** Heaters with pressure sensitive adhesive (PSA): not available at 10W/in².*

Ordering Example: KH-310/2, *is a 7.6 x 25 cm (3 x 10"), 115 Vac, 2.5 W/in2, Kapton heater,* ***$38.60***

Note: *Heaters are available in only the watt densities where total wattage is indicated.*

Accessory

Model No.	Price	Description
PE-1414	**$100**	Reference Book: Engineering Economy: Applying Theory to Practice

APPENDIX H-7: Thermocouple Wire

TFE and Kapton® Insulated Thermocouple Wire

New! "SLE" Special Limits of Error Available

ANSI color code shown | To order IEC color code see pg. H-9

TFE Insulated Thermocouple Wire

MADE IN USA

Convenient Length Spools Available

Duplex Insulated

Color coded TFE tape applied to conductors and jacket. Superior abrasion, moisture and chemical resistance.

ANSI Color Code:
Type J: Positive Wire, White; Negative Wire, Red; Overall, Brown
Type K: Positive Wire, Yellow; Negative Wire, Red; Overall, Brown
Type T: Positive Wire, Blue; Negative Wire, Red; Overall, Brown
Type E: Positive Wire, Purple; Negative Wire, Red; Overall, Brown

ALL MODELS AVAILABLE FOR FAST DELIVERY!

Calibration ANSI Code	AWG No.	Model Number	Price/ 1000'*	SLE/ 1000'**	Type Wire	Insulation		Max. Temp		Nominal Size mm (inches)	Wt.†/1000' kg (lb)
						Conductor	Overall	°C	°F		
J	20	TFE-J-20	$375	$425	Solid	Fused TFE Tape	Fused TFE Tape	260	500	1.5 x 2.5 (0.060 x 0.100)	5 (11)
	20S	TFE-J-20S	475	540	7 x 32	Fused TFE Tape	Fused TFE Tape	260	500	1.5 x 2.7 (0.060 x 0.105)	5 (11)
Iron -	24	TFE-J-24	285	320	Solid	Fused TFE Tape	Fused TFE Tape	260	500	1.3 x 1.9 (0.050 x 0.075)	3 (6)
Constantan	24S	TFE-J-24S	335	375	7 x 32	Fused TFE Tape	Fused TFE Tape	260	500	1.3 x 2.2 (0.050 x 0.085)	3 (6)
K	20	TFE-K-20	$475	$535	Solid	Fused TFE Tape	Fused TFE Tape	260	500	1.5 x 2.5 (0.060 x 0.100)	5 (11)
	20S	TFE-K-20S	735	835	7 x 32	Fused TFE Tape	Fused TFE Tape	260	500	1.5 x 2.7 (0.060 x 0.105)	5 (11)
CHROMEGA® -	24	TFE-K-24	350	390	Solid	Fused TFE Tape	Fused TFE Tape	260	500	1.3 x 1.9 (0.050 x 0.075)	3 (6)
ALOMEGA®	24S	TFE-K-24S	475	540	7 x 32	Fused TFE Tape	Fused TFE Tape	260	500	1.3 x 2.2 (0.050 x 0.085)	3 (6)
T	20	TFE-T-20	$375	$425	Solid	Fused TFE Tape	Fused TFE Tape	260	500	1.5 x 2.5 (0.060 x 0.100)	5 (11)
	20S	TFE-T-20S	475	540	7 x 32	Fused TFE Tape	Fused TFE Tape	260	500	1.5 x 2.7 (0.060 x 0.105)	5 (11)
Copper -	24	TFE-T-24	285	320	Solid	Fused TFE Tape	Fused TFE Tape	260	500	1.3 x 1.9 (0.050 x 0.075)	3 (6)
Constantan	24S	TFE-T-24S	335	375	7 x 32	Fused TFE Tape	Fused TFE Tape	260	500	1.3 x 2.2 (0.050 x 0.085)	3 (6)
E	20	TFE-E-20	$550	$625	Solid	Fused TFE Tape	Fused TFE Tape	260	500	1.5 x 2.5 (0.060 x 0.100)	5 (11)
	20S	TFE-E-20S	735	835	7 x 32	Fused TFE Tape	Fused TFE Tape	260	500	1.5 x 2.7 (0.060 x 0.105)	5 (11)
CHROMEGA® -	24	TFE-E-24	425	475	Solid	Fused TFE Tape	Fused TFE Tape	260	500	1.3 x 1.9 (0.050 x 0.075)	3 (6)
Constantan	24S	TFE-E-24S	520	585	7 x 32	Fused TFE Tape	Fused TFE Tape	260	500	1.3 x 2.2 (0.050 x 0.085)	3(6)

† *Weight of spool and wire rounded up to the next highest lb.; does not include packing material.*
* *Spool lengths 25', 50', 100', 200', 500' and 1000'. Other calibrations and lengths available, consult sales for pricing.*
** *To order special limits of error wire, add "-SLE" to model number before spool length*
Ordering Example: *TFE-J-24-SLE-1000 1000' (300 m) of Type J Iron-CONSTANTAN Special Limits of Error Duplex Insulated Wire, $320*

Kapton® Insulated Thermocouple Wire

Duplex Insulated

Fused Kapton tape applied to conductors and jackets. Excellent moisture and abrasion resistance, high dielectric strength (7 kV/mil) retains much physical integrity after gamma radiation. FEP is used as adhesive binding agent [melts at approx. 260°C (500°F)]

Calibration Color Code†	AWG No.	Model Number	Price/ 1000'*	SLE/ 1000'**	Type Wire	Insulation		Max. Temp		Nominal Size mm (inches)	Wt.†/1000' kg (lb)
						Conductor	Overall	°C	°F		
J	20	KK-J-20	$725	$825	Solid	Fused Polyimide Tape	Fused Polyimide Tape	316	600	1.5 x 2.5 (0.060 x 0.100)	5 (11)
	20	KK-J-20S	925	1060	7 x 32	Fused Polyimide Tape	Fused Polyimide Tape	316	600	1.5 x 2.7 (0.060 x 0.105)	5 (11)
Iron -	24	KK-J-24	600	685	Solid	Fused Polyimide Tape	Fused Polyimide Tape	316	600	1.3 x 1.9 (0.050 x 0.075)	3 (6)
Constantan	24	KK-J-24S	750	860	7 x 32	Fused Polyimide Tape	Fused Polyimide Tape	316	600	1.3 x 2.2 (0.050 x 0.085)	3 (6)
	30	KK-J-30	650	750	Solid	Fused Polyimide Tape	Fused Polyimide Tape	316	600	1.0 x 1.4 (0.040 x 0.055)	3 (5)
K	20	KK-K-20	$775	$885	Solid	Fused Polyimide Tape	Fused Polyimide Tape	316	600	1.5 x 2.5 (0.060 x 0.100)	5 (11)
	20	KK-K-20S	975	1115	7 x 32	Fused Polyimide Tape	Fused Polyimide Tape	316	600	1.5 x 2.7 (0.060 x 0.105)	5 (11)
CHROMEGA® -	24	KK-K-24	625	710	Solid	Fused Polyimide Tape	Fused Polyimide Tape	316	600	1.3 x 1.9 (0.050 x 0.075)	3 (6)
ALOMEGA®	24	KK-K-24S	775	885	7 x 32	Fused Polyimide Tape	Fused Polyimide Tape	316	600	1.3 x 2.2 (0.050 x 0.085)	3 (6)
	30	KK-K-30	640	730	Solid	Fused Polyimide Tape	Fused Polyimide Tape	316	600	1.0 x 1.4 (0.040 x 0.055)	3 (5)

† ***Note:*** *Kapton® wire is neither ANSI nor IEC color coded. Consult Sales for types T and E.*
* *Spool lengths 25', 50', 100', 200', 500' and 1000'. Other calibrations and lengths available, consult sales for pricing.*
** *To order special limits of error wire, add "-SLE" to model number before spool length*
Ordering Example: *KK-K-20-SLE-1000, 1000' (300 m) of Type K CHROMEGA®-ALOMEGA® Special Limits of Error Duplex Insulated Wire, $885*

OMEGA can cover any insulated wire with metal overbraiding to protect against wear and abrasion. Overbraiding adds durability and electrical shielding for improved performance.

H-23

APPENDIX H-8: Stepper and Servo Motor Drives

Stepper and Servo Motor Drives

NI MID-7604, NI MID-7602

- High-efficiency, bipolar chopper stepper drives
- User-selectable microstepping and peak current
- Integrated power supply
- CE approved and UL recognized

NI MID-7654, NI MID-7652

- High-efficiency servo amplifiers
- User-selectable peak current and continuous current
- Integrated power supply
- CE approved and UL recognized

Overview and Applications

The National Instruments MID-760x integrated stepper motor power drives and MID-765x integrated DC-brush servo motor power drives offer reliable, easy-to-connect drive solutions for National Instruments motion controllers. The NI MID-760x provides stepper motor control from the NI 7330, 7340, and 7350 controllers. The MID-7650 provides DC-brush servo motor control from NI 7340 and 7350 controllers. Because the MID-760x and the MID 7650 have all the required motion drive and motion I/O signals, they offer all the features of a universal motion interface wiring module with the enhancements of a powered motor drive in a single product. The NI MID power drives connect to motion controller boards through a single-shielded cable that transfers all motor commands, as well as motion I/O control and feedback signals.

The MID-7604 and MID-7602 are 4-axis and 2-axis stepper motor drive units, respectively. The MID-7654 and MID-7652 are 4-axis and 2-axis DC-brush servo motor drive units, respectively.

These compact, well integrated drives incorporate per-axis amplifiers, motor-power DC bus supplies, low-voltage motion I/O supplies, and pluggable screw terminal connectivity in a single rugged metal enclosure. This optimized system wiring design simplifies motion component selection.

High-Efficiency Architecture

The MID-760x power drives incorporate an efficient bipolar chopper architecture that converts step and direction control signals into winding currents for 2-phase stepper motors. The MID-765x power drives incorporate an efficient servo amplifier architecture that converts analog control signals into winding currents for DC-brush motors. The pulse width modulation driver technology in the MID-765x accurately controls motor winding current, while reducing motor heating, lowering ripple current, and improving overall motor performance. Active fan cooling provides optimal motion power drive operation.

Model	Stepper	Servo	NI 7330	NI 7350 NI 7340	(V)	Motor Drive (A)	Compact Current/Axis Diagnostic LEDs	Front Panel Enclosure and Microstepping	Front Panel Selectable Peak Current	Selectable Axes
MID-7604	✓	–	✓	✓	24	0.2 to 1.4	✓	✓	✓	4
MID-7602	✓	–	✓	✓	24	0.2 to 1.4	✓	✓	✓	2
MID-7654	–	✓	–	✓	48	0.8 to 5 continous 10 peak	✓	–	✓	4
MID-7652	–	✓	–	✓	48	0.8 to 5 continous 10 peak	✓	–	✓	2

Figure 1. Stepper and Servo Motor Drive Features

Stepper and Servo Motor Drives

Ordering Information

NI MID-7604 (4-axis stepper) 777936-0P
NI MID-7602 (2-axis stepper) 778003-0P
NI MID-7654 (4-axis servo) 778005-0P
NI MID-7652 (2-axis servo) 778004-0P
Cables
Refer to the cable guide on page 645.

Accessories
Rack-Mount Kit
MID-760x 777665-01
MID-765x 187374-01
Strain-Relief Bar for MID-76xx 187407-01
Panel-Mount Kit 187243-01

BUY ONLINE!

Visit ni.com/info and enter mid7602, mid7604, mid7652, and/or mid7654.

Specifications

The specifications below apply to only the MID-76xx. Please refer to your controller specifications to determine overall system specifications.

Some signals define compatibility as pass-through. This means the MID 76xx may have passive filtering on these signals, but the signals do not affect the voltage range. Consult your motion controller specifications to determine allowable voltage range and logic level compatibility of the signal.

MID-7604, MID-7602 Stepper Motor Drives

Driver type	IM481H modular hybrid, bipolar chopper
Chopping operating frequency	20 kHz
Motor bus voltage	24 VDC nominal
Current per phase	0.2 to 1.4 A_{peak} (0.14 to 1 A_{rms}) (factory setting is 0.2 A_{peak})
Microstepping selections	x2, 4, 8, 16, 32, 64, 128, 256 x5, 10, 25, 50, 125, 250

Power Supply

Input voltage	90-138 VAC/204-264 VAC, 47-63 Hz
Input fuse	1.5 A, 230 VAC 3 A, 115 VAC
Input fuse dimensions	5 x 20 mm

Host Bus Voltage Interlock

PC bus host voltage monitoring range	5 VDC

Physical

Dimensions	30.6 by 25.4 by 4.4 cm (12.1 by 10.0 by 1.7 in.)
Weight	4.5 kg (10 lb)

MID-7654, MID-7652 Servo Motor Drives

Driver type	Elmo Motion Control VIO 10/100
Peak current limit	1.7 to 10 A (default 1.7 A)
Continuous current limit	0.8 to 5 A (default 0.5 A)
DC-bus motor voltage	48 VDC nominal
Continuous power (all axes combined)	400 W at 25% duty cycle

Power Supply

Input voltage	90-132 VAC/198-264 VAC, 47-63 Hz
Input fuse	6 A, 230 VAC, 8 A, 115 VAC
Input fuse dimensions	0.25 by 1.25 in.

Host Bus Voltage Interlock

PC bus host voltage monitoring range	5 VDC ±5%

Physical

Dimensions	30.6 by 25.4 by 8.8 cm (12.0 by 10.0 by 3.5 in.)
Weight	10.2 kg (22.5 lb)

General (All MID 76xx drives)

Encoder Interface (Each Axis)

Inputs	Quadrature, incremental
Differential input threshold	±0.3 V (typical)
Single-ended input threshold	TTL/CMOS
Voltage range	0 to 5 VDC
Maximum quadrature frequency	20 MHz

Inhibit, Limit, and Home Switch Inputs (Each Axis)

Voltage range	0 to 12 VDC
Compatibility	Signal pass-through

Trigger Input

Noise filter (RC time constant)	100 ns
Compatibility	Signal pass-through

Breakpoint Output

Compatibility	Signal pass-through

Analog Input

Noise filter (RC time constant)	10 µs
Compatibility	Signal pass-through

Analog Output

Compatibility	Signal pass-through

Safety

Installation category II, pollution degree 2

Environment

Operating temperature	0 to 50 °C for 765x, 0 to 45 °C for 760x
Storage temperature	-20 to 70 °C
Relative humidity	10% to 90% (noncondensing)

APPENDIX H-9: Motion Controller

Low-Cost Stepper Motion Controllers

Technical Support for Motion Software

As a complement to your motion software product, consider:

Technical Support – FREE through applications engineers worldwide, Web resources, and Premier Support – ***ni.com/support***

Motion Control Fundamentals Training – Instructor-led courses – ***ni.com/training***

Professional Services – Feasibility, consulting, and integration through our Alliance Program members – ***ni.com/alliance***

For more information on NI services and support, visit ni.com/services

Ordering Information

NI PCI-7334 (4-axis stepper) 778417-01
NI PXI-7334 (4-axis stepper) 778444-01
Includes hardware and NI-Motion software, libraries, and examples

Accessories

NI Motion Assistant..778553-01
Universal Motion Interfaces ....see page 640
Drives...see page 642
Cables...see page 645

BUY ONLINE!

Visit ni.com/info and enter pxi7334, pci7334.

Specifications

Trajectory update rate range	62.5 to 500 µs/sample
Maximum update rate	62.5 µs/axis
4-axis update rate	250 µs total
Multi-axis synchronization	< 1 update sample
Trajectory parameters	
Position range	$\pm 2^{31}$ steps
Maximum relative move size	$\pm 2^{31}$ steps
Velocity range	1 to 4,000,000 steps/s
Acceleration/deceleration	61 to 128,000,000 steps/s2

System Safety

Watchdog timer function	Resets board to startup state
Shutdown input	Disable all axes and command outputs

Motion I/O

Stepper outputs	
Maximum pulse rate	4 MHz (full, half, and microstep)
Step output mode	Step and direction or CW/CCW
Encoder inputs	Quadrature, incremental, single-ended
Maximum count rate	20 MHz
Forward, reverse, and home inputs	
Number of inputs	3 per axis
Control	Individual enable/disable, stop on input, prevent motion, find home
Trigger inputs	1 per axis
Maximum repetitive capture rate	150 Hz
Breakpoint outputs	
Number of outputs	1 per axis, programmable polarity
Inhibit/enable output	
Number of outputs	1 per axis, programmable polarity
Analog inputs	12-bit resolution, ±10 V range, 50 µs scan rate

Digital I/O

Ports	4, 8-bit TTL ports, bit configurable, sink or source 24 mA
Open-loop PWM outputs	
Number of PWM outputs	2
Clock sources	Internal or external

Power Requirements

+5 VDC (±3%)	1 A
+12 VDC (±3%)	30 mA
-12 VDC (±3%)	30 mA
Power consumption	5.7 W, maximum

Physical

PCI	17.5 by 9.9 cm (6.9 by 3.9 in.)
PXI	16 by 10 cm (6.3 by 3.9 in)
Connectors	
Motion I/O connector	68-pin female high-density VHDCI type
Digital I/O connector	68-pin female high-density VHDCI type

Environment

Operating temperature	0 to 55 °C
Storage temperature	-20 to 70 °C
Relative humidity range	10 to 90% (noncondensing)

APPENDIX H-10: Image Acquisition

Low-Cost Single-Channel Color or Monochrome Image Acquisition

Programmable Gain and Offset

The PCI-1405 has programmable gain and offset circuitry for optimizing the input signal range.

I/O Connector and Cabling

Two external BNC connectors are used for the video source and digital I/O line. The PCI-1405 is shipped with a 2 m BNC cable.

Color Pattern Matching

Use color pattern matching to locate quickly known reference patterns, or fiducials, in a color image. With color pattern matching, you create a model or template of an object. The search tool first scans the image to match the color distribution, and then scores the match for shape. The score relates to how closely the model matches the pattern found. You should use color pattern matching to locate reference patterns that the color and spatial information in the pattern fully describe. Color can often simplify a monochrome problem by improving contrast or separation.

Ordering Information

NI PCI-1405 778838-01
Includes NI-IMAQ software and 2 m IMAQ-BNC-1 cable

Specifications

Typical for 25 °C unless otherwise noted.

Available Formats

RS-170, NTSC	30 frames/s interlaced
CCIR-601, PAL	25 frames/s interlaced

Video Input

Quantity	1 monochrome or color
Video 0	Single-ended (BNC)
Input impedance	75 Ω
Bandwidth	Typical 20 MHz (-3dB)
Input full-scale range	2 LSBrms maximum

A/D Conversion

Gray levels	256 (8 bits)
DNL	±1 LSB maximum
RMS noise	<0.5 LSB_{rms}
SNR	Typical 48 dB

External Synchronization and Trigger Signals

Trigger sense	TTL
Trigger polarity	Programmable (positive of negative)
Minimum detectable pulse width	20 ns
VIH (TTL)	2 V
VIL (TTL)	0.8 V

Pixel Clock

RS-170, NTSC	12.27 MHz ±5%
CCIR, PAL	14.75 MHz ±5%
Pixel jitter	<2 ns
Lock time	<1 frame

PCI Interface

Bus interface	Master, slave
Bus-master performance	132 MB/s (ideal)

Power Requirement

+5 VDC (±5%)	1.25 A
+12 VDC (±5%)	<200 mA

Physical

Dimensions	10.7 by 17.5 cm (4.2 by 6.9 in.)

Environment

Operating temperature	0 to 55 °C
Storage temperature	-20 to 70 °C
Relative humidity	5 to 90%, noncondensing

APPENDIX H-11: Data Acquisition Board

Low-Cost M Series Multifunction DAQ 16-Bit, 250 kS/s, up to 80 Analog Inputs

M Series – Low Cost

- 16, 32, or 80 analog inputs at 16-bit, 250 kS/s
- Up to 4 analog outputs at 16-bit, 833 kS/s (6 µs full-scale settling time)
- Programmable input range (±10, ±5, ±1, ±0.2 V) per channel
- Up to 48 TTL/CMOS digital I/O lines (up to 32 hardware-timed at 1 MHz)
- Two 32-bit, 80 MHz counter/timers
- Digital triggering
- NI-MCal calibration technology for improved measurement accuracy
- 6 DMA channels for fast data throughput
- NI-DAQmx measurement services software for simplified configuration and measurements
- 3-year warranty

Operating Systems
- Windows 2000/NT/XP

Recommended Software
- LabVIEW
- LabWindows/CVI
- Measurement Studio

Other Compatible Software
- Visual Studio.NET
- C/C++/C#
- NI SignalExpress

Measurement Services Software (included)
- NI-DAQmx

Family	Bus	Analog Inputs	Analog Input Resolution (bits)	Analog Outputs	Output Resolution (bits)	Max Output Rate (kS/s)	Output Range (V)	Digital I/O	Correlated (Clocked) DIO
NI 6220	PCI, PXI	16	16	–	–	–	–	24	8, up to 1 MHz
NI 6221	PCI, PXI	16	16	2	16	833	±10	24	8, up to 1 MHz
NI 6224	PCI, PXI	32	16	–	–	–	–	48	32, up to 1 MHz
NI 6225	PCI, PXI	80	16	2	16	833	±10	24	8, up to 1 MHz
NI 6229	PCI, PXI	32	16	4	16	833	±10	48	32, up to 1 MHz

Table 1. NI Low-Cost M Series Selection Guide

Overview and Applications

National Instruments low-cost M Series devices provide optimized functionality for cost-sensitive applications. They are ideal for applications including data logging and control, and measure sensors and high voltages when used in conjunction with NI signal conditioning. Synchronize the operations of multiple devices using the RTSI bus or PXI trigger bus.

Recommended Accessories

Signal conditioning is required for sensor measurements or voltage inputs greater than 10 V. National Instruments SCXI is a versatile, high-performance signal conditioning platform, optimized for high-channel-count applications. NI SCC provides portable, flexible signal conditioning options on a per-channel basis. For applications not requiring signal conditioning, refer to Table 2 for recommended cabling and accessories.

Recommended Software

National Instruments recommends using the latest version of NI-DAQmx measurement services software for application development in LabVIEW, LabWindows/CVI, and Measurement Studio. To check for the newest version of NI-DAQmx, go to ni.com/support/daq/versions. For custom driver development, use the Measurement Hardware DDK or customized register-level programming. M Series devices are compatible with the following versions (or later ones) of NI application software: LabVIEW, LabWindows/CVI, or Measurement Studio version 7.x; SignalExpress 1.x; VI Logger 2.0; or LabVIEW with the LabVIEW Real-Time Module 7.1. M Series devices do not work with the legacy Traditional NI-DAQ driver.

System Description	Terminal Block ①	Cable
High Performance	SCB-68, BNC-2110, TBX-68	SHC68-68-EPM
Basic Shielding	SCB-68, BNC-2110, TBX-68	SHC68-68

Table 2. Recommended Accessories (Two cables and accessories are required to access all pins on the NI 6224, 6225, and 6229 devices)

Ordering Information

PCI

NI PCI-6220	779065-01
NI PCI-6221	779066-01
NI PCI-6224	779067-01
NI PCI-6225	779295-01
NI PCI-6229	779068-01

PXI

NI PXI-6220	779112-01
NI PXI-6221	779113-01
NI PXI-6224	779114-01
NI PCI-6225	779296-01
NI PXI-6229	779115-01

Includes NI-DAQmx software.

Low-Cost M Series Multifunction DAQ
16-Bit, 250 kS/s, up to 80 Analog Inputs

Specifications

Typical at 25 °C unless otherwise noted.

Analog Input

Number of channels	
NI 6220/NI 6221	8 differential or 16 single ended
NI 6224/NI 6229	16 differential or 32 single ended
NI 6225	40 differential or 80 single ended
ADC resolution	16 bits
DNL	No missing codes guaranteed
INL	Refer to the *AI Absolute Accuracy Table*
Sampling rate	
Maximum	250 kS/s
Minimum	0 S/s
Timing accuracy	50 ppm of sample rate
Timing resolution	50 ns
Input coupling	DC
Input range	±10, ±5, ±1, ±0.2 V
Maximum working voltage for analog inputs (signal + common mode)	±11 V of AI GND
CMRR (DC to 60 Hz)	95 dB
Input impedance	
AI+ to AI GND	>10 GΩ in parallel with 100 pF
AI– to AI GND	>10 GΩ in parallel with 100 pF
Input bias current	±100 pA
Crosstalk (at 100 kHz)	
Adjacent channels	–75 dB
Non-adjacent channels	–90 dB
Small signal bandwidth (–3 dB)	700 kHz
Input FIFO size	4,095 samples
Scan list memory	4,095 entries
Data transfers	DMA (scatter-gather), interrupts, programmed I/O
Overvoltage protection (AI <0..79>, AI SENSE, AI SENSE 2)	
Device on	±25 V for up to two AI pins
Device off	±15 V for up to two AI pins
Input current during overvoltage condition	±20 mA max/AI pin

Settling Time for Multichannel Measurements

Accuracy, full scale step, all ranges	
±90 ppm of step (±6 LSB)	4 µs convert interval
±30 ppm of step (±2 LSB)	5 µs convert interval
±15 ppm of step (±1 LSB)	7 µs convert interval

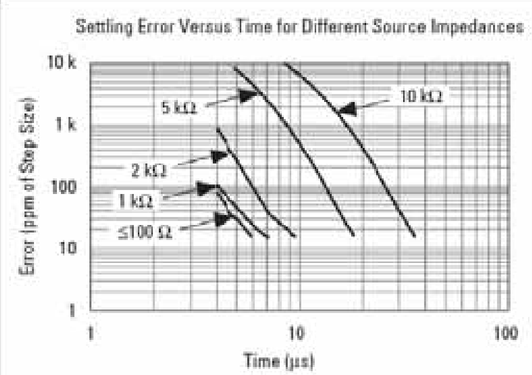

Typical Performance Graphs

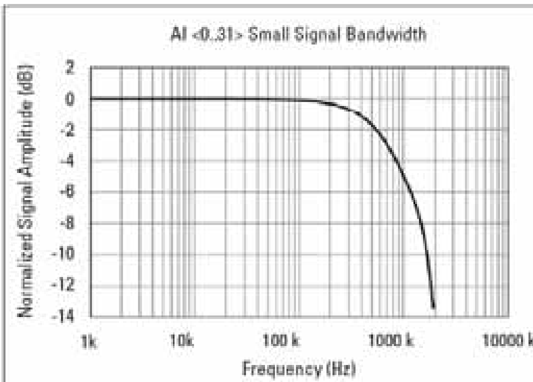

*Small signal bandwidth also applies to AI <32..79> for the NI 6225.

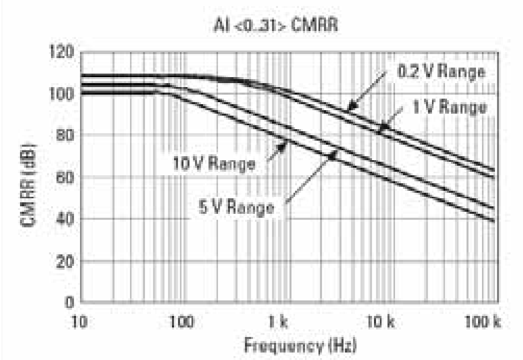

*CMRR also applies to AI <32..79> for the NI 6225.

Analog Output

Number of channels	
NI 6220	0
NI 6221	2
NI 6224	0
NI 6225	2
NI 6229	4
DAC resolution	16 bits
DNL	±1 LSB
Monotonicity	16 bit guaranteed
Maximum update rate	
1 channel	833 kS/s
2 channels	740 kS/s per channel
3 channels	666 kS/s per channel
4 channels	625 kS/s per channel
Timing accuracy	50 ppm of sample rate
Timing resolution	50 ns
Output range	±10 V
Output coupling	DC
Output impedance	0.2 Ω
Output current drive	±5 mA

Low-Cost M Series Multifunction DAQ 16-Bit, 250 kS/s, up to 80 Analog Inputs

Overdrive protection	±25 V
Overdrive current	10 mA
Power-on state	±20 mV
Power-on glitch	8.5 V peak for 14.5 ms
Output FIFO size	8,191 samples shared among channels used
Data transfers	DMA (Scatter-gather), interrupts, programmed I/O
AO waveform modes	Aperiodic waveform Periodic waveform regeneration mode from onboard FIFO Periodic waveform regeneration from host buffer including dynamic update
Settling time, full scale step 15 ppm (1 LSB)	6 µs
Slew rate	15 V/µs
Glitch energy	
Magnitude	100 mV
Duration	2.6 µs

Calibration (AI and AO)

Recommended warm-up time	15 minutes
Calibration interval	1 year

AI Absolute Accuracy Table

Nominal Range		Residual			Residual	Offset			Absolute	
Positive Full Scale	Negative Full Scale	Gain Error (ppm of Reading)	Gain Tempco (ppm/°C)	Reference Tempco	Offset Error (ppm of Range)	Tempco (ppm of Range/°C	INLError (ppm of Range)	Random Noise, σ (μV_{rms})	Accuracy at Full Scale[1] (µV)	Sensitivity[2] (µV)
10	–10	75	25	5	20	57	76	244	3100	97.6
5	–5	85	25	5	20	60	76	122	1620	48.8
1	–1	95	25	5	25	79	76	30	360	12.0
0.2	–0.2	135	25	5	80	175	76	13	112	5.2

AbsoluteAccuracy = Reading · (GainError) + Range · (OffsetError) + NoiseUncertainty

GainError = ResidualAIGainError + GainTempco · (TempChangeFromLastInternalCal) + ReferenceTempco · (TempChangeFromLastExternalCal)

OffsetError = ResidualAIOffsetError + OffsetTempco · (TempChangeFromLastInternalCal) + INL_Error

$$\text{NoiseUncertainty} = \frac{\text{RandomNoise} \cdot 3}{\sqrt{100}},$$ For a coverage factor of 3 σ and averaging 100 points

[1]Absolute accuracy at full scale on the analog input channels is determined using the following assumptions:

TempChangeFromLastExternalCal = 10 °C

TempChangeFromLastInternalCal = 1 °C

number_of_readings = 100

CoverageFactor = 3 σ

For example, on the 10 V range, the absolute accuracy at full scale is as follows:

GainError = 75 ppm + 25 ppm · 1 + 5 ppm · 10 GainError = 150 ppm

OffsetError = 20 ppm + 57 ppm · 1 + 76 ppm OffsetError = 153 ppm

$$\text{NoiseUncertainty} = \frac{244\ \mu V \cdot 3}{\sqrt{100}},$$ NoiseUncertainty = 73 µV

AbsoluteAccuracy = 10 V · (GainError) + 10 V · (OffsetError) + NoiseUncertainty

AbsoluteAccuracy = 3100 µV

[2]Sensitivity is the smallest voltage change that can be detected. It is a function of noise.

AO Absolute Accuracy Table

Nominal Range		Residual			Residual	Offset		Absolute
Positive Full Scale	Negative Full Scale	Gain Error (ppm of Reading)	Gain Tempco (ppm/°C)	Reference Tempco	Offset Error (ppm of Range)	Tempco (ppm of Range/°C	INLError (ppm of Range)	Accuracy at Full Scale[1] (µV)
10	–10	90	10	5	40	5	128	3230

[1]Absolute Accuracy at full scale numbers is valid immediately following internal calibration and assumes the device is operating within 10 °C of the last external calibration.

AbsoluteAccuracy = OutputValue · (GainError) + Range · (OffsetError)

GainError = ResidualGainError + GainTempco · (TempChangeFromLastInternalCal) + ReferenceTempco · (TempChangeFromLastExternalCal)

OffsetError = ResidualOffsetError + AOOffsetTempco · (TempChangeFromLastInternalCal) + INL_Error

Digital I/O/PFI

Static Characteristics

Number of channels	
NI 6220/NI 6221/NI 6225	24 total 8 (P0.<0..7>) 16 (PFI <0..15>/P1/P2)
NI 6224/NI 6229	48 total 32 (P0.<0..31>) 16 (PFI <0..15>/P1/P2)
Ground reference	D GND
Direction control	Each terminal individually programmable as input or output
Pull-down resistor	50 kΩ to 75 kΩ
Input voltage protection[1]	±20 V on up to two pins

[1] Stresses beyond those listed under Input voltage protection may cause permanent damage to the device.

Waveform Characteristics (Port 0 Only)

Terminals used	
NI 6220/NI 6221/NI 6225	Port 0 (P0.<0..7>)
NI 6224/NI 6229	Port 0 (P0.<0..31>)
Port/sample size	
NI 6220/NI 6221/NI 6225	Up to 8 bits
NI 6224/NI 6229	Up to 32 bits
Waveform generation (DO) FIFO	2,047 samples
Waveform acquisition (DI) FIFO	2,047 samples
DO or DI Sample Clock frequency	0 to 1 MHz
DO or DI Sample Clock source	Any PFI, RTSI, AI Sample or Convert Clock, AO Sample Clock, Ctr *n* Internal Output, and many other signals

PFI/Port 1/Port 2 Functionality

Functionality	Static digital input, static digital output, timing input, timing output
Timing output sources	Many AI, AO, counter, DI, DO timing signals
Debounce filter settings	125 ns, 6.425 µs, 2.54 ms, disable; high and low transitions; selectable per input

Low-Cost M Series Multifunction DAQ
16-Bit, 250 kS/s, up to 80 Analog Inputs

Recommended Operation Conditions

Level	Minimum	Maximum
Input high voltage (V_{IH})	2.2 V	5.25 V
Input low voltage (V_{IL})	0 V	0.8 V
Output high current (I_{OH})		
P0.<0..31>	–	–24 mA
PFI <0..15>/ P1/P2	–	–16 mA
Output low current (I_{OL})		
P0.<0..31>	–	24 mA
PFI <0..15>/P1/P2	–	16 mA

Electrical Characteristics

Level	Minimum	Maximum
Positive-going threshold (VT+)	–	2.2 V
Negative-going threshold (VT–)	0.8 V	–
Delta VT hysteresis (VT+ – VT–)	0.2 V	–
I_{IL} input low current (V_{in} = 0 V)	–	–10 μA
I_{IH} input high current (V_{in} = 5 V)	–	250 μA

Digital I/O Characteristics

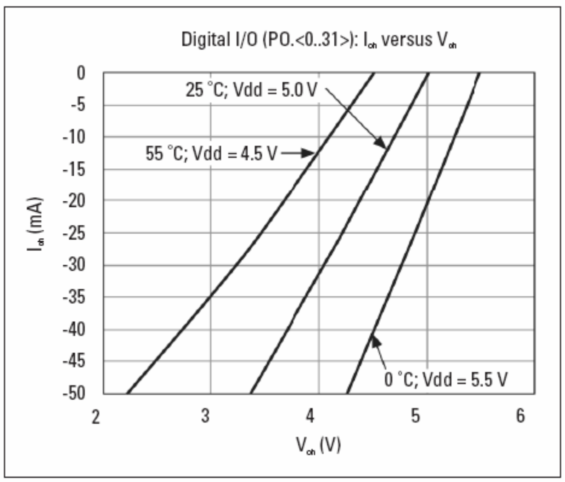

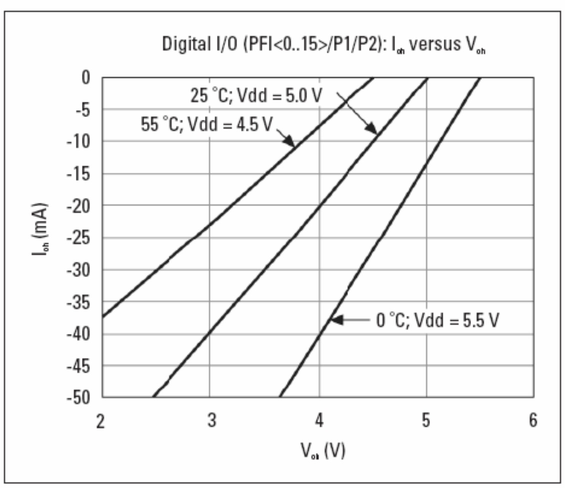

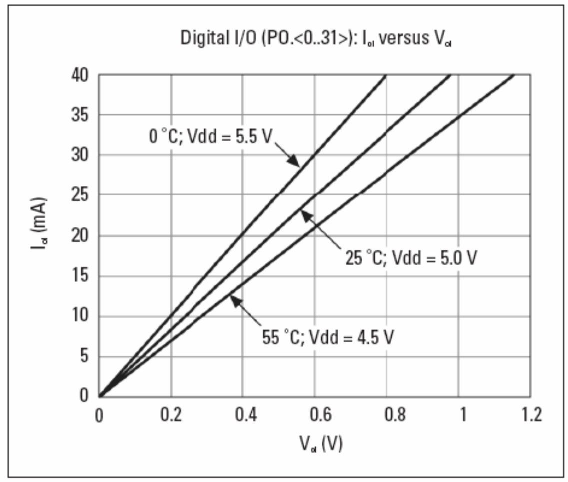

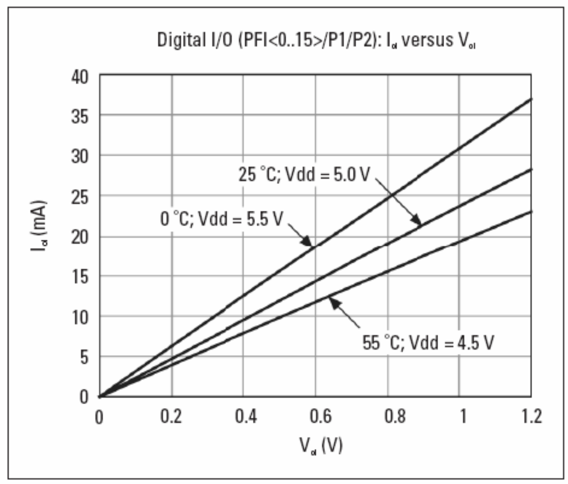

General-Purpose Counter/Timers

Number of counter/timers 2
Resolution.. 32 bits
Counter measurements.................................. Edge counting, pulse, semi period, period, two-edge separation
Position measurements.................................. X1, X2, X4 quadrature encoding with Channel Z reloading; two-pulse encoding
Output applications....................................... Pulse, pulse train with dynamic updates, frequency division, equivalent time sampling
Internal base clocks .... 80, 20, 0.1 MHz
External base clock frequency .... 0 to 20 MHz
Base clock accuracy .... 50 ppm
Inputs.. Gate, Source, HW_Arm, Aux, A, B, Z, Up_Down
Routing options for inputs.............................. Any PFI, RTSI, PXI_TRIG, PXI_STAR, analog trigger, many internal signals
FIFO.. 2 samples
Data transfers .... Dedicated scatter-gather DMA controller for each counter/timer; interrupts; programmed I/O

Low-Cost M Series Multifunction DAQ 16-Bit, 250 kS/s, up to 80 Analog Inputs

Frequency Generator

Number of channels	1
Base clocks	10 MHz, 100 kHz
Divisors	1 to 16
Base clock accuracy	50 ppm

Output can be available on any PFI or RTSI terminal.

Phase-Locked Loop (PLL)

Number of PLLs	1
Reference signal	PXI_STAR, PXI_CLK10, RTSI <0..7>
Output of PLL	80 MHz timebase; other signals derived from 80 MHz timebase including 20 MHz and 100 kHz timebases

External Digital Triggers

Source	Any PFI, RTSI, PXI_TRIG, PXI_STAR
Polarity	Software-selectable for most signals
Analog input function	Start Trigger, Reference Trigger, Pause Trigger, Sample Clock, Convert Clock, Sample Clock Timebase
Analog output function	Start Trigger, Pause Trigger, Sample Clock, Sample Clock Timebase
Counter/timer functions	Gate, Source, HW_Arm, Aux, A, B, Z, Up_Down
Digital waveform generation (DO) function	Sample Clock
Digital waveform acquisition (DI) function	Sample Clock

Device-To-Device Trigger Bus

PCI devices	RTSI <0..7>[1]
PXI devices	PXI_TRIG <0..7>, PXI_STAR
Output selections	10 MHz Reference Clock; frequency generator output; many internal signals
Debounce filter settings	125 ns, 6.425 µs, 2.54 ms, disabled; high and low transitions; selectable per input

[1] In other sections of this document, RTSI refers to RTSI <0..7> for PCI devices or PXI_TRIG <0..7> for PXI devices.

Bus Interface

PCI or PXI	3.3 V or 5 V signal environment
DMA channels	6, analog input, analog output, digital input, digital output, counter/timer 0, counter/timer 1

Power Requirements

Current draw from bus during no-load condition	
+5 V	0.02 A
+3.3 V	0.25 A
+12 V	0.15 A
Current draw from bus during AI and AO overvoltage condition	
+5 V	0.02 A
+3.3 V	0.25 A
+12 V	0.25 A
Power available from +5 V terminal	1 A max, each connector, with self-resetting fuse
Other power limit for PXI devices	Current drawn from +5 V terminals and all P0/PFI/P1/P2 terminals should not exceed 2 A

Physical

Dimensions	
PCI	9.7 by 15.5 cm (3.8 by 6.1 in.)
PXI	Standard 3U PXI
I/O connector	
NI 6220/NI 6221	1 68-pin VHDCI
NI 6224/NI 6225/NI 6229	2 68-pin VHDCI

Maximum Working Voltage[1]

Channel-to-earth	11 V, Installation Category I
Channel-to-channel	11 V, Installation Category I

[1] Maximum working voltage refers to the signal voltage plus the common-mode voltage.

Environmental

Operating temperature	0 to 55 °C
Storage temperature	–20 to 70 °C
Relative Humidity	10 to 90%, noncondensing
Maximum altitude	2,000 m
Pollution Degree (indoor use only)	2

Safety

This product is designed to meet the requirements of the following standards of safety for electrical equipment for measurement, control, and laboratory use:

- IEC 61010-1, EN 61010-1
- UL 61010-1
- CAN/CSA C22.2 No. 61010-1

For UL and other safety certifications, refer to the product label, or visit **ni.com/certification**, search by model number or product line, and click the appropriate link in the Certification column.

Electromagnetic Compatibility

Emissions	EN 55011 Class A at 10 m; FCC Part 15A above 1 GHz
Immunity	EN 61326:1997 + A2:2001, Table 1

CE, C-Tick, and FCC Part 15 (Class A) Compliant

For EMC compliance, operate this device with shielded cabling.

CE Compliance CE

This product meets the essential requirements of applicable European Directives, as amended for CE marking, as follows:

Low-Voltage Directive (safety)	73/23/EEC
Electromagnetic Compatibility Directive (EMC)	89/336/EEC

Refer to the Declaration of Conformity (DoC) for this product for any additional regulatory compliance information. To obtain the DoC for this product, visit **ni.com/certification**, search by model number or product line, and click the appropriate link in the Certification column.

Multifunction DAQ and SCXI Signal Conditioning Accuracy Specifications Overview

Module	Empirical Accuracy
SCXI-1102	±0.25 °C at 250 °C ±24 mV at 9.5 V
SCXI-1112	±0.21 °C at 300 °C
SCXI-1125	±2.2 mV at 2 V

Table 1. Possible Empirical Accuracy with System Calibration

		Absolute Accuracy							Relative Accuracy	
Nominal Range (V)		% of Reading			System Noise (mV)		Temp Drift	Absolute Accuracy	Resolution (µV)	
Positive FS	Negative FS	24 Hours	1 Year	Offset (µV)	Single Point	Averaged	(%/°C)	at Full Scale (mV)	Single Point	Averaged
10.0	-10.0	0.0354	0.0371	947.0	981.0	87.0	0.0006	4.747	1145.0	115.0
5.0	-5.0	0.0054	0.0071	476.0	491.0	43.5	0.0001	0.876	573.0	57.3
2.5	-2.5	0.0354	0.0371	241.0	245.0	21.7	0.0006	1.190	286.0	28.6
1.0	-1.0	0.0354	0.0371	99.2	98.1	8.7	0.0006	0.479	115.0	11.5
0.5	-0.5	0.0354	0.0371	52.1	56.2	5.0	0.0006	0.243	66.3	6.6
0.25	-0.25	0.0404	0.0421	28.6	32.8	3.0	0.0006	0.137	39.2	3.9
0.1	-0.1	0.0454	0.0471	14.4	22.4	2.1	0.0006	0.064	27.7	2.8
0.05	-0.05	0.0454	0.0471	9.7	19.9	1.9	0.0006	0.035	25.3	2.5
10.0	0.0	0.0054	0.0071	476.0	491.0	43.5	0.0001	1.232	573.0	57.3
5.0	0.0	0.0354	0.0371	241.0	245.0	21.7	0.0006	2.119	286.0	28.6
2.0	0.0	0.0354	0.0371	99.2	98.1	8.7	0.0006	0.850	115.0	11.5
1.0	0.0	0.0354	0.0371	52.1	56.2	5.0	0.0006	0.428	66.3	6.6
0.5	0.0	0.0404	0.0421	28.6	39.8	3.0	0.0006	0.242	48.2	3.9
0.2	0.0	0.0454	0.0471	14.4	22.4	2.1	0.0006	0.111	27.7	2.8
0.1	0.0	0.0454	0.0471	9.7	19.9	1.9	0.0006	0.059	25.3	2.5

Table 2. NI PCI-6052E Analog Input Accuracy Specifications

Note: Accuracies are valid for measurements following an internal (self) E Series calibration. Averaged numbers assume averaging of 100 single-channel readings. Measurement accuracies are listed for operational temperatures within ±1 °C of internal calibration temperature and ±10 °C of external or factory-calibration temperature. One-year calibration interval recommended. The absolute accuracy at full scale calculations were performed for a maximum range input voltage (for example, 10 V for the ±10 V range) after one year, assuming 100 point averaging of data.

APPENDIX H-12: Signal Conditioning Modules

Portable, Modular Signal Conditioning Modules

Specifications

Typical for 25 °C unless otherwise noted.

SCC-TC Series

Input Characteristics

Number of channels	1 differential
Input signals	Thermocouples of type J, K, T, B, E, N, R, and S, ±100 mV
Input signal gain	100
Maximum input working voltage	±12 V of chassis ground
Overvoltage protection to DAQ device	±42 V_{pk} (powered on or off)
Nonlinearity	±0.004% maximum
Gain error	±0.08% of reading, maximum
Input impedance	
Normal powered on	10 MΩ
Powered off or overload	10 kΩ
Open thermocouple detection current	250 nA maximum
Common-mode rejection ratio	110 dB minimum
Bandwidth	2 Hz, dual-pole RC filter
System noise	5 μV_{rms}, referred to input
Stability	
Offset temperature coefficient	±0.6 µV/°C maximum
Gain temperature coefficient	±0.0005%/°C
Cold-junction sensor (thermistor)	
Output	1.91 V (at 0 °C) to 0.58 V (at 55 °C)
Accuracy (15 to 35 °C)	0.4 °C maximum

Power Requirements

Analog	60 mW

SCC-RTD01

Analog Input

Number of input channels	2 differential
Input range	±400 mVDC (fixed gain of 25 on each channel)
Maximum working voltage (signal + common mode)	Each input should remain within ±12 V of ground
Overvoltage protection	±42 V_{pk}/60 VDC (powered on or off)
Input impedance	2 MΩ in parallel with 4.7 nF powered on; 20 kΩ min powered off
Filter type	Lowpass 3-pole Sallen and Key filter
-3 dB cutoff frequency	30 Hz
System noise	4.5 μV_{rms} (referred to input)

Transfer Characteristics

Gain	25
Gain error	±1.2%
Gain-error temperature coefficient	±10 ppm/°C
Offset error	±250 mV RTI
Offset-error temperature coefficient	±1.6 mV/°C
Nonlinearity	10 ppm of full scale
Recommended warm-up time	5 minutes (SCC system only)

Amplifier Characteristics

CMRR	110 dB at 60 Hz
Output range	±10 V

Excitation

Number of channels	1
Constant-current source	1 mA, ±0.4 µA or 0.04%
Maximum voltage level without losing regulation	24 V
Drift	±127 ppm/°C

Environment

Operating temperature	0 to 50 °C
Relative humidity	5 to 90% noncondensing

Power Requirements

Analog	135 mW maximum
Digital	153 mW maximum

SCC-SG0x

Input Characteristics

Number of channels	2 differential
Input signal range	±100 mV
Output signal range	±10 V
Gain	100
Overvoltage protection	±28 Vpk (powered on or off)
Input impedance	10 MΩ powered on, 10 kΩ powered off or overload
Gain error	±0.8% of reading maximum
Offset error	±5 µV
Bandwidth	1.6 kHz (single-pole RC filter)
Excitation voltage	2.5 V ±0.4%

Excitation current drive

SG01, SG02	42 mA (with 2 120 Ω gauges)
SG03, SG04	60 mA (with 2 350 Ω gauges)
Excitation drift	13 mV/°C

Power Requirements

Analog	103 mW
Digital	115 mW

SCC-SG11

Number of channels	2
Control signal	1 DIO channel
Resistor for each channel	301 kΩ ±1%, socketed
Resistor temperature coefficient	±100 ppm/°C

Power Requirements

Digital	100 µW

SCC-SG24

Input Characteristics

Number of channels	2 differential
Input signal range	± 100 mV
Output signal range	±10 V
Gain	100
Overvoltage protection	±42 VDC powered on and powered off
Input impedance	20 MΩ powered on >60 kΩ powered off or overload
Gain error	± 0.20% of reading max
Offset error	±50 µV typ, 325 µV max before calibration[1]
Bandwidth	1.6 kHz single-pole buffered RC filter
Excitation voltage	10 V ±0.05%
Excitation current drive	60 mA, based on two full-bridge 350 Ω strain gauges
Excitation drift	10 ppm/°C

Power Requirements

Analog	340 mW
Digital	930 mW

[1]By factory-default the nulling resistors are not installed in the SCC-SG24. Refer to the user manual for information on installing the nulling resistors.

SCC-ACC01

Analog Input

Number of input channels	1 differential
Input range	±5 VAC (fixed gain of 2)
Input coupling	AC
-3 dB cutoff frequency	0.8 Hz
Filter type	Lowpass 3-pole Bessel
-3 dB cutoff frequency	19 kHz
Passband flatness	±0.3 dB, 10 Hz to 5 kHz ±1 dB, 5 Hz to 10 kHz
Maximum working voltage (signal + common mode)	Each input should remain within ±12 V of ground
Overvoltage protection	±40 VAC + DC (powered on or off)
Input impedance	5 MΩ in series with 0.39 µF (powered on or off)
System noise	130 mV_{rms} (referred to input)

Transfer Characteristics

Gain	5
Gain error	±1%
Gain-error temperature coefficient	±10 ppm/°C
Offset error	±3 mV (referred to input)
Offset-error temperature coefficient	±1.6 mV/°C
Nonlinearity	10 ppm of full scale
Recommended warm-up time	5 minutes

Portable, Modular Signal Conditioning Modules

Specifications (continued)

Amplifier Characteristics
CMRR .... 80 dB at 60 Hz
Output range .... ±10 V

Excitation
Number of channels 1
Constant-current source .... 4 mA
Maximum voltage level
without losing regulation .... 24 V
Drift .... ±127 ppm/°C

Environment
Operating temperature .... 0 to 50 °C
Relative humidity .... 5 to 90% noncondensing

Power Requirements
Analog .... 80 mW
Digital .... 330 mW

SCC-AI Series

Input Characteristics
Number of channels .... 2 differential, isolation per module
Input impedance .... 1 MΩ (SCC-AI01, SCC-AI02)
100 MΩ (all others)

Safety Isolation
Working common mode voltage .... 300 V, Category II[1]
Differential maximum voltage .... 250 VDC/VAC
Gain error .... Adjustable to 0
Offset error .... Adjustable to 0

[1]Test isolation voltage is 2,350 VAC for 2 s.

Power Requirements
Analog .... 375 mW
Digital .... 525 mW

Module	Input Range	Output Range	Gain	Filter Bandwidth
SCC-AI01	±42 V	±8.4 V	0.2	10 kHz
SCC-AI02	±20 V	±10 V	0.5	10 kHz
SCC-AI03	±10 V	±10 V	1	10 kHz
SCC-AI04	±5 V	±10 V	2	10 kHz
SCC-AI05	±1 V	±10 V	10	10 kHz
SCC-AI06	±100 mV	±10 V	100	10 kHz
SCC-AI07	±50 mV	±10 V	200	10 kHz
SCC-AI13	±10 V	±10 V	1	4 Hz
SCC-AI14	±5 V	±10 V	2	4 Hz

SCC-A10

Input Characteristics
Number of channels .... 2 differential
Input range .... ±100 VDC
Output range .... ±10 V
Overvoltage protection .... 250 V_{rms} to DAQ device
Gain error .... ±0.14% of reading, maximum
Offset error .... ±6.5 mV maximum reffered to input
Input impedance
Normal powered on or off .... 1 MΩ
Full power bandwidth .... 10 kHz

Power Requirements
Analog .... 90 mW

SCC-AO10

Output Characteristics
Number of output channels .... 1 nonreferenced single ended
Input range .... ±10 V
Output range .... ±10 V
Current drive .... ±30 mA
Gain nonlinearity .... 0.5% of full-scale output range
Propagation delay .... 10 µs
Output noise .... 2 mV_{rms} typ; 3 mV_{rms} max
Bandwidth .... 26 kHz
Slew rate .... 1.4 V/µs

Safety Isolation
Channel-to-earth (signal + common mode) .... ±300 V, Category II[2]

Environment
Operating temperature .... 0 to 50 °C
Relative humidity .... 10 to 90% noncondensing
Stability
Output offset temperature coefficient .... 200 µV/°C
Gain temperature coefficient .... 300 ppm/°C

Power Requirements
Analog .... 150 mW
Digital .... 875 mW

SCC-CI20

Input Characteristics
Number of channels .... 2 differential
Input range .... 0 to 20 mA
Output range .... 0 to 5 V
Gain error .... ±0.1% of reading maximum
Offset error .... ±0.6 mV maximum
Input resistor .... 249 Ω, 0.05%, 0.25 W
Full power bandwidth .... 10 kHz

Power Requirements
Analog .... 75 mW

SCC-CO20

Output Characteristics
Number of channels 1
Output referencing .... Nonreferenced (floating)
Input range .... 0 to 10 V
Output range .... 0 to 20 mA
Voltage compliance .... 12.5 V

Safety Isolation
Working common-mode voltage .... 300 V, Category II

Environment
Operating temperature .... 0 to 50 °C
Relative humidity .... 10 to 90%, noncondensing

Power Requirements
Analog .... 175 mW
Digital .... 645 mW

SCC-LP

Amplifier Characteristics
Number of input channels .... 2 differential
Input signal range .... ±10 V
Output signal range .... ±5 V
Gain 0.5
Overvoltage protection .... ±40 V
Input impedance .... 10 GΩ in parallel with 10 pF powered on 10 kΩ powered off or overload
Gain error .... Adjustable to 0%
Offset error (RTI) .... 350 µV typical, 1.5 mV maximum

Filter characteristics
Filter type .... 4th-order Butterworth
Stop-band attenuation rate .... 80 dB/decade
Cutoff frequency .... SCC-LP01 = 25 Hz
SCC-LP02 = 50 Hz
SCC-LP03 = 150 Hz
SCC-LP04 = 1 kHz

[2]Safe for use with the transients associated with local level mains supplies of up to 300 V, Installation Category (Overvoltage Category) II. 300 V CAT II local level mains supplies can see occasional transients of up to 1500 V.

Portable, Modular Signal Conditioning Modules

Specifications (continued)

Passband ripple: Fc = cutoff frequency

	Typical	Maximum
DC to ¼F_c	0 ± 0.04 dB max	0 ± 0.1 dB max
DC to ½F_c	0 ± 0.06 dB max	0 ± 0.2 dB max
DC to ¾F_c	-0.2 ± 0.25 dB max	-0.2 ± 0.4 dB max
DC to F_c	-3 ± 0.3 dB max	-3 ± 0.5 dB max

System Noise

THD at F_c .... <-90 dB
Wide band noise (DC to 1 MHz, (referred to input) .... 100 µV_{rms}
Narrow band noise (DC to 33 kHz,
(referred to input) .... 6 µV_{rms}

Stability

Gain temperature coefficient .... 10 ppm/°C typical, 20 ppm/°C maximum
Offset drift (RTI) .... 3.4 µV/°C typical, 27 µV/°C maximum

Power Requirements

SCC-LP01, LP02
Analog .... 135 mW
SCC-LP03, LP04
Analog .... 475 mW

SCC-FV01

Input Characteristics

Number of input channels .... 2 referenced single ended
Input range .... 100 mV_{pk} to 5 V_{pk}
Input coupling .... DC
Minimum input frequency .... 0 Hz
Minimum input pulse width (5V pulse train) .... 1.5 µs
Overvoltage protection .... ±40 VAC + DC (powered on or off)
Input Impedance
Signal > threshold .... 400 kΩ
Signal < threshold .... 10 MΩ
Threshold .... Zero crossing
Hysteresis .... 200 mV

Transfer Characteristics

Rise/fall time .... 80 ms (0 to +63%)
Step response .... 220 ms at 90%; 360 ms at 99%
Output offset .... 5 mV max
Output offset temperature coefficient .... 10 ppm/°C
Gain error temperature coefficient .... 100 ppm/°C
Nonlinearity .... ±0.05% full scale
Output ripple .... 30 mV_{p-p} at 10Hz
Output range .... 0 to +10 V
Recommended warm up time .... 5 minutes

Power Requirements

Analog .... 60 mW

SCC-DI01

Input Characteristics

Number of channels 1
Input range .... 24 VDC or 24 VAC

Digital logic levels

Level	Minimum	Maximum
Input low voltage (DC or Peak AC)	—	±1 V
Input high voltage		
DC	±2 VDC	±24 VDC
1 kHz AC	4 V_{rms}	24 VAC

Input current
5 V input .... 1.5 mA
24 V input .... 7.0 mA
Isolation .... 24 VDC from computer ground

Power Requirements

Digital .... 61 mW

SCC-DO01

Output Characteristics

Number of channels 1
Compatibility .... TTL-compatible
Supply voltage range .... 5 to 24 VDC

Digital Logic Levels

Configuration 1

Logic Level	Output Voltage Level Between Vout and Vcom
Low (I_{01} =0 mA)	0 V
High (I_{01} =25 mA)	22 VDC at V_{ss} = 24 V 3 VDC at V_{ss} = 5 V

Configuration 2

Logic Level	Output Voltage Level Between Vout and Vcom
Low (I_{02} =25 mA)	0.4 V
High (I_{02} =0 mA)	V_{ss}

Maximum continuous load current (I_o)
Configuration 1 .... 86 mA
Configuration 2 .... 120 mA
Minimum load resistance (at V_{SS}=24 V)
RLOAD1 .... 196Ω

RLOAD2 .... 84Ω

Power Requirements

Digital .... 70 mW

SCC-RLY01

Number of channels 1
Nominal switching capacity .... 5 A at 250 VAC, 5 A at 30 VDC
Contact resistance .... 30 mΩ
Switching time
Operate time (NC to NO) .... 5 ms (10 ms max)
Release time (NO to NC) .... 4 ms (5 ms max)
Maximum speed .... 30 operations/s at rated load
Contact lifetime .... 5 x 10^7 operations at 180 operations/minute (minimum)

SCC-PWR Series

SCC-PWR01

Input .... +5 VDC ±5% from an external source,
or +5 VDC from DAQ device
Output .... +5 VDC, 100% efficiency, ±15 VDC, 62% efficiency

SCC-PWR02

Input .... 90 to 264 VAC, 1 A maximum
Output .... +5 VDC, 1 A, ±15 VDC, ±0.3 A

SCC-PWR03

Input .... 7 to 42 VDC
Output .... +5 VDC, 75% efficiency, ±15 VDC, 46% efficiency

Physical

Dimensions
SCC Modules .... 8.9 by 2.9 by 1.9 cm (3.5 by 1.2 by 0.7 in.)
SC-2345 connector block .... 24.1 by 26.2 by 3.94 cm (9.5 by 10.3 by 1.6 in.)
SC-2345 with configurable connectors .... 30.7 by 25.4 by 4.3 cm (12.1 by 10 by 1.7 in.)
External AC adapter (for SCC-PWR02) .... 15.5 by 8.5 by 4.8 cm (6.1 by 3.3 by 1.9 in.)
Connectors
SC-2345 cable .... 68-pin male SCSI II
SCC input .... Removable screw terminal or minithermocouple connector
SCC output .... 20-pin right-angle male connector

Certification and Compliance

SCC-AIxx .... 300 V, Category II working voltage
SCC-AO10 .... 300 V, Category II working voltage

European Compliance

EMC .... EN 61326 Group I Class A, 10m, Table 1 Immunity
Safety .... EN 61010-1

North American Compliance

EMC .... FCC Part 15 Class A using CISPR

Australia and New Zealand Compliance

EMC .... AS/NZS 2064.1/2 (CISPR-11)

For additional regulatory compliance information click on "Declaration of conformity" at *ni.com/hardref.nsf/*
For assistance in configuring your SCC DAQ system, please visit *ni.com/advisors* and click on "SCC Advisor"

APPENDIX I: Procedure for Running a Sample Test

The following section will go through the procedures of running a sample test. Preparation of the sample for testing must first be performed. First, the bath must be filled with the physiological solution that the sample has been kept in during culture. Carefully remove the sample from the solution and measure its length, width, and thickness. Record this data for later testing input. Turn on the PID temperature controller and set to 37°C (or desired temperature). The heating pads should turn on and the solution will begin to heat up. See PID controller instruction manual for operational details.

While the bath solution is heating up, cut 8 pieces of silk sutures approximately 3-4 inches in length. Obtain 16 standard fly fishing hooks size #16. Tie a hook to both ends of each piece of suture with a clinch knot. (See APPENDIX J for clinch knot tying instructions) Attach four hooks to each side of the sample so that two small loops are created on each side. Hooks should be spaced as evenly as possible and approximately a 1/8 – 1/4 of an inch from the edge. Once the bath has reached the desired temperature (37°C) the sample can be mounted into the device.

Turn on both the power button and the enable button on the front of the NI-MID 7604 board. Open up LabVIEW 7.1 located on the desktop. Open the INITIALIZE.vi program within LabVIEW. Run the program by clicking on the right arrow in the top-left corner of the window. Use the axis jog buttons to move the four arms inward, to provide adequate space to attach the sutures to the pulleys. Loop each suture around a pulley while using the axis jog buttons to move the arms out. Continue to move all axis arms out as needed until the sample becomes taut. Use the control buttons to move the sample up, down, left, or right as needed to center the sample. Finally, use the threshold range control to adjust the threshold image until only the four markers are visible. Once satisfied with the initial parameters press the stop button to end the INITIALIZE.vi program.

Immediately after ending the INITIALIZE.vi program, open the NI Measurement and Automation Explorer program located on the desktop. In the collapsible tree on the left open the folders in order shown below.

open *Devices and Interfaces* folder → open *PCI-7334(1)* folder → open *Interactive* folder → open *1-D Interactive* folder

The new screen in the main window should display an interface for controlling the four stepper motors. Within the *trajectory parameters* section select Axis 1 from the Axis collapsible list. Within the *current trajectory data* section press the reset position button and click apply. Repeat this process for all four axes to reset all current motor positions. This step is very important and cannot be skipped. Failure to have current positions reset before final testing may result in damaging the motors and/or linear rails. Once reset is complete, Measurement and Automation Explorer may be closed.

The sample and device are now ready for final testing. Open Labview 7.1 from the desktop. Open the FINAL.vi program within Labview. Next, enter the following required data into the appropriate data inputs. The example values will change depending on the testing parameters desired by the user. For this example the test performed will be a 10% strain of the sample in 1 second. Enter 0.1 into the percent strain input. Enter 0.1 into the strain rate input. Enter the measured length, width, and thickness of the sample. Enter the length of the stretching arm attached to the force transducers. Enter the exact same threshold range parameters as set in the INITIALIZE.vi program. The device is now ready for testing.

Run the program by clicking on the right arrow button located in the top left corner of the window. Monitor test while program is running. If at any time there is a malfunction in the program or device, click stop to end the program. If motors do not halt after clicking stop, turn off the enable button on the NI-MID 7604 board. Once the test is complete, the user will be prompted to save the data gathered to file as an excel spreadsheet. Name the file and click save to desired location.

Graphs can be cleared by right clicking on the graph and selecting *data operations* and then *clear graph*. Memory of position is saved between tests. In order to return to the initial position, enter 0 into the percent strain input and run the FINAL.vi program again. The device can also be reset for a new test again with the INITIALIZE.vi program; however this again requires the resetting of current axis positions within Measurement and Automation Explorer before final testing.

APPENDIX J: Clinch Knot Instructions

Source: http://www.killroys.com/knots/clinch.htm

Use to tie hook to end of suture.

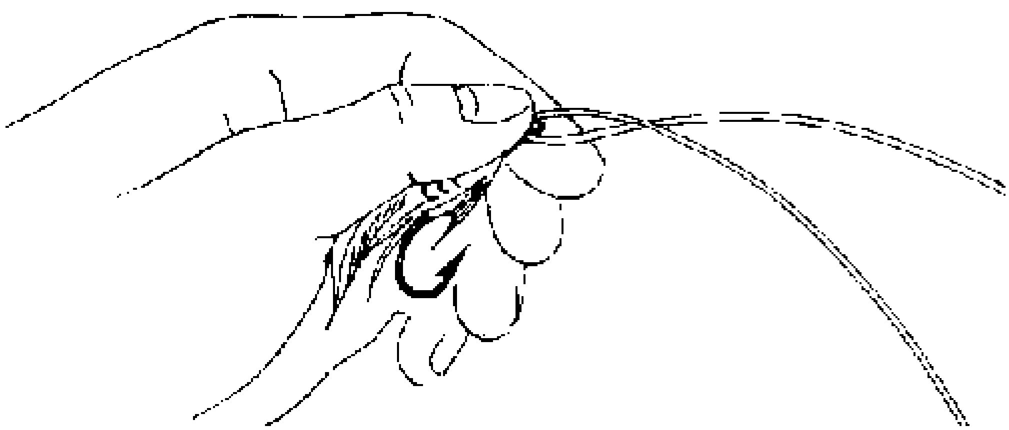

step 1:

Insert one end of suture through eye of hook.

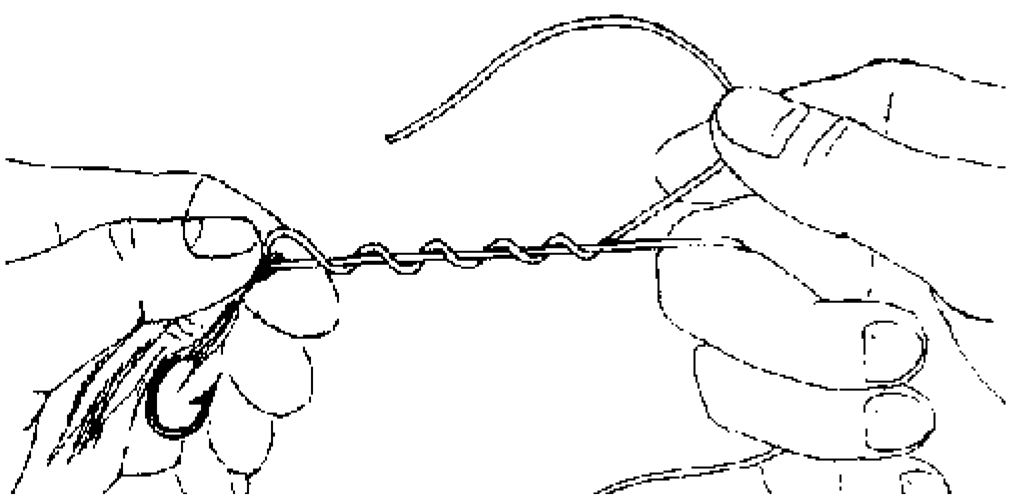

step 2:

Hold hook in left hand and with right hand wind the end of the suture around standing part of suture five times, keeping a small loop immediately adjacent to hook eye open. This loop is easy to keep open if you pinch it between thumb and forefinger of left hand.

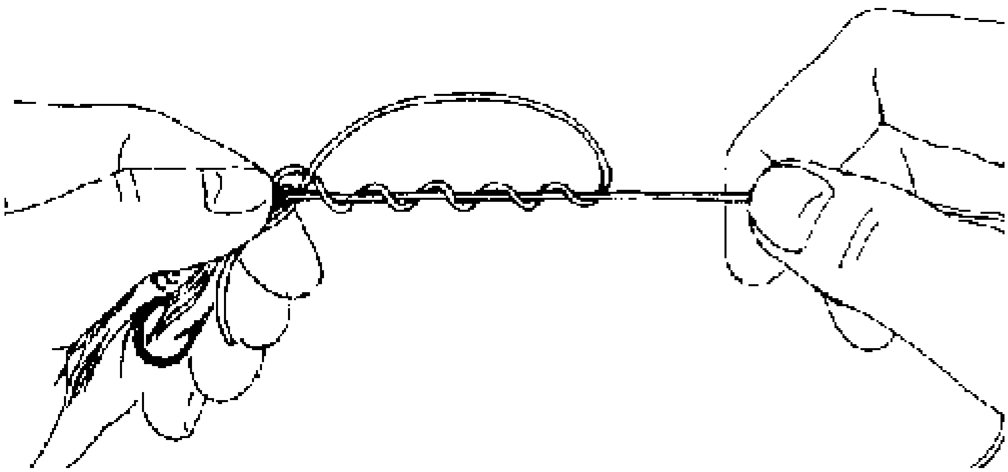

step 3:

Bring wrapped end of suture back through loop next to the hook eye and grasp with thumb and forefinger of left hand.

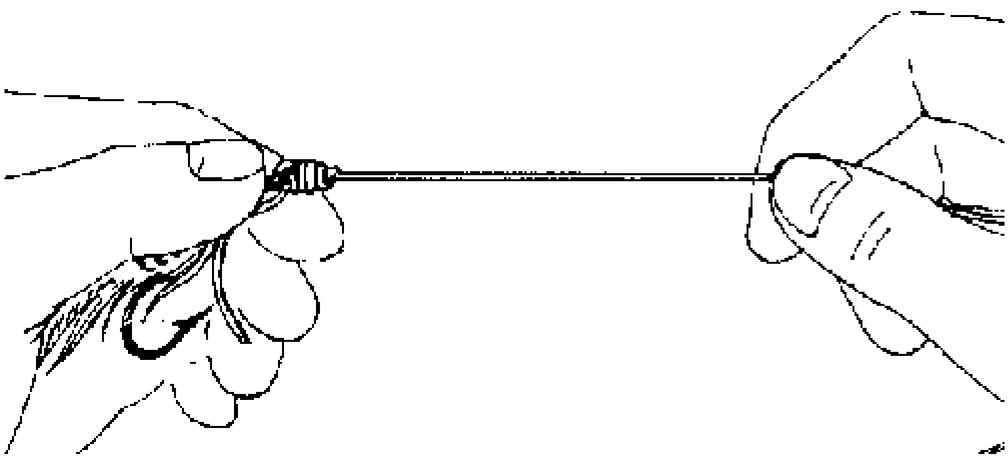

step 4:

Tighten by pulling the standing part of suture and the hook in opposite directions. Do not pull on the wrapped end of the suture - merely hold it alongside the hook. Trim loose end of suture close to knot.